2023

Development of Novel Cellular Assay Model and Therapeutic Deep Eutectic Solvents to Optimize the Activity of Anticancer Agents

Nizam Uddin
South Dakota State University, nizamsdstate@gmail.com

DEVELOPMENT OF NOVEL CELLULAR ASSAY MODEL AND THERAPEUTIC DEEP EUTECTIC SOLVENTS TO OPTIMIZE THE ACTIVITY OF ANTICANCER AGENTS

BY

NIZAM UDDIN

A dissertation submitted in partial fulfilment of the requirements for the

Doctor of Philosophy

Major in Biochemistry

South Dakota State University

2023

DISSERTATION ACCEPTANCE PAGE
NIZAM UDDIN

This dissertation is approved as a creditable and independent investigation by a candidate for the Doctor of Philosophy degree and is acceptable for meeting the dissertation requirements for this degree. Acceptance of this does not imply that the conclusions reached by the candidate are necessarily the conclusions of the major department.

Douglas Raynie
Advisor Date

Douglas Raynie
Department Head Date

Nicole Lounsbery, PhD
Director, Graduate School Date

I dedicate the dissertation to my lovely parents, Fatema Yeasmin and Shahab Uddin for continuous mental support, prayer, love, care, and encouragement that made possible for me to work diligently.

ACKNOWLEDGEMENTS

First, I would like to express my gratitude to Allah Almighty to provide strength, guide in right direction and helped to achieve my goal in long PhD journey.

My beloved mom Fatema Yeasmin and dad Shahab Uddin provided me with continuous support, courage, prayer, and mental strength to accomplish my dream. Without them it would have been impossible to reach my destination. I am forever grateful to them. Their love and affection were my inspiration.

I am very grateful and greatly indebted to my advisor, Dr. Douglas E. Raynie for continuous feedback, enlightening with analytical science-based research ideas, guidance, mentorship, counseling, motivation, and support in my critical time in the dept. You are an amazing and great advisor. I am forever grateful to you to back me up in critical and uncertain time in the department. Without your analytical lab support, I could have never materialized my dream of establishing novel methods and becoming a successful PhD holder. I always pray to God for your good health and long life.

I would like to thank my committee member Dr. Fathi Halaweish for providing constructive feedback and reviews. His biochemistry lab resources encouraged to execute novel idea from my PhD project in pharmacological experimental setting. I am thankful to another committee member Dr. Jay Shore for helping to do DSC study and guided me perfectly to redesign molecular modeling technique. I am also thankful to Dr. Surtaj Iram for providing logistic support to design and implement my first research project.

My caring, beautiful and charming wife Fariha Tabassum Aniqa continuously refilled me with fuel to move forward to finish my project work and dissertation writing. I want to thank her from my deep heart to support and motivate me in my tough time.

I specially express my gratitude to Jennifer and Trevor for being the most helpful colleagues with charming personalities. You made my research projects and work life easier. Dr. Jennifer kyerematen assisted in designing my novel cell-based efflux assay for detecting drug resistance and executing in the laboratory. Trevor Ostlund helped me to design and implement cell-based assays for my therapeutic solvent project. I want to thank Dr. Md Sajjadur Rahman to assist me in designing and preparing therapeutic solvents and HPLC method development in my analytical projects. I want to thank my friends, Mavis and Michael for helping me to perform solvatochromism experiment. I want to thank Kakan for assisting me in performing IR and NMR studies. I am thankful to all Dr. Raynie's analytical research lab members for their gratitude, trust, and appreciation.

Finally, I am forever grateful to the Department of Chemistry and Biochemistry to provide continuous financial assistance throughout my PhD journey.

CONTENTS

LIST OF ABBREVIATIONS

ABC	ATP-binding cassette
ADMET	Absorption, Distribution, Metabolism Excretion and Toxicity
ADP	Adenosine Diphosphate
ATP	Adenosine Triphosphate
MRP1	Multidrug Resistance Protein 1
BCRP	Breast Cancer Resistance Protein
E217βG	17β-estradiol glucuronide
FDA	Food and drug administration
GFP	Green Fluorescent Protein
MDR	Multidrug Resistance
NBD	Nucleotide Binding Domain
GSH	Reduced Glutathione
GSSG	Oxidized Glutathione
TMD	Transmembrane Domain
P-gp	Permeability Glycoprotein
HEK293	Human Embryonic Kidney 293
DMSO	Dimethyl Sulfoxide
EGFR	Epidermal Growth Factor Receptor.
PI3K	Phosphoinositide 3-kinases
π*	Dipolarity/polarizability parameter
℃	Degree Celsius
DES	Deep Eutectic Solvents

DMSO-d6	Deuterated dimethyl sulfoxide
Dod	Dodecyl Gallate
EG/ET	Ethyl Gallate
FTIR	Fourier transformed infra-red
HPLC	High Performance Liquid Chromatography
UV	Ultraviolet Spectroscopy
HBA	Hydrogen Bond acceptor
HBD	Hydrogen Bond Donor
α	Hydrogen Bond Acidity
β	Hydrogen Bond Basicity
MTT	3-(4,5-dimethylthiazol-2-yl)-2,5-diphenyl-2H-tetrazolium bromide
^{1}H-NMR	Proton Nuclear Magnetic Resonance
^{13}C-NMR	Carbon Nuclear Magnetic Resonance
PBS	Phosphate Buffered Saline
HBSS	Hank's Balanced Salt Solution
MDCK	Madin-Darby canine kidney cells
THEDES	Therapeutic Deep Eutectic Solvent
P	Parental
G1	GAP 1
S	Synthesis
G2	GAP 1
M	Mitosis

LIST OF FIGURES

LIST OF TABLES

ABSTRACT

DEVELOPMENT OF NOVEL CELLULAR ASSAY MODEL AND THERAPEUTIC DEEP EUTECTIC SOLVENTS TO OPTIMIZE THE ACTIVITY OF ANTICANCER AGENTS

NIZAM UDDIN

2023

Multidrug resistance (MDR) is the major burden behind chemotherapeutic treatment failure. It is the principal mechanism by which cancer cells evade chemotherapeutic treatment. As a result, aggressive cancer cells survive and continue uncontrolled cell division. Multidrug resistance affects survival rate of almost all types of cancer patients and death toll rises at an alarming rate. There are seven different mechanisms for evolving MDR. The most common mechanism in efflux activity of overexpressed ABC transporters. MRP1 is a prominent ABC transporter that pumps out a wide variety of anticancer drugs from the cells and thereby reduces intracellular drug concentrations and develops chemoresistance. Currently there are several protocols available to assess interaction between MRP1 and probable substrate anticancer drugs. However, these protocols have several limitations in common, such as expansive instrument set up, trained personnel, complex image analysis, separation of drugs from cell lysate, preparation of membrane vesicle, and results are based on accumulation of secondary fluorescence or radiolabeled substrates. To the best of our knowledge, there are no known protocols that can directly detect interaction between MPP1 and chemotherapeutic agents and categorize as MRP1 substrates. To solve this issue, in first project we developed an easy to follow and efficient novel mammalian cell-based efflux assaying using HPLC-UV technique to detect whether

MRP1 considers anticancer drug as substrate and directly pumps the drug of the cancer cells. We chose MDCK-II parental and MDCK-II MRP1 overexpressed cells to establish the assay. To evaluate the efficacy of novel protocol, the result was compared with a known MRP1 substrate anticancer drug vincristine (positive control). To conduct the assay, we chose total seven MRP1 modulator anticancer drugs identified previously in our laboratory. We exclusively focused on extracellular media for pumped-out drugs from both cell lines. Initially, incubation (1 hour) and efflux time points (2 hours) were optimized. In the final step, parental and MRP1 overexpressed cells were incubated with drugs for 1 hour. After that, cells were washed and replaced with fresh transport buffer and waited for 2 hours to collect pumped out drugs from the cells. Then the solution was injected into HPLC for determining concentration. Our research idea is that if the drug works as MRP1 substrate, it will be pumped out directly by MRP1 and extracellular concentration will significantly increase compared to parental cells (no MRP1 overexpression). Our idea worked perfectly and we identified some anticancer drugs namely, alisertib, mesalamine and celecoxib that are highly susceptible to MRP1 mediated drug resistance. Next, we validated our novel protocol using popular MTT assay. We used same cell lines for MTT. From MTT we noticed that for these substrate drugs cell viability was high in MRP1 overexpressed cells compared to parental cells. It confirmed the outcome of the novel efflux assay. The novel protocol will pioneer direct and rapid detection of new MRP1 substrates with accuracy. It could also be applied to other prominent ABC transporters to identify specific substrates. The novel assay will also promote development of ABC transporter specific inhibitors to inhibit activity of transporters and restore the pharmacological potential of chemotherapeutic agents.

In second project, we formulated a novel therapeutic deep eutectic solvent (THEDES) where anticancer natural product Ethyl Gallate and acetylcholine chloride were used as components. The main aim of the project is to evaluate the spectroscopic properties and possibility of biological application of the novel formulation. To prepare THEDES, ethyl gallate was mixed with choline chloride, acetylcholine chloride, glycerol, and PEG 400 in different molar ratios. We successfully prepared DES by mixing all the ingredients. We selected ethyl gallate and acetylcholine chloride-based DES (1:2) for further assessment. To characterize the spectroscopic and physicochemical properties, we conducted IR, NMR and solvatochromism. IR, ^{1}HNMR and ^{13}CNMR indicate nonbonding interaction between components in formulating DES. Solvatochromism provides polarity parameters in different temperatures. Solubility study was performed to assess high concentration of drug delivery in the aqueous medium. The novel solvent tremendously improved the solubility of ethyl gallate in aqueous medium. DES improved solubility of ethyl gallate 38 times higher than pure form. Quantum calculations were performed to analyze the extent of nonbonding interaction between both ingredients in the solvent. Electrostatic potential analysis represents possible electrophilic and nucleophilic attack between hydrogen bond donor and hydrogen bond acceptor. Thermogravimetric assay showed melting point depressed from 154 to below zero-degree celsius for DES. Furthermore, we presented the bio application of the green solvent. Cell viability assessments were performed on drug resistant MRP1 overexpressed cells and pancreatic cancer cells. In both cases DES showed comparatively better performance than pure ethyl gallate. Based on cell viability, we further conducted cell cycle analysis using flow cytometer. The result is interesting, and it shows DES could stop cancer cell growth in G1 phase. To get probable insight about

molecular mechanism of pancreatic cancer cell growth inhibition, we performed molecular modeling studies against various key protein parameters responsible for pancreatic cancer cell proliferation and we found that ethyl gallate based DES mostly works by inhibiting HER2 and Akt.

Poorly water-soluble anticancer agent dodecyl gallate was incorporated in tetra butyl ammonium bromide and polyethylene glycol -400 to formulate DES. Structural properties were calculated and compared between two dodecyl gallate incorporated DESs. Both DES improved water solubility of dodecyl gallate. IR spectroscopic assessment confirmed hydrogen bonding interaction between dodecyl gallate-TBABR (1:1) and dodecyl gallate-PEG400 (1:1). According to solvatochromism, both DES are closely related to polarity of commonly available ionic liquids and organic solvents. Computational study provides us informative analysis about electrostatic potential for analyzing hydrogen bonding interaction between DES components. Thermal decomposition shows that DESs were found thermally stable formulations up to 250 °C.

Overall, the newly formulated therapeutic solvents demonstrated good bioactivities compared to pure form of gallate compounds. It opens door for the anticancer therapies to be incorporated into novel solvent to accelerate pharmacological properties and successful drug delivery in near future.

CHAPTER ONE: PROBLEM STATEMENT AND BACKGROUND

1.1. Introduction

1.2. Problem statement

The main goal of this study is to develop a bioanalytical assay and novel therapeutic solvent formulation to optimize the efficacy of anticancer agents. To reach the goal two specific objectives will be achieved.

In the first objective, a novel cell-based efflux assay will be developed using HPLC-UV to identify substrates of MRP1 drug resistant protein. To conduct the experiment 6 MRP1 modulators were selected based on previous laboratory research projects. To establish the assay, we will focus on extracellular concentration instead of intracellular conc. Currently several protocols are followed to determine ABC transporter mediated drug resistance and all the protocols are based on either fluorescent or radioactive molecule accumulation or intracellular drug content determination. This novel protocol exclusively focuses on pumped out drug from MRP1 overexpressed cell lines. It will simplify direct and rapid detection of MRP1 substrate anticancer drugs.

In the second objective our prime research interest is mainly focused on formulation of novel THDESs where poorly water-soluble ethyl gallate and dodecyl gallate will be used as primary ingredients. Analysis of structural and spectroscopic properties of the new formulations, cell- viability assessment, solvatochromism, and solubility experiments will be performed. The new formulations will significantly increase the solubility and bioavailability of ethyl gallate. It will lead to breakthrough in pharmaceutical drug development and delivery research. The novel formulation will shape the anticancer therapy to treat various types of cancer.

1.3. Chemoresistance

Cancer is a deadly disease, and it can affect any part of our body. Each year millions of people die due to cancer. When cancel cells grow in uncontrolled manner, they spread and affect different organs of human body. According to the American Cancer Society, 1 in 3 women and 1 in 2 men will undergo cancer diagnosis in future [1,2]. Chemotherapy is the most used cancer treatment option for managing different stages of cancer. Along with chemotherapy, hormone therapy, immune therapy, radiation therapy, targeted therapy and surgery are other available treatment options. Resistance to chemotherapy is becoming evident day by day and emerging as the major treatment obstacle. Cancers develop resistance against all types of chemotherapeutic agents and, as a result, the survival rate and health condition of cancer patients is impacted [3,4]. Approximately 90% mortality is related to cancer drug resistance directly or indirectly [5].

1.4. Factors affect chemoresistance

Several factors govern development of chemoresistance. These are mainly categorized by two classes. Intrinsic chemoresistance and acquired chemoresistance (Figure 1.1) [1]. Intrinsic resistance develops before administration of chemotherapy. It might also develop concurrently in the time of chemotherapeutic treatment. Tumor heterogenicity due to inherent genetic mutation, differentiation, self-renewal, overexpression efflux transporters, mi RNA heterogenicity, proteomic heterogenicity, etc. are known as intrinsic factors [6]. Acquired resistance develops after chemotherapeutic treatment [6]. This type of resistance develops due to mutation in target protein, tumor microenvironment heterogenicity, genetic alteration of up and downstream regulating factors, reduced drug absorption, alteration in cell death pathway, impaired drug metabolism, etc. are some crucial factors behind

developing acquired resistance [7,8]. The figure below outlines simple diagram of acquired and intrinsic resistance (Figure 1.1).

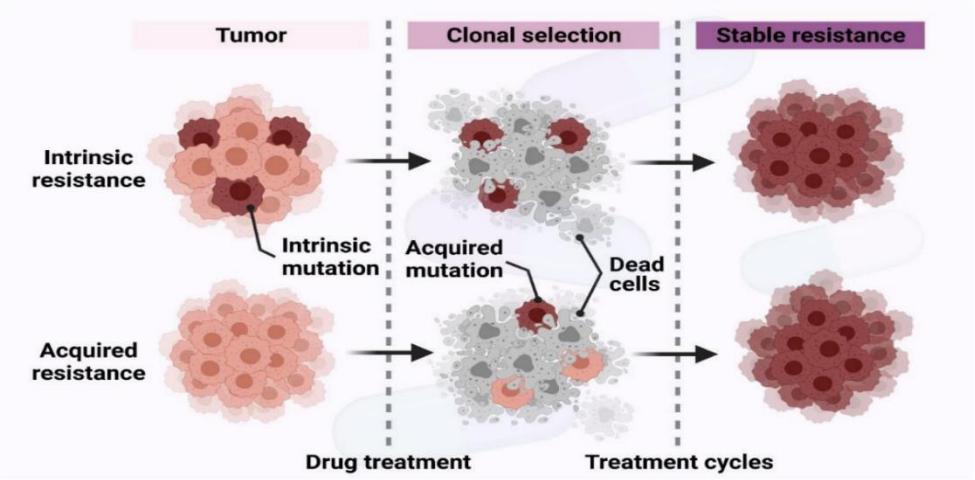

Figure 1.1. Acquired and intrinsic resistance. Intrinsic resistance occurs before any chemotherapeutic treatment and acquired resistance develops due to chemotherapeutic treatment. Genetic mutation is the root cause of development of chemoresistance. Both types of resistance might happen concurrently during tumor growth and development [1].

1.5. ABC transporters and functions

Drug molecules cross the biological barrier through active and passive diffusion. As a part of biological membrane transporter proteins facilitate the transport of drugs, as well as other endogenous and endogenous molecules of drugs. There are 400 transporters available in our body and out of these 400, 30-40 transporters are known to exchange drug molecules. Drug transporters have a wide impact on the pharmacological activities of drugs which include pharmacokinetics, pharmacodynamics, efficacy, toxicity, and drug safety profile [9–13].

Drug transporters are divided into two major families: ATP-binding cassette (ABC) and solute carrier (SLC)[14,15]. Among these two families, ABC transporters efflux the drug molecule out of the cells against the drug concentration gradient with the help of ATP hydrolysis (Figure 1.2). Normally they are membrane-bound proteins and they have conserved structure functions. This family of proteins needs two NBD (nuclear binding domain) and two TBD (transmembrane binding domain) to function. In our body these transporters are distributed in liver, kidney, brain, and intestine. These transporters have the unique ability to transport xenobiotics, endobiotic, and a wide variety of amphipathic and hydrophobic molecules across the biological membrane [16–20].

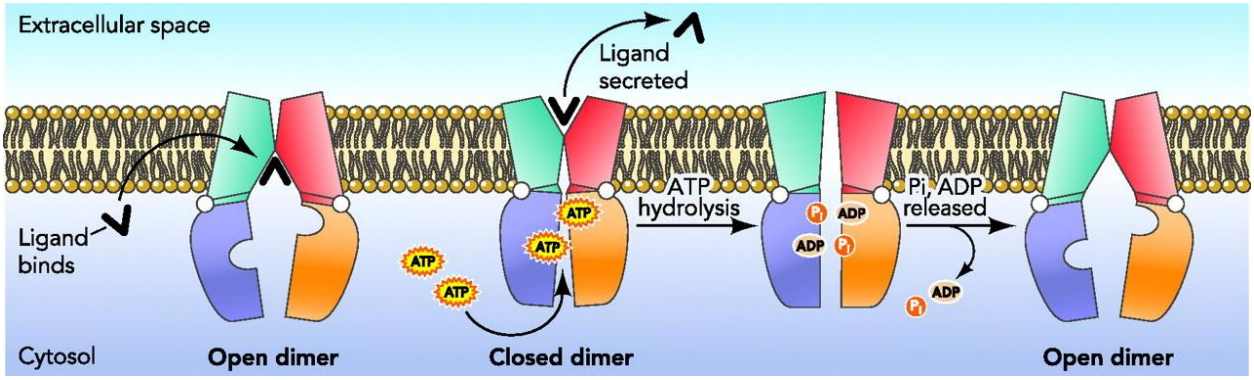

Figure 1.2. A simple ATP-driven mechanism of ABC transporters. Ligand binding to active pocket of TBD (transmembrane domain) induces conformational change in nucleotide binding region (NBD). Two ATP molecules bind to the NBDs and cause energy release. Energy released by the formation of the closed NBD dimer triggers conformational change in the transmembrane binding domain. ATP hydrolysis dissolve closed NBD dimer and further triggers conformational changes in the TMDs. In the final step, release of phosphate and ADP restores the ABC transporter to the open NBD dimer for next efflux cycle [21].

Cancer is one of the leading causes of death and the deadliest disease around the world. Day by day the number of cancer death is increasing. The cancer cells develop resistance towards chemotherapy. As a result, chemotherapy fails to show efficacy. The most common cause of multidrug resistance (MDR) is altered function of ABC transporters which efflux chemotherapeutic drug molecules out of the tumor cells. Faulty efflux is linked with overexpression and gene amplification of these transporters. Overexpression of these transporters is a common phenomenon in different types of cancer such as lung cancer ovarian cancer, colorectal cancer, prostate cancer, breast cancer, etc. P-gp is the first ABC transporter found to be expressed in kidney proximal tubule, apical membrane of hepatocytes, blood brain barrier and mucosal membrane. P-gp transports a wide variety of cytotoxic agents, immune suppressive agents, anthelmintic, cardiac glycosides and so on [22–26]. In addition, P-gp also transports lipid, hormone, peptide and cytokines like endogenous compounds[27–30]. MRP1 is the second most expressed ABC transporter. It confers resistance to chemotherapy for example, methotrexate, doxorubicin and vincristine. Substrates of MRP1 includes hydrophobic molecules, ionic conjugates, and some non-conjugates [31]. In addition to the drug molecules, this protein also transports glutathione conjugates and free glutathione as endogenous compounds [32,33]. BCRP is another type of transporter which are predominantly expressed in various organs and transport a wide variety of exogenous and endogenous compounds across the biological membranes [34–36].

To overcome the drug resistance associated with ABC transporters, selective ABC transporter inhibitors are used to inhibit the efflux activity and sensitize the cancer cells towards the chemotherapy. Third generation MDR inhibitors have high selectivity towards

ABC transporters and already showed promising results however, there are some reports of clinical trial about poor outcome [37–39]. That is why there is need of highly selective and high-affinity modulators to alter the function of these proteins. Scientists are also looking for targeting the MDR expression using novel approaches. The role of ABC transporters and evaluating their functions play important role in drug discovery and development research. Selecting the proper efflux-based transport experiment will help us to avoid variability in different assays and to set and validate proper acceptance criteria for ABC transporter specific substrates and inhibitors.

1.6. Treatment option for chemoresistance

Due to dynamic tumor heterogeneity in growing numbers of patients and high complexity of tumor microenvironments, it is challenging to treat and overcome chemoresistance. However, development of high-throughput screening of inhibitor and modulator drugs, and high throughput cancer genomics introduced a new era for treating chemoresistance. The following figure outlined some strategies to combat against chemoresistance [2].

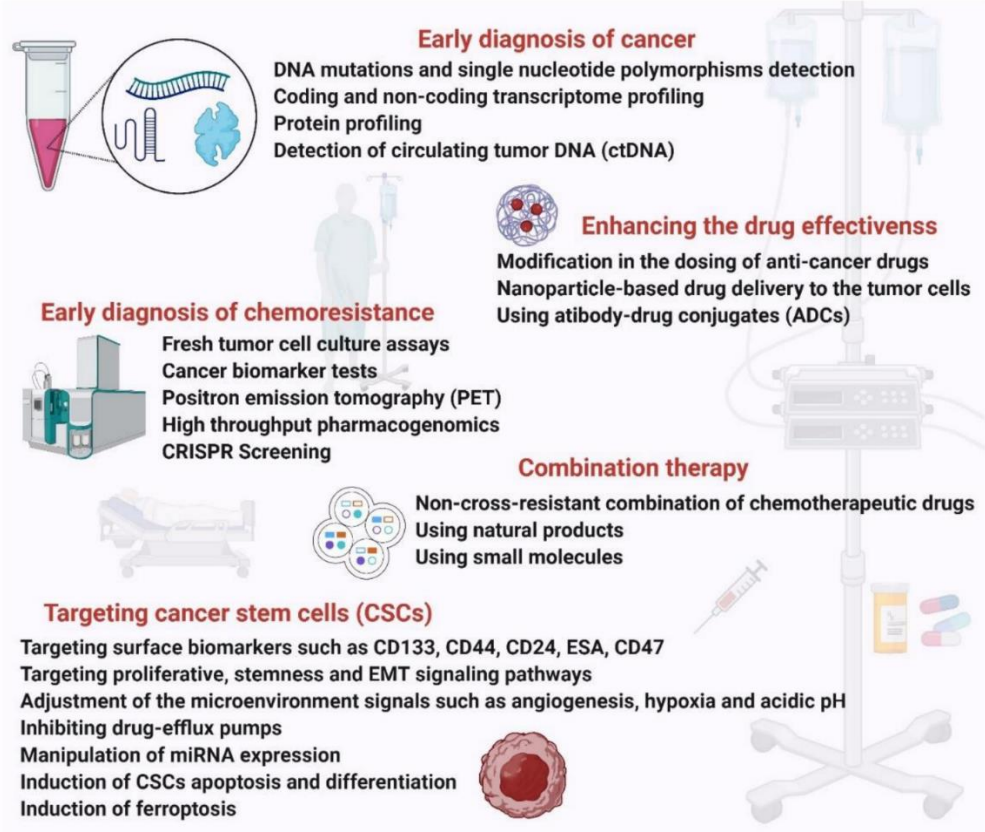

Figure 1.3. Strategies to battle against chemoresistance. Chemoresistance reduces effectiveness of chemotherapy. Early diagnosis followed by treatments with novel combination therapies and targeting cancer stem cells [1].

Early detection of chemoresistance will accelerate improvement of chemotherapeutic treatment. Genomics, proteomics, biomarker, and other tests for cancer are emerging rapidly to detect genes and proteins responsible for early development of chemoresistance [40]. Recently nanoparticle-based medicine introduced a new era in chemotherapy treatment (Figure 1.3). Nanoparticle treatments deliver chemotherapeutic agents in the targeted site of action and boost cytotoxicity (Figure 1.3). Using nanoparticle-based drug delivery it was possible to treat germ cell and hematological cancers, but the approach showed poor response in solid tumor treatment [41][42]. Nowadays natural products are

used extensively to combat drug resistance. Diverse structural scaffolds and pharmacological potential rendered them an effective strategy against chemoresistance [43]. Natural product-based drug discovery works by two approaches. First, natural products inhibit the efflux activity of ABC transporters and second, they induce cell death through different mechanisms like, apoptosis, necrosis, autophagy, etc. [44]. Another robust and effective strategy is the use of combination therapy. Frequent mutation of cancer cells causes failure of monotherapy. As a result, there is an urgent need to coadminister transporter inhibitor in the conventional chemotherapy to treat resistance [45,46]. There is growing interest in identifying effective inhibitors or modulators through high throughput screening from available drug libraries by treating in combination with traditional chemotherapeutic agents. In a high-throughput assay, 16 new MRP1 inhibitors were reported. Their activity was confirmed though flow cytometers and confocal microscopic assessment. Afatinib, doramapimod, celecoxib, mifepristone, MK-2206, and rosiglitazone reversed MRP1-mediated drug resistance in vincristine, doxorubicin and etoposide treated lung cancer cell lines [47]. In a different study four compounds, namely CHIR-124, Elesclomol, Tyrphostin-9 and Brefeldin A were identified as potential P-glycoprotein inhibitors though cell-based P-gp efflux models [48]. Cancer stem cells are a subpopulation of cancer cells that initiate tumor formation and metastasis. These cells are responsible for causing chemoresistance and are identified in a variety of cancers such as brain cancer, thyroid cancer, colon cancer, and others. To improve clinical outcomes, targeting stem cells will be a valuable alternative strategy to treat chemoresistance. The antihyperglycemic agent metformin resensitized chemoresponse to tumor metastasis inducing apoptosis. It induces apoptosis in breast cancer cell lines [1,49].

1.7. Available protocols to assess drug resistance

Lots of assays are available for determining the efflux activity of ABC transporters. These can be classified as *in vitro* assays, *in vivo* assays and *ex vivo* assays.

1.7.1. *In vitro* assays

1.7.1.1. Membrane vesicle-based assay

To perform this assay, plasma membranes with overexpression of specific transporters are prepared from a variety of cells and tissues. Since transporter proteins do not traverse biological membranes, the membranes are prepared as inside out vesicles. Transport of the drug molecules and quantification are determined in the presence of ATP because the proteins are ATP-driven pumps. Here AMP is used as negative control. The membrane vesicles are prepared using a rapid filtration technique [50–52]. If the drug molecules work as substrates, there will be high amount of molecules deposited inside the vesicle. On the other hand, if the drug molecules work as inhibitors, it will deposit low amount of probe substrates. Control experiment is performed where there is no overexpression of transporter proteins. This experiment is used to assess the effect of endogenously expressed transporters. This assay also adds benefits in determining the kinetic parameters: Km and inhibitory concentration (IC_{50}). Km is for substrates and IC_{50} is for inhibitors [53]. Using LC/MS/MS and LC-UV the compounds can be quantified. Other approaches are also used such radiolabeling and fluorescence intensities [47,54–61] . This is a straightforward assay and can be easily developed to a high throughput screening assay.

Recently Iram et al developed a novel approach to assess the transport efficiency, known as the Fluorescence Spectroscopy-Based FRET approach. The research group engineered two Color MRP1 constructs [57]. Using a distinctive GFP sequence, the final two

recombinant sequences of protein were separated between the N and C terminus with distinctive amino acid linkers. After getting the two color MRP1 constructs, they were expressed in MRP1-overexpressed cell line using mammalian transfection reagent. By utilizing flow cytometry, both GFP-and RFP-expressing cells were sorted out. The author constructed different constructs for the experiment: GR-638, GR-881, GR-888, and GR-905. Among the different constructs, GR-881, GR-888, and GR-905 showed very promising results in a substrate free FRET efficiency experiment. GR-881 was chosen based on overall FRET efficiency. Membrane vesicle was prepared from these two color MRP1 overexpressed cells. To further validate the two-color biosensor-based model screening using 40 anticancer drugs was conducted. Drugs were incubated with GR-881 biosensor and then FRET intensity was measured in fluorometer. The percent change in FRET is calculated using the equation: $(1 - IDA/ID) \times 100$, where IDA means acceptance fluorophore and ID means donor fluorophores. Among the 40 drugs, 10 hits showed conformational change when interacted with MRP1. The compounds might be substrate or modular. Due to the large pocket of the MRP1, it can show nonspecific interaction with the test compounds which might provide a false positive result. Further investigation is needed to confirm the interaction of the test compounds with MRP1. The figure below presents the FRET efficiency for the best hits in GR-881 construct [57].

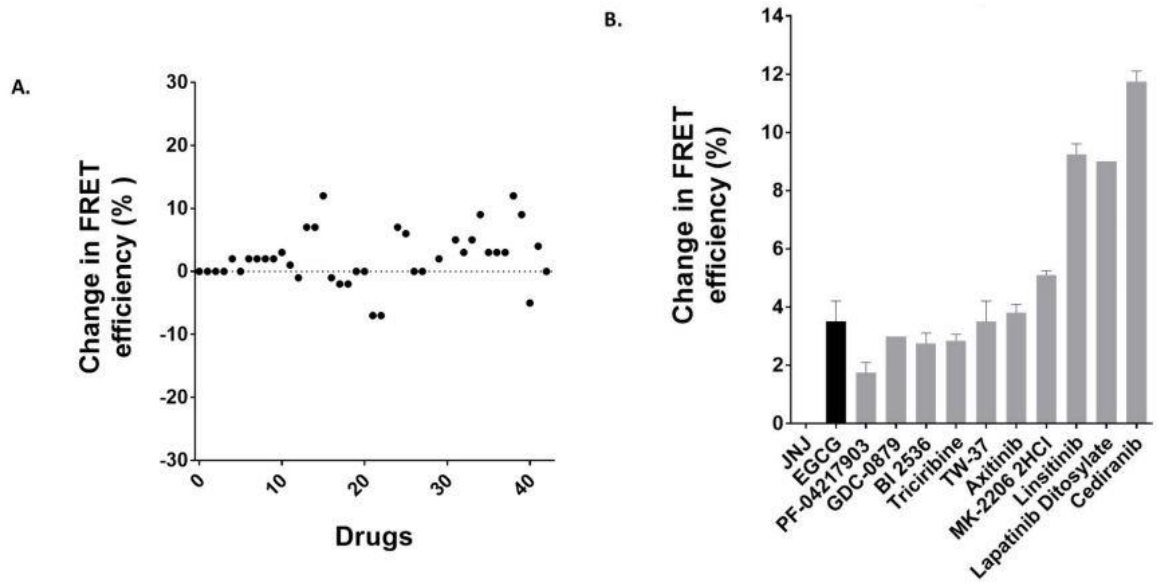

Figure 1.4. A) screening of 40 anticancer drugs with two color GR-881 construct. B) top 10 anti-cancer hits which presented high FRET efficiency. Image used form corresponding author's consent [58].

Membrane vesicles can also be purchased commercially. Variability should be assessed before selecting the commercial vesicles with the help of probe inhibitors and substrates. This technique is suited for compounds with low nonspecific binding and low permeability. Compounds with high nonspecific binding and high permeability might give false results. Additionally, precaution should be taken to prepare the vesicles because the protocols are technically complicated and time consuming.

1.7.1.2. ATPase assay

ABC transporters export compounds out of cells with the help of ATP hydrolysis [62]. Therefore, ATPase activity has been utilized to evaluate the interaction between transporter proteins and substrates/inhibitors. By trapping the ABC transporter with vanadate, the

experiment is performed to determine the substrate and inhibitors. The sensitivity of vanadate changes due to the presence of substrates and modulators. When ATP hydrolysis occurs, inorganic phosphate is released. Using a simple colorimetric method, the amount can be calculated. The amount of the released is correlated with the efflux activity of the transporter proteins. Those compounds which are substrates of can stimulate the ATPase activity of the transporters. This can be quantified by determining the high amount of Pi (phosphates) released in the reaction medium. To determine the ATPase inhibitory activity, probe substrates and inhibitors are used [63–66]. Besides the Pi quantification strategy, there are other approaches to detect the unmetabolized the ATP. These are luminescence-based using luciferase. This strategy is an alternative to the direct ATPase assay. Low intensity corresponds to high ATP consumption and high intensity indicates low ATP consumption. If the amount of unmetabolized ATP is high, it can be correlated with low release of Pi in the ATPase assay. On the other hand, inhibitors of ABC transporters show high amount of unmetabolized ATP and low release of Pi. This assay also helps us to perform and analyze kinetic experiments related to substrates and modulators [67,68].

Though the assays are simple to perform, it is not always easy to differentiate between substrate and modulator because of high cell variability. Compounds might stimulate or inhibit the transport activity at high or low concentrations. Sometimes the lipids and endogenous components of membrane become vanadate sensitive and interfere with signal. Sometimes compounds do not interact directly with the ABC transporters and as a result produce a false result.

1.7.1.3. Photoaffinity Labeling Assays

These assays have been used to determine the binding of substrates and modulators to the ABC transporters. To evaluate the binding affinity and binding sites, the transporter proteins or the membranes expressed by these proteins are incubated with specific radiolabeled compounds. These samples are then irradiated with strong UV radiation and separated by sodium dodecyl sulphate gel electrophoresis. Using autoradiography, the radiolabeled proteins are visualized [69]

There is another way to assess the substrate-transporter binding interaction. This is nucleotide trapping. A radiolabeled ATP known as 8-azido-ATP is used to analyze the transient cycle during the ATP hydrolysis. This method was applied at first for P glycoprotein. In this technology under normal condition, radiolabeled ATP binds to ABC transporter. This is quantified and visualized by size fractionation and autoradiography. Normally the ATP hydrolysis occurs rapidly. Here phosphate mimicking vanadate is used, and it stabilizes the transition state by trapping the nucleotide agent in the nucleotide binding domain. The greater is the formation of transition state, the greater is the rate of transport of substrate [70–73].

The protocols to perform both techniques are complicated and not easy to use. Moreover, these are not a preferable routine screening to distinguish between substrate and modulators.

1.7.1.4. Monoclonal antibody (MAB) strategy to react with cell surface transporters and inhibition of the activity

Specialized MABs are used to tag the extracellular epitope of ABC transporters. Among all ABC transporters, MDR1 was first targeted, and function of the protein was modified.

MABs namely MRK16 and MRK17 were generated successfully to treat specific ABC transporter. MRK16 showed activity in modulating the transport of vincristine. Moreover, it also inhibited the growth of human MDR-expressing cells in tumor xenocraft model. Another monoclonal antibody was developed by a research group which is known as UIC2. UIC2 inhibited the efflux activity of MDR1 substrates. In addition, it increased the cytotoxicity of substrate compounds of the protein. It was found that the antibody interacts with the MDR in its transition state. It can block the function of the MDR1 in transient state [74–77].

Antibody-mediated inhibition of human ABC transporter has potential clinical application. But there is no specific information about how the MABs interact with the transporters. Recently, scientists mapped the epitopes of P-gp-specific monoclonal antibodies MRK-16, UIC2 and 4E3 to understand how these agents interact with the extracellular loops 1 and 4 of the p-glycoprotein. Their findings demonstrate that, the discontinuous epitopes of these antibodies are located in the same region of the two loops (ECL) of P-gp [78].

1.7.1.5. Cytotoxicity assays

Cytotoxicity assays are used as markers of substrates or modulators of the ABC transporters. With the help of IC_{50} values it is possible to distinguish between substrates and inhibitors. For the substrate, the IC_{50} value (concentration inhibits cell growth by 50 %) of wild-type cell will be less than the IC_{50} value of overexpressed cells. The inhibitor will increase or decrease the IC_{50} values of the probe substrates in overexpressed cell line. The resistance-reversal agents show its activity by fold resistance [79–83].

Table 1.1. The effects of selected MRP1 inhibitors on the IC_{50} values of vincristine in H69 and H69AR cells.

Cells/Treatment	IC_{50}[a] (nM)	Fold resistance[b]
H69	0.5 ± 0.2	1.0
H69AR	23.1 ± 3.0	45.5
H69AR + MK571 10 μM	9.8 ± 0.4	19.4
H69AR + Tipifarnib 1 μM	6.4 ± 0.3	12.7
H69AR + AZD1208 2 μM	11.4 ± 0.7	22.6
H69AR + Rapamycin 10 μM	4.0 ± 0.9	7.8
H69AR + Deforolimus 10 μ	8.7 ± 1.1	17.1
H69AR + Everolimus 10 μM	6.6 ± 1.9	13.1
H69AR + TAK-733 10 μM	5.5 ± 0.5	10.8
H69AR + Temsirolimus 10 μM	9.0 ± 0.6	17.7

[a]Mean ± SEM of n ≥ 3 independent experiments.
[b]Fold resistance is the ratio between IC_{50} value of each drug and IC_{50} value of vincristine alone in H69 cells (0.5 ± 0.2). Table was collected following the permission of the author.

From the above Table 1.1 we can see that parenteral H69 shows good sensitivity towards vincristine. That is why the IC_{50} and fold resistance values are very low. In case of H69 AR cells both values are higher than the control cells because the cells are overexpressed MRP1 proteins. It kicks out most of the drugs from inside. TAK-733 and rapamycin reduce the resistance to around 10-fold. This result indicates the ability of these drugs to reverse the resistance of MRP1 overexpressed cell line. These agents might be potent inhibitors. If any agent works as a substrate, it will not potentiate the fold resistance in the treated overexpressed cell lines. The inhibitors might contribute to reduction of the poor clinical outcome of the chemotherapeutic agent which is related to the cancer chemotherapy [54].

The MTT assay is a widely accepted protocol to conduct cell viability and toxicity. There is another method to determine the cytotoxicity which is LDH assay. In MTT assay, metabolically active cells convert MTT salt to formazan. Solubilizing agent is used to dissolve the crystal and the amount in colored solution is quantified. LDH is another type of coulometric assay. This assay works on the principle that lactate dehydrogenase is released by the damaged plasma membrane [84]. Both assays are flexible and convenient. However, one study found that MTT interacts with efflux activity of p-glycoprotein and if the tested compound is substrate then it might give erroneous results [85].

1.7.1.6. Western blot analysis and qPCR

To check the overexpression of ABC transporter proteins, an immunoblotting technique is applied. This technique helps to confirm and select the proper cell line which shows overexpression of specific transporter proteins. Moreover, the techniques confirm whether the inhibitor inhibits the expression of protein or not. If the expression is low in the presence of any inhibitor it means the drug not only inhibits efflux mechanism but also reduces the expression. To perform this experiment the protein concentration is determined. After that, following protein gel electrophoresis and membrane blocking, the samples are then incubated overnight with primary and secondary antibody. Chemiluminescence agent is used to detect the target protein. Proper normalization is necessary for densitometry data generated from the experiment and to main the quality control standard [86–90].

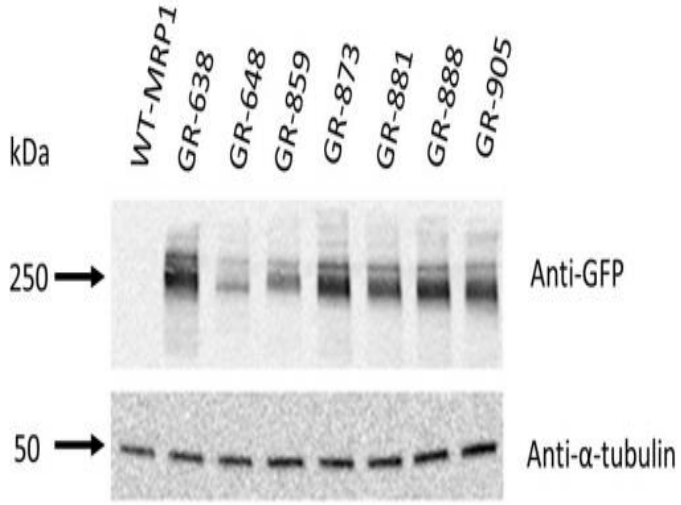

Figure 1.5. Expression of different two color MRP1 and WT MRP1. Picture collected with author permission. Rabbit polyclonal anti-GFP antibody and mouse monoclonal anti-α tubulin were used for the detection [58].

Iram et al carried out the western blot experiment to assess the overexpression of different constructs of two color MRP1. From the Figure 1.5 it can be concluded that wild type MRP1 was not expressed as expected but GR-881, GR-905, GR-638, and GR-888 demonstrated high expression using anti GFP antibody. Based on the high expression the researcher selected the constructs for further step [58].

Quantitative PCR is utilized by researchers to detect the specific gene expression. This technique is a common detection and quantification technique in the field of molecular biology. From a single cell it can quantify from small to large amount of mRNA. In addition to standard process, it adds the use of fluorescent dye and fluorometer. Normally SYBR Green fluorescent dye is used for this protocol. This dye binds to the double stranded DNA. PCR amplification and accumulation depend on parameters of cycle threshold. In the time of PCR reaction, between the forward and reverse primers, annealing of the probe takes place. During the reaction, primer extension and replication happens. After every cycle, the more is the amount of probe cleavage, the higher is the fluorescence intensity [89].

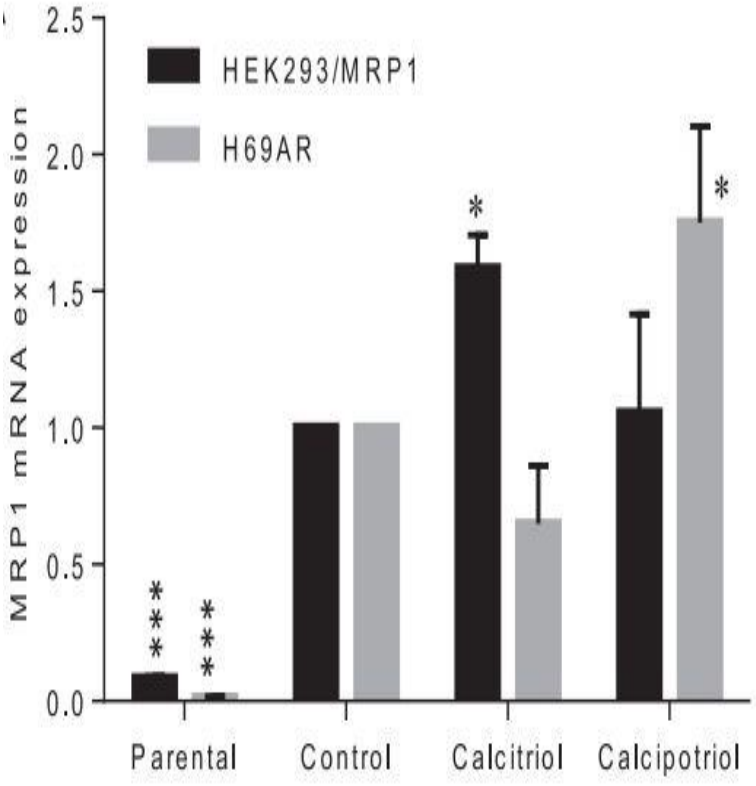

Figure 1.6. Effect of calcitriol and calcipotriol on the mRNA expression of MRP1 protein. Image used with the permission from the corresponding author. Results are presented as presented as mean S.E.M (n=3). where *P < 0.05; ***P < 0.001 when compared against control [56].

Tan et al performed qPCR analysis to assess the modulatory activity of calcitriol and caclipotriol on the transport activity of MRP1. Both drugs significantly reduced the mRNA overexpression index when compared with control [56].

There is another approach which is known as FRET-based approach. Here one dye works as donor sye and another dye works as an acceptor. In close proximity donor side emits energy to excite the acceptor side. Finally, both sides emit fluorescence of different wavelength and the fluorometer signal is monitored. Recently Iram et al generated two color MRP1 construct using pTagRFP-N vector as primary backbone by using QPCR technique. For example, to construct GR-638, C terminal 2.6-kb fragment of MRP1 (encodes amino acid sequence 639–1531 as stop codon) was generated using PCR. He

generated the following forward and reverse primers: 5’ GTA CCG CGG GGG GGC ACG AAC AGC ATC ACC G 3’(forward) and 5’ GTA ACC GGT CT CAC CAA GCC GGC GTC TTT GGC CAT G 3’(reverse). In the second step, cloning size of 0.7-kb insert fragment was used to code for GFP. Forward primer 5’ GTA GTC GAC ATG GTG AGCAAG GGC GAG GAG 3’ and reverse primer 5’ GTA GTC GAC ATG GTG AGCAAG GGC GAG GAG 3’ were used to amplify GFP code. In the final step, N terminal 2 Kb fragment of MRP1 (represents amino acid sequence 1-638) was amplified using the forward primer, 5’ GTA GAG CTC ATG GCG CTC CGG GGC TTC TGC AG 3’ and reverse primer 5’ CTA GTC GAC GCC GTC TTT GAC AGG CCG TCG CTC 3’. All the inserts were incorporated into the background frame to create the main construct. After that both N and C terminals were separated by inserting valine–aspartate and proline–arginine amino acid linkers. After removing the stop codon of MRP1 the C terminal end of the sequence was ligated to the backbone. There were five amino acids —threonine, glycine, leucine, alanine, and threonine incorporated in between these two segments. The efficiency of the two-color construct was evaluated using FRET efficiency [58].

1.7.1.7. *In silico* analysis

Nowadays, different computational methods are used to predict the interaction between ABC transporters and substrate. From molecular docking to machine learning algorithms, scientists are utilizing all possible modeling approaches. Several published pharmacophore models are available for ABCB1, ABCC1 and ABCG2. Pharmacophore models highlight receptor and protein interaction with hydrophobic and hydrophilic features. However, due to overlapping substrate specificity, multiple pharmacophore models pave the way to overcome the limitation of traditional pharmacophore models [91,92]. Li et al presented

this approach recently for ABCB1 [93]. The extension of this protocol might also show promising results for other ABC transporters. Pharmacophore-based QSAR models consider physicochemical properties of both drug and receptor. It helps the researcher cancel out unwanted drug receptor interaction for designing better inhibitor. Scientists are constantly trying different modeling approaches to distinguish between substrate and inhibitors. Scientist mainly look at the physiochemical properties, especially hydrogen and hydrophobic bonding interactions between the binding pocket of the ABC transporter and substrates. Other parameters to be considered are molar mass, logP, surface electron geometry, free energy change , HOMO-LUMO, and pharmacokinetic parameters (absorption, distribution, metabolism, excretion and toxicity) [91,94,95].

Though the ABC transporters have long amino acid chains, full and high-resolution structures are available online in the RCSB protein databank. The structures are available both in substrate bound and apo form. 5UJ9 is the Cryo-EM structure of bovine ABCC1 and 5UJA is the structure of same MRP1 bound to LTC4, a substrate of MRP1. This is the crystal structure nucleotide binding domain 1 of human MRP1. For small structures it is easy to perform crystallization with very high resolution. 3G5U is the crystal structure available in the data bank for P glycoprotein. For the full structures mentioned here, the resolutions are above 3 Å. Other ABC transporter PDB files are also available in the databank. Crystal structure helps to figure out binding site and amino acids participating in the binding interaction. These features help to proceed further for molecular docking and molecular modeling analysis to design novel inhibitors and assess substrate-ABC transporter interaction [24,96,97] .

1.7.1.8. *Ex vivo* assays

ABC transporters (Pgp, MRP1 and BCRP) are expressed mainly in the liver, kidney, intestine, and brain. For example, P glycoprotein is found in intestinal mucosa. It has great influence on absorption of different small molecules in the intestine. *Ex vivo* methods are followed because it is effective to assess the transport activity using specific animal organs. The organ is then kept in a specialized chamber and normal biological environment of the body is maintained in the chamber. After the experiment, the fluid of the chamber bath is collected for measurement of substrate concentration [98–101].

Shukla et al studied the effect of curcumin on ABCG2, which was expressed in rat brain capillary. The author found that curcumin inhibited and increased the bioavailability and Cmax of sulfasalazine, a substrate of ABCG2. For the experiment, brains of rats were decapitated and then collected the capillary for assessing the inhibitory effect [100]. Parasrampura et al investigated the activity of some Pgp inhibitors on the function of P-gp. To conduct the experiment, at first peripheral blood mononuclear cells were isolated from buffy coat and then washed with buffer. The cells were then incubated with rhodamine 123 in the presence of inhibitors. The buffer containing the fluorescence was collected and measured. In this experiment cyclosporin showed very good inhibitory activity [99]. Ballent et al reported the interaction between ABC transporters and anthelmintic drugs. The study was performed by isolating rat intestine and adjusting it in using diffusion chamber. Ivermectin significantly reduced Rho 123 efflux activity [98]. In another study Verstraelen et al compared overexpression of MDR1, BCRP and MRP3 between *ex vivo* models, rabbit and porcine corneas and human cornea cells. Here, the rabbit cornea model confirmed overexpression of MDR1. Overexpression was confirmed using immunoblot,

PCR and bidirectional transport using specific probe substrates and inhibitors of the specific proteins [101].

1.7.2. *In vivo* assay

In vivo animal models are utilized to perform the ABC transporter activity for substrates and modulators. *In vivo* animal model study in the final step in confirming whether the test compound is a substrate or modulator or both and to clear picture about the pharmacokinetics of the substrates and modulators. Scientists prefer the gene knockout mouse model with wild type mice to understand the effect of the ABC transporter. To generate the gene knockout model, the target gene of the ABC transporters is silenced using gene editing tools. Sometimes naturally occurring mutations are also common for ABC transporters. Until now, natural mutants of P glycoprotein and MRP2 have been detected in mice and dogs. MDR1a and MDR1b knockout mouse models were found to be effective in evaluating the brain uptake and ADME parameters and toxicity profile of Pgp substrates cyclosporin A, vinblastine, toperamide, donepezil, and digoxin [102–106]. To perform this assay the target vector was constructed and cloned from 129 CCE-derived stem cells. The mouse model was generated by injecting in the blastocysts followed by reimplantation. Clinical hematology parameters were monitored and Pgp content analysis was done using monoclonal antibody. For the pharmacokinetic analysis, drugs were injected into the tail vein. After certain time brain, liver, and intestine were collected radioactivity of [^{3}H] digoxin was measured using liquid scintillation counting and HPLC was used to quantify paclitaxel. A research group generated MRP1 knockout mice gene editing in the embryonic stem cells to observe if there is increased accumulation of cerebro spinal fluid (CSF) etoposide in the absence of MRP1. The study has huge impact on assessing

pharmacokinetic and distribution of etoposide through blood brain barrier [107]. Another research group found that MRP1 inhibitor reversan increases the chemotherapeutic index of vincristine, etoposide, doxorubicin in neuroblastoma mouse model. The author deleted the MRP1 gene in the neuroblastoma cells and then injected into the mouse flanks for the *in vivo* experiment. After that the mice were set for further drug treatment [108]. In addition, BCRP1 knockout mouse model was found to be effective in assessing the BCRP1 mediated efflux of sulfasalazine and nitrofurantoin [100,109].

In order to test the efficacy of substrates or modulators it is imperative to conduct in vivo experiments. But precaution should be maintained while selecting transgenic animal models. Deletion of ABC transporter associated gene might upregulate or downregulate the expression of other ABC transporter proteins and enzymes. Moreover, interspecies difference among the ABC transporters should be taken into consideration when extrapolating data from animals to human trial.

Table 1.2. General flow chart for detecting and quantifying the transported substrate and modulators of ABC transporters.

Selection of test compounds, probe substrates, probe inhibitors and suitable cell line overexpressing the specific ABC transporters. HEK, H69, MDCK, and CACO-2 cell lines are commonly used worldwide.

Optimization and validation of membrane vesicle based transport study to get initial idea of the transport efficiency of the specific ABC transporters and then proceed to cell-based accumulation and efflux assay to see whether the drugs really work as substrate/modulator in the live cell system. It helps to set acceptable parameters to analyze the outcome.

Measurement of the transported fluorescence or radiolabeled substrates using flow cytometry and liquid scintillation counting. The inhibitory or inducing activity of the test compound is assessed. This is possible to figure out from the amount of transported substrates. To directly measure the quantity, LCMSMS, HPLC-MS or HPLC-UV-based analytical protocols are applied.

Further validation of the property of the compounds as substrate and or modulator using MTT reversal assay, FRET based approach, in vivo animal models, ex vivo model, and in silico molecular modeling analysis (molecular docking algorithm figures out binding affinity and molecular dynamics check the stability of the drug molecule in the binding site).

Table 1.3. A short list of substrates and modulators of all types of ABC transporters [34,47,54,62,110–129].

ABC transporter	Distribution	Substrate	Modulator
P glycoprotein	Highly expressed in intestine and cancer cells. Expression also observed in kidney, brain, testes, overy, placenta	Vincristine, vinblastine, doxorubicin, daunorubicine, methotrexate, mitoxanthrone, etoposide, docetaxel, paclitaxel, verapamil, amiodarone, rifampin, tetracycline,levofloxacin, ritonavir, amprenavir, indinavir, losartan, diltiazem, prazosin, erythromycin, cyclosporine A, sirolimus, amitryptiline, fluoxetine, morphine, loperamide, phenytoin, phenobarbital, tandutinib, nilotinib, imatinib mesylate, hydrocortisone, corticosterone, theaflavin, quercetin, rutin, tamarixetin	Verapamil, cyclosporin A, valspodar, dexverapamil, biricodar, quercetin, baicalein, tariquidar, laniquidar, annamycin, trifluoperazine, biricodar, dexniguldipine, cycleanin, camptothecin, ergotamine, harmine, piperine, epigallocatechin gallate, kaempferol, myricetin, avermectin, amiodarone, avermectin, capsaicin, piperine, EGCG, curcumin, tannic acid, nelfinavir,
MRP1	Highly expressed in kidney, testis, lung, placenta, heart and cancer cells. Moderately expressed in brain, small	doxorubicin, daunorubicin, vinblastine, vincristine, etoposide, paclitaxel, methotrexate, estradiol-17-β-D-glucuronide, LTC4, difloxacin, grepafloxacin, sn-3, imatinib, gefitinib,	MK571, cyclosporin A LTC4, verapamil, genistein, indomethacin, glibenclamide, probenecid, rifampicin, dexamethasone,

	intestine, colon, and peripheral blood mononuclear cells	ciprofloxacin, cyclophosphamide, calcein-AM, benzylpenicillin	quercetin, rapamycin, AZD1208, tipifarnib, rapamycin, everolimus , deforolimus, , temsirolimus, TAK-733, afatinib, celecoxib, doramapimod, mifepristone, MK-2206, rosiglitazone, calcitriol, calcipotriol
MRP2-MRP9	Low level in brian, kidney, prostate, liver and placenta, overy, testes	lopinavir, olmesartan, anthracyclines, cisplatin, etoposide, methotrexate, vincristine, topotecan, mercaptopurine, glutathione. doxorubicin, daunorubicin, E217G, LTC4, LTD4,LTE4, cascade blue, pyranine and sulforhodamine 101, paracetamol glutathione, cysteine conjugates, paclitaxel, tenofovir disoproxil, alectinib	methotrexate, mk-571, etoposide, celecoxib, probenecid, diclofenac, indomethacin, sulfinpyrazone, rofecoxib, furosemide, spironolactone, leflunomide, curcumin, glucuronide, ibrutinib, tariquidar, sodium butyrate
BCRP	Highly expressed in liver, brain, placenta, small intestine, and cancer cells	methotrexate, sulphasalazine, estrone 3-sulphate, hematoporphyrin, E217βG, uric acid, SN-38, prazosin, pheophobide A,	fumitremorgin C, Ko143, GF120918, ritonavir, nelfinavir, biochanin A, chrysin, gefitinib, imatinib,

		nitrofurantoin, imatinib, gefitinib, genistein, mitoxantrone, 2-amino-1-methyl-6-phenylimidazo [4,5-b] pyridine, quercetin, (rosuvastatin, rosuvastatin, simvastatin, zidovudine, lamivudine, topotecan, rosuvastatin, tariquidar	cyclosporin A, novobiocin, quercetin, oxotremorine, phenobarbita, etoposide, phenobarbital, rifampicin, omeprazole, resveratrol

List of substrates and modulators for the P-glycoprotein, MRP1 and BCRP

1.8. Therapeutic deep eutectic solvent

Over the past decade ionic liquids have emerged potential solvent system in analytical chemistry. In the field of science and engineering it became widely studied solvent topic. Ionic liquids are prepared from organic salts and their melting points stay below 100°C. Due to their solvency power, non-flammability, low vapor pressure, and thermal stability, they have diverse applications in the fields of biotechnology, pharmaceuticals, environmental science, and medical science. Ionic liquid has been employed in drug discovery and development research to enhance transdermal permeability, solubility of active pharmaceutical ingredients and synthesis of drug candidates. Although it displayed some favorable features, there are limitations because of high cost in synthesis, poor biodegradability, poor biocompatibility, and toxicity to cellular organelles. As an alternative of ILs, DES is emerging as popular and highly promising class of green solvent because of lots of benefits over ILs. DES comprise four subtypes and among these types, class III is the most prominent. To prepare type III DES, the most used and widely accepted HBA is choline chloride. It is mixed with HBD such as urea, ethylene glycol or glycerol in a two or three fold molar ratio. Due to low cost, readily availability, biocompatibility and

simple preparation steps, type III DES turned out to be attractive class among types of deep eutectic solvents. It became an inseparable part in several research fields such as pharmaceuticals, extraction and separation, organic synthesis, nanomaterials, and biomedical sciences.

Deep eutectic solvents are emerging as an attractive solvent due to low toxicity, simple preparation procedure, inexpensive starting material, and biodegradability. It is a mixture of two or more components that results in lowering the melting point of the mixture. Binary mixture is common in the scientific community. It is prepared by mixing one hydrogen bond acceptor (quaternary ammonium salt) and hydrogen bond acceptor following a certain molar ratio. The low melting point of the new solvent is less than the melting points of the pure substance that are used to prepare the DES.

Therapeutic deep eutectic solvents are another emerging practical application of deep eutectic solvent. To form THEDES, active pharmaceutical ingredients (API) are mixed with another component and the mixture is heated to form DES. It enhances the solubility, permeability, and stability of the API. Moreover, THEDES prevents recrystallization of API. API incorporated in THEDES shows promise in topical and transdermal drug delivery. THEDES successfully improved the transdermal permeability of ibuprofen, irtaconaole, propranolol, testosterone and lidocaine [130,131]. The enhanced capacity of transdermal permeation could be attributed to menthol, low melting point of the mixture, and increased solubility in the membrane [131][130]. Lu and coworkers reported that NSAIDs such as acetaminophen, aspirin, ibuprofen, ketoprofen and naproxen are more highly soluble in DES than in water [132]. Silva and coworkers formulated menthol and fatty acid-based THEDES and reported excellent wound healing properties with potential

antibacterial activity [133]. In another article they unraveled the anticancer potential of limomene based deep eutectic solvents prepared with menthol and ibuprofen in different ratios [134]. Recently one research group prepared a eutectic based transdermal delivery system for risperidone. They formulated eutectic solvent of the antipsychotic drug with some fatty acids. Application of the formulation showed enhanced skin permeation and no inflammation to the skin of animal models [135]. Combining THEDES with a biodegradable polymer opens a new window for efficient controlled pharmaceutical drug delivery over long period of time [136]. Aroso et al developed a specialized drug delivery system by impregnating menthol:ibuprofen deep eutectic solvent with starch:poly-ϵ-caprolactone and carried out sustainable delivery of bioactive molecules from the polymer matrix. They found that ibuprofen showed fast release when it is incorporated in as THDES compared to ibuprofen impregnated alone in the polymer matrix [137]. Recently, THDES was advantageous in gelatin-based drug delivery. Mano et al incorporated choline chloride/mandelic acid-based DES in gelatin by electrospinning and reported that the new nanofiber presented excellent dissolving capacity and enhanced oral bioavailability of drug [138]. Several experimental reports are published on THEDES but little work has been done on correlation between experimental studies and computational simulation using molecular dynamics. Solvation of lidocaine in different deep eutectic solvent was explained by intermolecular interaction between lidocaine and other components in DES coupled with the structure of the solvation state [139]. Structural properties of a menthol-based deep eutectic solvent, menthol:acetic acid (1:1), was investigated using experimental and computed IR-VCD analysis, Principal component analysis and cluster state analysis using molecular dynamics and density functional theory at the ωB97XD/6-311G (d,p)

level [140]. In another research work, thermodynamic property analysis, quantum calculation, and hydrogen bonding interaction assessment were performed on nine different choline chloride based DES and it was determined that 1:1 and 1:2 clusters are more energetically favorable and the clusters are stabilized by several hydrogen bonds formed between donor and acceptor molecules [141]. With the help of density functional theory, molecular dynamics, PCA analysis, favorable cluster analysis, and behavior of non-bonding interaction, detailed atomic-level interactive property between HBA and HBD is possible.

1.9. Features of Deep Eutectic Solvent

Introduced by Abbott et al. in 2004, DES became hot topic not only in the field of chemistry, biochemistry, and but also in the fields of pharmaceutical sciences, nutraceutical, and cosmetic sciences. Since the advent of DES, a number of patents is increasing day by day [142,143]. Before use of DES, ionic liquids (IL) were used extensively for manifold applications. Despite manifold applications, extensive use of IL greatly reduced due to high toxicity, poor biodegradability, and costly production steps. For this reason, there is a constant search for new and alternative solvents that will overcome major drawbacks of ILs. DES became the topic of attraction and considered as alternative of IL because of very low toxicity, rapid biodegradability, low volatility, availability of starting materials, formulation stability, non-flammability, and tuneability [142,143]. DES differ from IL in two particular aspects, chemical formulation and source of raw materials [144]. DES are mainly formed by mixing hydrogen bond donor and hydrogen bond acceptor in a certain molar ratio. On the other hand, IL are formulated by mixing two ionic components through formation of ionic bonding. In case of DES, ion-

dipole attractions mainly govern HBA and HBD interaction in DES. Other types of bonding e.g., Van der Waals force, and electrostatic forces occasionally contribute to DES formulation [142,144]. DES is applicable in biomass production process, extraction of plant components, and stabilization of natural pigments. As an ecofriendly green solvent and sustainable catalyst, DES has been utilized in traditional organic synthesis reactions for example, Diels-Alder, Halogenation, Knoevenagel, Henry, Perkin, Paal-Knorr, and Biginelli reactions. There is a class of DES which is known as NADES (Natural Deep Eutectic Solvents). In this type of DES natural compounds, like vitamin or amino acids, are used as DES components. NADES have novel application of DES in the field of physiology [142–144].

Natural compounds are obtained mainly from plants, microorganisms, fungi and algae. Along with primary metabolites, natural compounds play significant roles in body defense mechanisms and nutritional requirements. To extract these compounds several traditional and modern methods are currently followed [142–144]. Different polarities of organic solvents and water are primarily used to extract different categories of natural products. However, several major concerns are associated with currently available protocols. These ambiguous concerns ultimately affect the physicochemical properties and utilities of extracted compounds. There is an urgent need of the use of alternative cheap solvent that will be greener and sustainable than current solvents. From numerous applications it has been proved that DES satisfies most of the criteria to be a suitable alternative solvent in this situation. It significantly improves the extraction yield as well as quality of finished products [142–144].

Recently biotransformations showed noticeable improvement in DES. Two types of biotransformation are commonly used to synthesize metabolites [144,145]. First is harvested enzyme-based biocatalysts and microorganism-based biocatalysts. For high yield and optimum production of metabolites both methods require non aqueous solvent system for high yield. Due to adverse effect, instability of products, product post treatment, and contamination from microbes recently DES emerged as a suitable and highly efficient nonaqueous green solvent system for biotransformation. DES-inspired biocatalysts improved solubility of products, chemical inertness, chemical stability, and efficiency of enzyme. Numerous studies prove the superior efficacy of DES over traditional organic solvents [142,144].

Application of DES in biomacromolecule preservation is evident from recently published literature. For example, preservation of DNA molecules in DES is governed through efficient dissolution by forming hydrogen bonding networks between DES components and phosphate backbone of DNA. Moreover, different structures of DNA, such as triplex and quadruplex, are structurally stable in DES due to distinctive physicochemical properties. Since the last decade there has been considerable improvement observed in nanotechnology. Due to improved diffusion coefficient, surface tension, and viscosity, DES significantly improved assembly of nanoparticles in nanostructure format and facilitates synthesis. Presence of hydrogen bonding, Ostwald ripening, single atom attachment and coalescence might enhance coordination of nanoparticles in nanostructure [146,147].

1.10. Pharmaceutical application of deep eutectic solvent

The number of pharmaceutical solvents is limited, and development of novel solvent became the priority. Solvents play a major role in drug design and delivery to the appropriate site of action. Use of solvent is also applicable in reaction media for synthesis of drug molecules. This section will focus on potential application of DES in the field of drug delivery and drug design [142].

To treat various heath disorders the most important aspect of the drug discovery process is appropriate delivery in the proper location. In this case solubility is a critical issue and it hinders therapeutic activity of drug molecules. Additionally, some drugs suffer from hydrolysis because of long term storage in water medium. Traditionally, organic solvents have been used tremendously to increase drug solubility in water but due to toxicity and other health and environment concerns application of organic solvents are not a viable solution. DES works as a versatile green solvent for increasing solubility of poorly water-soluble drugs [142,144]. Several experimental studies confirm the applicability of DES to increase solubility and delivery of pharmaceutical drugs. Li et al found that solubility of itraconazole, posaconazole, lidocaine, and piroxicam increased significantly in the choline chloride-based DES ChCl:glycolic acid compared to water. The DES ratio was 1:2. Moreover, solubility was also found to be significant in tertiary solvents [148]. According to Morrison et al, solubility of poorly water soluble danazol, griseofulvin, itraconazole, and AMG517 were better in ChCl:urea (1:2) and ChCl:malonic acid (1:1) than water [149]. To formulate therapeutic DES, active pharmaceutical ingredient API is used as one component of DES. As a result, solubility of the API is enhanced at a high rate. Stott et al improved transdermal delivery, solubility and permeability of ibuprofen incorporated in

DES composed of a series of terpene molecules including menthol, menthone, thymol, etc. [131]

Natural deep eutectic solvent showed potential in stabilizing antimicrobial drugs. In a different study it has been reported that DES stabilized the beta lactam ring of two commonly used antibiotics, namely imipenem and clavulanic acid. Beta lactam is highly unstable and prone to degradation due to nucleophilic or electrophilic attack. Deep eutectic solvent composed from betaine:urea in 1:1.5 ratio retained antimicrobial potency of the drugs even after seven days of preservation [150]. On the other hand, storage of the antibiotics in water for consecutive days drastically reduced the potency. In the treatment of antibiotic drug resistance, application of DES is becoming apparent [150]. Antibiotic resistance is emerging as a major health hazard globally. It can occur in any time or any day. Due to overuse and misuse, the problem is accelerating day by day. Existing antimicrobial medication is losing efficacy in treating a growing number of microbial infections for example, tuberculosis, pneumonia, and others. To treat drug-resistant bacteria, scientists are developing new treatment options and antimicrobial photodynamic therapy is one of the options. Recently DES has been introduced in preparing photodynamic therapy to maximize functions of porphyrin molecules. Several disadvantages limit the use of organic solvent to dissolve porphyrin. That is why DES comes in the form of solubilizing agent of porphyrin and acts as photosensitizer compound porphyrin solubilizer [142].

Successful drug delivery remains a hurdle for the pharmaceutical scientists. From oral administration to site action is a long route for drug molecules to reach and exert appropriate mechanism of action. On the way drug molecules undergo degradation due to

multiple physiological factors. To assist in successful drug delivery, nowadays polymer technology evolved as a drug delivery vehicle. Polymerization and micelle formation capacity can encapsulate drug in the inner core of micelle. DES can act as hydrophobic core in the inner moiety of micelle and dissolve hydrophobic drugs. Outer shell of micelle is shaped by polymeric career and thus polymer based micelle carries drugs and take to the desired place by navigating through the internal body environment [151,152].

Application of DES is an interesting topic in improving efficacy of chemotherapeutic agents. DES can improve solubility and delivery of anticancer agents or itself can act as anticancer medication when drug molecules can be incorporated in the solvent system. In addition, DES can facilitate synthesis of novel anticancer agents. Proper analysis of DES mechanism of action should be conducted for designing better chemotherapeutic drugs and rendering the normal cells harmless [153].

The overall dissertation is about establishing bioanalytical chemistry-based methods and therapeutic solvents to enhance therapeutic activity of anticancer drugs and drug like candidates. In this research I explored all available protocols established for detecting interaction between ABC transporters and probable anticancer substrates. In first aim, a novel method to directly detect and quantify probable anticancer substrate chemotherapeutic drugs was designed and developed. To establish the assay MDCK-II MRP1 and its parental cell lines were selected. We exclusively focused on extracellular conc. Instead of measuring intracellular conc. The idea simplifies the outcome of the protocol and makes it easy to follow, directly detectable and reproducible. The novel protocol was confirmed and validated by MTT cell viability assay. In second aim, two

projects were designed and performed to provide substantial evidence regarding physicochemical and biological activities of therapeutic deep eutectic solvent prepared from ethyl gallate and dodecyl gallate. Both molecules have multifaceted therapeutic activities including anticancer properties. Limited water solubility limits desired therapeutic activity of these potential candidates. We conducted several experiential protocols to assess the structural and pharmacological properties of DES. DESs were identified as promising medium for future drug delivery research.

1.11. References

[1] A. Ramos, S. Sadeghi, H. Tabatabaeian, Battling Chemoresistance in Cancer: Root Causes and Strategies to Uproot Them, Int. J. Mol. Sci. . 22 (2021). https://doi.org/10.3390/ijms22179451.

[2] X. Wang, H. Zhang, X. Chen, Drug resistance and combating drug resistance in cancer, Cancer Drug Resist. 2 (2019) 141–160. https://doi.org/10.20517/cdr.2019.10.

[3] S. Murray, E. Briasoulis, H. Linardou, D. Bafaloukos, C. Papadimitriou, Taxane resistance in breast cancer: Mechanisms, predictive biomarkers and circumvention strategies, Cancer Treat. Rev. 38 (2012) 890–903. https://doi.org/https://doi.org/10.1016/j.ctrv.2012.02.011.

[4] C. Vulsteke, A.M. Pfeil, M. Schwenkglenks, R. Pettengell, T.D. Szucs, D. Lambrechts, M. Peeters, P. van Dam, A.S. Dieudonné, S. Hatse, P. Neven, R. Paridaens, H. Wildiers, Impact of genetic variability and treatment-related factors on outcome in early breast cancer patients receiving (neo-) adjuvant chemotherapy with 5-fluorouracil, epirubicin and cyclophosphamide, and docetaxel, Breast Cancer Res. Treat. 147 (2014) 557–570. https://doi.org/10.1007/s10549-014-3105-5.

[5] R. Baskar, K.A. Lee, R. Yeo, K.-W. Yeoh, Cancer and radiation therapy: current advances and future directions., Int. J. Med. Sci. 9 (2012) 193–199. https://doi.org/10.7150/ijms.3635.

[6] B. Mansoori, A. Mohammadi, S. Davudian, S. Shirjang, B. Baradaran, The Different Mechanisms of Cancer Drug Resistance: A Brief Review., Adv. Pharm. Bull. 7 (2017) 339–348. https://doi.org/10.15171/apb.2017.041.

[7] M.M. Gottesman, Mechanisms of cancer drug resistance., Annu. Rev. Med. 53 (2002) 615–627. https://doi.org/10.1146/annurev.med.53.082901.103929.

[8] F.U. Vaidya, A. Sufiyan Chhipa, V. Mishra, V.K. Gupta, S.G. Rawat, A. Kumar, C. Pathak, Molecular and cellular paradigms of multidrug resistance in cancer., Cancer Reports (Hoboken, N.J.). (2020) e1291. https://doi.org/10.1002/cnr2.1291.

[9] K.M. Giacomini, S.-M. Huang, D.J. Tweedie, L.Z. Benet, K.L.R. Brouwer, X. Chu, A. Dahlin, R. Evers, V. Fischer, K.M. Hillgren, K.A. Hoffmaster, T. Ishikawa, D. Keppler, R.B. Kim, C.A. Lee, M. Niemi, J.W. Polli, Y. Sugiyama, P.W. Swaan, J.A. Ware, S.H. Wright, S.W. Yee, M.J. Zamek-Gliszczynski, L. Zhang, Membrane transporters in drug development., Nat. Rev. Drug Discov. 9 (2010) 215–236. https://doi.org/10.1038/nrd3028.

[10] B. Feng, M. V Varma, C. Costales, H. Zhang, L. Tremaine, In vitro and in vivo approaches to characterize transporter-mediated disposition in drug discovery, Expert Opin. Drug Discov. 9 (2014) 873–890. https://doi.org/10.1517/17460441.2014.922540.

[11] R.H. Ho, R.B. Kim, Transporters and drug therapy: implications for drug disposition and disease., Clin. Pharmacol. Ther. 78 (2005) 260–277. https://doi.org/10.1016/j.clpt.2005.05.011.

[12] D.A. Volpe, Transporter assays as useful in vitro tools in drug discovery and development, Expert Opin. Drug Discov. 11 (2016) 91—103. https://doi.org/10.1517/17460441.2016.1101064.

[13] J. König, F. Müller, M.F. Fromm, Transporters and drug-drug interactions: important determinants of drug disposition and effects., Pharmacol. Rev. 65 (2013) 944–966. https://doi.org/10.1124/pr.113.007518.

[14] M.K. DeGorter, C.Q. Xia, J.J. Yang, R.B. Kim, Drug transporters in drug efficacy and toxicity., Annu. Rev. Pharmacol. Toxicol. 52 (2012) 249–273. https://doi.org/10.1146/annurev-pharmtox-010611-134529.

[15] B. Döring, E. Petzinger, Phase 0 and phase III transport in various organs: combined concept of phases in xenobiotic transport and metabolism., Drug Metab. Rev. 46 (2014) 261–282. https://doi.org/10.3109/03602532.2014.882353.

[16] P. Borst, R.O. Elferink, Mammalian ABC transporters in health and disease., Annu. Rev. Biochem. 71 (2002) 537–592. https://doi.org/10.1146/annurev.biochem.71.102301.093055.

[17] M. Dean, T. Fojo, S. Bates, Tumour stem cells and drug resistance., Nat. Rev. Cancer. 5 (2005) 275–284. https://doi.org/10.1038/nrc1590.

[18] G. Szakács, A. Váradi, C. Özvegy-Laczka, B. Sarkadi, The role of ABC transporters in drug absorption, distribution, metabolism, excretion and toxicity (ADME–Tox), Drug Discov. Today. 13 (2008) 379–393. https://doi.org/https://doi.org/10.1016/j.drudis.2007.12.010.

[19] B. Sarkadi, L. Homolya, G. Szakács, A. Váradi, Human multidrug resistance ABCB and ABCG transporters: participation in a chemoimmunity defense system., Physiol. Rev. 86 (2006) 1179–1236. https://doi.org/10.1152/physrev.00037.2005.

[20] G. Szakács, J.K. Paterson, J.A. Ludwig, C. Booth-Genthe, M.M. Gottesman, Targeting multidrug resistance in cancer., Nat. Rev. Drug Discov. 5 (2006) 219–234. https://doi.org/10.1038/nrd1984.

[21] K.J. Linton, Structure and Function of ABC Transporters, Physiology. 22 (2007) 122–130. https://doi.org/10.1152/physiol.00046.2006.

[22] R.B. Kim, Drugs as P-glycoprotein substrates, inhibitors, and inducers, Drug Metab. Rev. 34 (2002) 47–54. https://doi.org/10.1081/DMR-120001389.

[23] F.J. Sharom, ABC multidrug transporters: structure, function and role in chemoresistance., Pharmacogenomics. 9 (2008) 105–127. https://doi.org/10.2217/14622416.9.1.105.

[24] S.G. Aller, J. Yu, A. Ward, Y. Weng, S. Chittaboina, R. Zhuo, P.M. Harrell, Y.T.

Trinh, Q. Zhang, I.L. Urbatsch, G. Chang, Structure of P-glycoprotein reveals a molecular basis for poly-specific drug binding., Science. 323 (2009) 1718–1722. https://doi.org/10.1126/science.1168750.

[25] L. Mora Lagares, N. Minovski, M. Novič, Multiclass Classifier for P-Glycoprotein Substrates, Inhibitors, and Non-Active Compounds, Molecules. 24 (2019) 2006. https://doi.org/10.3390/molecules24102006.

[26] T.D. Lee, O.W. Lee, K.R. Brimacombe, L. Chen, R. Guha, S. Lusvarghi, B.G. Tebase, C. Klumpp-Thomas, R.W. Robey, S. V Ambudkar, M. Shen, M.M. Gottesman, M.D. Hall, A High-Throughput Screen of a Library of Therapeutics Identifies Cytotoxic Substrates of P-glycoprotein., Mol. Pharmacol. 96 (2019) 629–640. https://doi.org/10.1124/mol.119.115964.

[27] D.C. Wolf, S.B. Horwitz, P-glycoprotein transports corticosterone and is photoaffinity-labeled by the steroid., Int. J. Cancer. 52 (1992) 141–146. https://doi.org/10.1002/ijc.2910520125.

[28] Y. Liu, L. Huang, T. Hoffman, M. Gosland, M. Vore, MDR1 substrates/modulators protect against beta-estradiol-17beta-D-glucuronide cholestasis in rat liver., Cancer Res. 56 (1996) 4992–4997.

[29] F.J. Sharom, The P-glycoprotein multidrug transporter, Essays Biochem. 50 (2011) 161–178. https://doi.org/10.1042/bse0500161.

[30] R.P. Oude Elferink, J. Zadina, MDR1 P-glycoprotein transports endogenous opioid peptides., Peptides. 22 (2001) 2015–2020. https://doi.org/10.1016/s0196-9781(01)00564-2.

[31] S.P.C. Cole, Multidrug resistance protein 1 (MRP1, ABCC1), a "multitasking" ATP-binding cassette (ABC) transporter, J. Biol. Chem. 289 (2014) 30880–30888. https://doi.org/10.1074/jbc.R114.609248.

[32] J. Yin, J. Zhang, Multidrug resistance-associated protein 1 (MRP1/ABCC1) polymorphism: from discovery to clinical application, Zhong Nan Da Xue Xue Bao. Yi Xue Ban. 36 (2011) 927–938. https://doi.org/10.3969/j.issn.1672-7347.2011.10.002.

[33] J.F. Lu, D. Pokharel, M. Bebawy, MRP1 and its role in anticancer drug resistance, Drug Metab. Rev. 47 (2015) 406–419. https://doi.org/10.3109/03602532.2015.1105253.

[34] Z. Ni, Z. Bikadi, M.F. Rosenberg, Q. Mao, Structure and function of the human breast cancer resistance protein (BCRP/ABCG2)., Curr. Drug Metab. 11 (2010) 603–617. https://doi.org/10.2174/138920010792927325.

[35] F. Staud, P. Pavek, Breast cancer resistance protein (BCRP/ABCG2)., Int. J. Biochem. Cell Biol. 37 (2005) 720–725. https://doi.org/10.1016/j.biocel.2004.11.004.

[36] A.H. Schinkel, Functions of the ABC transporter breast cancer resistance protein (BCRP/ABCG2), Cancer Res. 65 (2005) 1475 LP – 1476.

http://cancerres.aacrjournals.org/content/65/9_Supplement/1475.6.abstract.

[37] L.D. Cripe, H. Uno, E.M. Paietta, M.R. Litzow, R.P. Ketterling, J.M. Bennett, J.M. Rowe, H.M. Lazarus, S. Luger, M.S. Tallman, Zosuquidar, a novel modulator of P-glycoprotein, does not improve the outcome of older patients with newly diagnosed acute myeloid leukemia: a randomized, placebo-controlled trial of the Eastern Cooperative Oncology Group 3999., Blood. 116 (2010) 4077–4085. https://doi.org/10.1182/blood-2010-04-277269.

[38] R.J. Kelly, D. Draper, C.C. Chen, R.W. Robey, W.D. Figg, R.L. Piekarz, X. Chen, E.R. Gardner, F.M. Balis, A.M. Venkatesan, S.M. Steinberg, T. Fojo, S.E. Bates, A pharmacodynamic study of docetaxel in combination with the P-glycoprotein antagonist tariquidar (XR9576) in patients with lung, ovarian, and cervical cancer., Clin. Cancer Res. 17 (2011) 569–580. https://doi.org/10.1158/1078-0432.CCR-10-1725.

[39] S. Shukla, C.-P. Wu, S. V Ambudkar, Development of inhibitors of ATP-binding cassette drug transporters – present status and challenges, Expert Opin. Drug Metab. Toxicol. 4 (2008) 205–223. https://doi.org/10.1517/17425255.4.2.205.

[40] T.H. Lippert, H.-J. Ruoff, M. Volm, Current status of methods to assess cancer drug resistance., Int. J. Med. Sci. 8 (2011) 245–253. https://doi.org/10.7150/ijms.8.245.

[41] A.Z. Wang, R. Langer, O.C. Farokhzad, Nanoparticle delivery of cancer drugs., Annu. Rev. Med. 63 (2012) 185–198. https://doi.org/10.1146/annurev-med-040210-162544.

[42] W.P. Peters, G.L. Rosner, J.J. Vredenburgh, E.J. Shpall, M. Crump, P.G. Richardson, M.W. Schuster, L.B. Marks, C. Cirrincione, L. Norton, I.C. Henderson, R.L. Schilsky, D.D. Hurd, Prospective, Randomized Comparison of High-Dose Chemotherapy With Stem-Cell Support Versus Intermediate-Dose Chemotherapy After Surgery and Adjuvant Chemotherapy in Women With High-Risk Primary Breast Cancer: A Report of CALGB 9082, SWOG 9114, and NCIC MA, J. Clin. Oncol. 23 (2005) 2191–2200. https://doi.org/10.1200/JCO.2005.10.202.

[43] P. Wang, H.L. Yang, Y.J. Yang, L. Wang, S.C. Lee, Overcome Cancer Cell Drug Resistance Using Natural Products, Evidence-Based Complement. Altern. Med. 2015 (2015) 767136. https://doi.org/10.1155/2015/767136.

[44] W.H. Talib, A.R. Alsayed, M. Barakat, M.I. Abu-Taha, A.I. Mahmod, Targeting Drug Chemo-Resistance in Cancer Using Natural Products., Biomedicines. 9 (2021). https://doi.org/10.3390/biomedicines9101353.

[45] D.A. Yardley, Drug Resistance and the Role of Combination Chemotherapy in Improving Patient Outcomes, Int. J. Breast Cancer. 2013 (2013) 137414. https://doi.org/10.1155/2013/137414.

[46] H. Wang, Y. Huang, Combination therapy based on nano codelivery for overcoming cancer drug resistance, Med. Drug Discov. 6 (2020) 100024.

https://doi.org/https://doi.org/10.1016/j.medidd.2020.100024.

[47] A. Sampson, B.G. Peterson, K.W. Tan, S.H. Iram, Doxorubicin as a fluorescent reporter identifies novel MRP1 (ABCC1) inhibitors missed by calcein-based high content screening of anticancer agents., Biomed. Pharmacother. 118 (2019) 109289. https://doi.org/10.1016/j.biopha.2019.109289.

[48] R. Zahra, M. Furqan, R. Ullah, A. Mithani, R.S.Z. Saleem, A. Faisal, A cell-based high-throughput screen identifies inhibitors that overcome P-glycoprotein (Pgp)-mediated multidrug resistance, PLoS One. 15 (2020) e0233993. https://doi.org/10.1371/journal.pone.0233993.

[49] S.M. Samuel, E. Varghese, L. Koklesová, A. Líšková, P. Kubatka, D. Büsselberg, Counteracting Chemoresistance with Metformin in Breast Cancers: Targeting Cancer Stem Cells., Cancers (Basel). 12 (2020). https://doi.org/10.3390/cancers12092482.

[50] V.L. Lew, A. Hockaday, C.J. Freeman, R.M. Bookchin, Mechanism of spontaneous inside-out vesiculation of red cell membranes, J. Cell Biol. 106 (1988) 1893–1901. https://doi.org/10.1083/jcb.106.6.1893.

[51] M. Horio, M.M. Gottesman, I. Pastan, ATP-dependent transport of vinblastine in vesicles from human multidrug-resistant cells, Proc. Natl. Acad. Sci. U. S. A. 85 (1988) 3580–3584. https://doi.org/10.1073/pnas.85.10.3580.

[52] J.E. Karlsson, C. Heddle, A. Rozkov, J. Rotticci-Mulder, O. Tuvesson, C. Hilgendorf, T.B. Andersson, High-activity p-glycoprotein, multidrug resistance protein 2, and breast cancer resistance protein membrane vesicles prepared from transiently transfected human embryonic kidney 293-epstein-barr virus nuclear antigen cells., Drug Metab. Dispos. 38 (2010) 705–714. https://doi.org/10.1124/dmd.109.028886.

[53] V.D. Makhey, A. Guo, D.A. Norris, P. Hu, J. Yan, P.J. Sinko, Characterization of the regional intestinal kinetics of drug efflux in rat and human intestine and in Caco-2 cells., Pharm. Res. 15 (1998) 1160–1167. https://doi.org/10.1023/a:1011971303880.

[54] B.G. Peterson, K.W. Tan, B. Osa-Andrews, S.H. Iram, High-content screening of clinically tested anticancer drugs identifies novel inhibitors of human MRP1 (ABCC1)., Pharmacol. Res. 119 (2017) 313–326. https://doi.org/10.1016/j.phrs.2017.02.024.

[55] S.H. Iram, S.P.C. Cole, Differential functional rescue of Lys(513) and Lys(516) processing mutants of MRP1 (ABCC1) by chemical chaperones reveals different domain-domain interactions of the transporter., Biochim. Biophys. Acta. 1838 (2014) 756–765. https://doi.org/10.1016/j.bbamem.2013.11.002.

[56] K.W. Tan, A. Sampson, B. Osa-Andrews, S.H. Iram, Calcitriol and Calcipotriol Modulate Transport Activity of ABC Transporters and Exhibit Selective Cytotoxicity in MRP1-overexpressing Cells., Drug Metab. Dispos. 46 (2018) 1856–1866. https://doi.org/10.1124/dmd.118.081612.

[57] S.H. Iram, S.J. Gruber, O.N. Raguimova, D.D. Thomas, S.L. Robia, ATP-Binding Cassette Transporter Structure Changes Detected by Intramolecular Fluorescence Energy Transfer for High-Throughput Screening., Mol. Pharmacol. 88 (2015) 84–94. https://doi.org/10.1124/mol.114.096792.

[58] B. Osa-Andrews, K.W. Tan, A. Sampson, S.H. Iram, Development of Novel Intramolecular FRET-Based ABC Transporter Biosensors to Identify New Substrates and Modulators., Pharmaceutics. 10 (2018). https://doi.org/10.3390/pharmaceutics10040186.

[59] D. Cihalova, F. Staud, M. Ceckova, Interactions of cyclin-dependent kinase inhibitors AT-7519, flavopiridol and SNS-032 with ABCB1, ABCG2 and ABCC1 transporters and their potential to overcome multidrug resistance in vitro., Cancer Chemother. Pharmacol. 76 (2015) 105–116. https://doi.org/10.1007/s00280-015-2772-1.

[60] J. Mo, M. Kang, J.-X. Ye, J.-B. Chen, H.-B. Zhang, C. Qing, Gibberellin derivative GA-13315 sensitizes multidrug-resistant cancer cells by antagonizing ABCB1 while agonizes ABCC1., Cancer Chemother. Pharmacol. 78 (2016) 51–61. https://doi.org/10.1007/s00280-016-3051-5.

[61] E. Gozalpour, R. Greupink, A. Bilos, V. Verweij, J.J.M.W. van den Heuvel, R. Masereeuw, F.G.M. Russel, J.B. Koenderink, Convallatoxin: a new P-glycoprotein substrate., Eur. J. Pharmacol. 744 (2014) 18–27. https://doi.org/10.1016/j.ejphar.2014.09.031.

[62] Y.H. Choi, A.-M. Yu, ABC transporters in multidrug resistance and pharmacokinetics, and strategies for drug development., Curr. Pharm. Des. 20 (2014) 793–807. https://doi.org/10.2174/13816128005140214165212.

[63] Q. Mao, E.M. Leslie, R.G. Deeley, S.P. Cole, ATPase activity of purified and reconstituted multidrug resistance protein MRP1 from drug-selected H69AR cells, Biochim. Biophys. Acta. 1461 (1999) 69—82. https://doi.org/10.1016/s0005-2736(99)00150-9.

[64] E.-M. Collnot, C. Baldes, M.F. Wempe, R. Kappl, J. Huttermann, J.A. Hyatt, K.J. Edgar, U.F. Schaefer, C.-M. Lehr, Mechanism of inhibition of P-glycoprotein mediated efflux by vitamin E TPGS: influence on ATPase activity and membrane fluidity., Mol. Pharm. 4 (2007) 465–474. https://doi.org/10.1021/mp060121r.

[65] Z. Fekete, Z. Rajnai, T. Nagy, K.T. Jakab, A. Kurunczi, K. Gemes, K. Heredi-Szabo, F. Fulop, G.K. Toth, M. Czerwinski, G. Loewen, P. Krajcsi, Membrane Assays to Characterize Interaction of Drugs with ABCB1., J. Membr. Biol. 248 (2015) 967–977. https://doi.org/10.1007/s00232-015-9804-y.

[66] Y. Tajima, H. Nakagawa, A. Tamura, O. Kadioglu, K. Satake, Y. Mitani, H. Murase, L.O. Regasini, V. da S. Bolzani, T. Ishikawa, G. Fricker, T. Efferth, Nitensidine A, a guanidine alkaloid from Pterogyne nitens, is a novel substrate for human ABC transporter ABCB1., Phytomedicine. 21 (2014) 323–332. https://doi.org/10.1016/j.phymed.2013.08.024.

[67] Z.-X. Wu, Q.-X. Teng, C.-Y. Cai, J.-Q. Wang, Z.-N. Lei, Y. Yang, Y.-F. Fan, J.-Y. Zhang, J. Li, Z.-S. Chen, Tepotinib reverses ABCB1-mediated multidrug resistance in cancer cells., Biochem. Pharmacol. 166 (2019) 120–127. https://doi.org/10.1016/j.bcp.2019.05.015.

[68] R. Zaja, J. Loncar, M. Popovic, T. Smital, First characterization of fish P-glycoprotein (abcb1) substrate specificity using determinations of its ATPase activity and calcein-AM assay with PLHC-1/dox cell line., Aquat. Toxicol. 103 (2011) 53–62. https://doi.org/10.1016/j.aquatox.2011.02.005.

[69] A. Patel, A.K. Tiwari, E.E. Chufan, K. Sodani, N. Anreddy, S. Singh, S. V Ambudkar, R. Stephani, Z.-S. Chen, PD173074, a selective FGFR inhibitor, reverses ABCB1-mediated drug resistance in cancer cells., Cancer Chemother. Pharmacol. 72 (2013) 189–199. https://doi.org/10.1007/s00280-013-2184-z.

[70] P. Roerig, P. Mayerhofer, A. Holzinger, J. Gartner, Characterization and functional analysis of the nucleotide binding fold in human peroxisomal ATP binding cassette transporters., FEBS Lett. 492 (2001) 66–72. https://doi.org/10.1016/s0014-5793(01)02235-9.

[71] A.C. Hobson, R. Weatherwax, G.F. Ames, ATP-binding sites in the membrane components of histidine permease, a periplasmic transport system., Proc. Natl. Acad. Sci. U. S. A. 81 (1984) 7333–7337. https://doi.org/10.1073/pnas.81.23.7333.

[72] H. Chavan, M.M.T. Khan, G. Tegos, P. Krishnamurthy, Efficient purification and reconstitution of ATP binding cassette transporter B6 (ABCB6) for functional and structural studies., J. Biol. Chem. 288 (2013) 22658–22669. https://doi.org/10.1074/jbc.M113.485284.

[73] S. Shukla, R.W. Robey, S.E. Bates, S. V Ambudkar, The calcium channel blockers, 1,4-dihydropyridines, are substrates of the multidrug resistance-linked ABC drug transporter, ABCG2., Biochemistry. 45 (2006) 8940–8951. https://doi.org/10.1021/bi060552f.

[74] E.B. Mechetner, I.B. Roninson, Efficient inhibition of P-glycoprotein-mediated multidrug resistance with a monoclonal antibody., Proc. Natl. Acad. Sci. U. S. A. 89 (1992) 5824–5828. https://doi.org/10.1073/pnas.89.13.5824.

[75] H. Hamada, T. Tsuruo, Functional role for the 170- to 180-kDa glycoprotein specific to drug-resistant tumor cells as revealed by monoclonal antibodies., Proc. Natl. Acad. Sci. U. S. A. 83 (1986) 7785–7789. https://doi.org/10.1073/pnas.83.20.7785.

[76] E. Okochi, T. Iwahashi, T. Tsuruo, Monoclonal antibodies specific for P-glycoprotein., Leukemia. 11 (1997) 1119–1123. https://doi.org/10.1038/sj.leu.2400658.

[77] Y. Heike, T. Tsuruo, Antibodies in the study of multiple drug resistance., Cytotechnology. 12 (1993) 91–107. https://doi.org/10.1007/BF00744659.

[78] S. Vahedi, S. Lusvarghi, K. Pluchino, Y. Shafrir, S.R. Durell, M.M. Gottesman, S.

V Ambudkar, Mapping discontinuous epitopes for MRK-16, UIC2 and 4E3 antibodies to extracellular loops 1 and 4 of human P-glycoprotein, Sci. Rep. 8 (2018) 12716. https://doi.org/10.1038/s41598-018-30984-8.

[79] Z. Zhang, N. Guan, T. Li, D.E. Mais, M. Wang, Quality control of cell-based high-throughput drug screening, Acta Pharm. Sin. B. 2 (2012) 429–438. https://doi.org/https://doi.org/10.1016/j.apsb.2012.03.006.

[80] J.L. Gordon, M.A. Brown, M.M. Reynolds, Cell-Based Methods for Determination of Efficacy for Candidate Therapeutics in the Clinical Management of Cancer., Dis. (Basel, Switzerland). 6 (2018). https://doi.org/10.3390/diseases6040085.

[81] Y. Yang, N. Ji, Q.-X. Teng, C.-Y. Cai, J.-Q. Wang, Z.-X. Wu, Z.-N. Lei, S. Lusvarghi, S. V Ambudkar, Z.-S. Chen, Sitravatinib, a Tyrosine Kinase Inhibitor, Inhibits the Transport Function of ABCG2 and Restores Sensitivity to Chemotherapy-Resistant Cancer Cells in vitro , Front. Oncol. . 10 (2020) 700. https://www.frontiersin.org/article/10.3389/fonc.2020.00700.

[82] L. Florento, R. Matias, E. Tuano, K. Santiago, F. Dela Cruz, A. Tuazon, Comparison of Cytotoxic Activity of Anticancer Drugs against Various Human Tumor Cell Lines Using In Vitro Cell-Based Approach., Int. J. Biomed. Sci. 8 (2012) 76–80.

[83] M.R. Ansbro, S. Shukla, S. V Ambudkar, S.H. Yuspa, L. Li, Screening compounds with a novel high-throughput ABCB1-mediated efflux assay identifies drugs with known therapeutic targets at risk for multidrug resistance interference., PLoS One. 8 (2013) e60334. https://doi.org/10.1371/journal.pone.0060334.

[84] S.-J. Oh, H.-K. Han, K.-W. Kang, Y.-J. Lee, M.-Y. Lee, Menadione serves as a substrate for P-glycoprotein: implication in chemosensitizing activity., Arch. Pharm. Res. 36 (2013) 509–516. https://doi.org/10.1007/s12272-013-0052-3.

[85] K.-S. Vellonen, P. Honkakoski, A. Urtti, Substrates and inhibitors of efflux proteins interfere with the MTT assay in cells and may lead to underestimation of drug toxicity., Eur. J. Pharm. Sci. 23 (2004) 181–188. https://doi.org/10.1016/j.ejps.2004.07.006.

[86] P. Limtrakul, S. Anuchapreeda, D. Buddhasukh, Modulation of human multidrug-resistance MDR-1 gene by natural curcuminoids., BMC Cancer. 4 (2004) 13. https://doi.org/10.1186/1471-2407-4-13.

[87] S.C. Taylor, A. Posch, The design of a quantitative western blot experiment., Biomed Res. Int. 2014 (2014) 361590. https://doi.org/10.1155/2014/361590.

[88] T.A.J. Butler, J.W. Paul, E.-C. Chan, R. Smith, J.M. Tolosa, Misleading Westerns: Common Quantification Mistakes in Western Blot Densitometry and Proposed Corrective Measures., Biomed Res. Int. 2019 (2019) 5214821. https://doi.org/10.1155/2019/5214821.

[89] R.S. Bartlett, M.E. Jette, S.N. King, A. Schaser, S.L. Thibeault, Fundamental approaches in molecular biology for communication sciences and disorders., J.

Speech. Lang. Hear. Res. 55 (2012) 1220–1231. https://doi.org/10.1044/1092-4388(2011/11-0152).

[90] P.S. Souza, J.P. Madigan, J.-P. Gillet, K. Kapoor, S. V Ambudkar, R.C. Maia, M.M. Gottesman, K.L. Fung, Expression of the multidrug transporter P-glycoprotein is inversely related to that of apoptosis-associated endogenous TRAIL., Exp. Cell Res. 336 (2015) 318–328. https://doi.org/10.1016/j.yexcr.2015.06.005.

[91] M.A. Demel, R. Schwaha, O. Kramer, P. Ettmayer, E.E. Haaksma, G.F. Ecker, In silico prediction of substrate properties for ABC-multidrug transporters., Expert Opin. Drug Metab. Toxicol. 4 (2008) 1167–1180. https://doi.org/10.1517/17425255.4.9.1167.

[92] S. V Molinski, Z. Bozoky, S.H. Iram, S. Ahmadi, Biophysical Approaches Facilitate Computational Drug Discovery for ATP-Binding Cassette Proteins., Int. J. Med. Chem. 2017 (2017) 1529402. https://doi.org/10.1155/2017/1529402.

[93] W.-X. Li, L. Li, J. Eksterowicz, X.B. Ling, M. Cardozo, Significance analysis and multiple pharmacophore models for differentiating P-glycoprotein substrates., J. Chem. Inf. Model. 47 (2007) 2429–2438. https://doi.org/10.1021/ci700284p.

[94] A. Golbraikh, X.S. Wang, H. Zhu, A. Tropsha, Predictive QSAR Modeling: Methods and Applications in Drug Discovery and Chemical Risk Assessment BT - Handbook of Computational Chemistry, in: J. Leszczynski (Ed.), Springer Netherlands, Dordrecht, 2016: pp. 1–38. https://doi.org/10.1007/978-94-007-6169-8_37-2.

[95] I. Ponzoni, V. Sebastián-Pérez, M.J. Martínez, C. Roca, C. De la Cruz Pérez, F. Cravero, G.E. Vazquez, J.A. Páez, M.F. Díaz, N.E. Campillo, QSAR Classification Models for Predicting the Activity of Inhibitors of Beta-Secretase (BACE1) Associated with Alzheimer's Disease, Sci. Rep. 9 (2019) 9102. https://doi.org/10.1038/s41598-019-45522-3.

[96] Z.L. Johnson, J. Chen, Structural Basis of Substrate Recognition by the Multidrug Resistance Protein MRP1., Cell. 168 (2017) 1075-1085.e9. https://doi.org/10.1016/j.cell.2017.01.041.

[97] O. Ramaen, N. Leulliot, C. Sizun, N. Ulryck, O. Pamlard, J.-Y. Lallemand, H. van Tilbeurgh, E. Jacquet, Structure of the human multidrug resistance protein 1 nucleotide binding domain 1 bound to Mg2+/ATP reveals a non-productive catalytic site., J. Mol. Biol. 359 (2006) 940–949. https://doi.org/10.1016/j.jmb.2006.04.005.

[98] M. Ballent, L. Mate, G. Virkel, J. Sallovitz, P. Viviani, C. Lanusse, A. Lifschitz, Intestinal drug transport: ex vivo evaluation of the interactions between ABC transporters and anthelmintic molecules., J. Vet. Pharmacol. Ther. 37 (2014) 332–337. https://doi.org/10.1111/jvp.12112.

[99] D.A. Parasrampuria, M. V Lantz, L.Z. Benet, A human lymphocyte based ex vivo assay to study the effect of drugs on P-glycoprotein (P-gp) function., Pharm. Res.

18 (2001) 39–44. https://doi.org/10.1023/a:1011070509191.

[100] S. Shukla, H. Zaher, A. Hartz, B. Bauer, J.A. Ware, S. V Ambudkar, Curcumin inhibits the activity of ABCG2/BCRP1, a multidrug resistance-linked ABC drug transporter in mice., Pharm. Res. 26 (2009) 480–487. https://doi.org/10.1007/s11095-008-9735-8.

[101] J. Verstraelen, S. Reichl, Expression analysis of MDR1, BCRP and MRP3 transporter proteins in different in vitro and ex vivo cornea models for drug absorption studies., Int. J. Pharm. 441 (2013) 765–775. https://doi.org/10.1016/j.ijpharm.2012.10.007.

[102] S. Marchetti, N.A. de Vries, T. Buckle, M.J. Bolijn, M.A.J. van Eijndhoven, J.H. Beijnen, R. Mazzanti, O. van Tellingen, J.H.M. Schellens, Effect of the ATP-binding cassette drug transporters ABCB1, ABCG2, and ABCC2 on erlotinib hydrochloride (Tarceva) disposition in in vitro and in vivo pharmacokinetic studies employing Bcrp1-/-/Mdr1a/1b-/- (triple-knockout) and wild-type mice., Mol. Cancer Ther. 7 (2008) 2280–2287. https://doi.org/10.1158/1535-7163.MCT-07-2250.

[103] A. Doran, R.S. Obach, B.J. Smith, N.A. Hosea, S. Becker, E. Callegari, C. Chen, X. Chen, E. Choo, J. Cianfrogna, L.M. Cox, J.P. Gibbs, M.A. Gibbs, H. Hatch, C.E.C.A. Hop, I.N. Kasman, J. Laperle, J. Liu, X. Liu, M. Logman, D. Maclin, F.M. Nedza, F. Nelson, E. Olson, S. Rahematpura, D. Raunig, S. Rogers, K. Schmidt, D.K. Spracklin, M. Szewc, M. Troutman, E. Tseng, M. Tu, J.W. Van Deusen, K. Venkatakrishnan, G. Walens, E.Q. Wang, D. Wong, A.S. Yasgar, C. Zhang, The impact of P-glycoprotein on the disposition of drugs targeted for indications of the central nervous system: evaluation using the MDR1A/1B knockout mouse model., Drug Metab. Dispos. 33 (2005) 165–174. https://doi.org/10.1124/dmd.104.001230.

[104] A.H. Schinkel, E. Wagenaar, C.A. Mol, L. van Deemter, P-glycoprotein in the blood-brain barrier of mice influences the brain penetration and pharmacological activity of many drugs, J. Clin. Invest. 97 (1996) 2517–2524. https://doi.org/10.1172/JCI118699.

[105] G.J. Sills, P. Kwan, E. Butler, E.C.M. de Lange, D.-J. van den Berg, M.J. Brodie, P-glycoprotein-mediated efflux of antiepileptic drugs: preliminary studies in mdr1a knockout mice, Epilepsy Behav. 3 (2002) 427–432. https://doi.org/https://doi.org/10.1016/S1525-5050(02)00511-5.

[106] D. Spieler, C. Namendorf, T. Namendorf, M. von Cube, M. Uhr, Donepezil, a cholinesterase inhibitor used in Alzheimer's disease therapy, is actively exported out of the brain by abcb1ab p-glycoproteins in mice, J. Psychiatr. Res. 124 (2020) 29–33. https://doi.org/https://doi.org/10.1016/j.jpsychires.2020.01.012.

[107] J. Wijnholds, E.C. deLange, G.L. Scheffer, D.J. van den Berg, C.A. Mol, M. van der Valk, A.H. Schinkel, R.J. Scheper, D.D. Breimer, P. Borst, Multidrug resistance protein 1 protects the choroid plexus epithelium and contributes to the blood-cerebrospinal fluid barrier., J. Clin. Invest. 105 (2000) 279–285.

https://doi.org/10.1172/JCI8267.

[108] C.A. Burkhart, F. Watt, J. Murray, M. Pajic, A. Prokvolit, C. Xue, C. Flemming, J. Smith, A. Purmal, N. Isachenko, P.G. Komarov, K. V Gurova, A.C. Sartorelli, G.M. Marshall, M.D. Norris, A. V Gudkov, M. Haber, Small-molecule multidrug resistance-associated protein 1 inhibitor reversan increases the therapeutic index of chemotherapy in mouse models of neuroblastoma., Cancer Res. 69 (2009) 6573–6580. https://doi.org/10.1158/0008-5472.CAN-09-1075.

[109] G. Merino, M. Perez, R. Real, E. Egido, J.G. Prieto, A.I. Alvarez, In Vivo Inhibition of BCRP/ABCG2 Mediated Transport of Nitrofurantoin by the Isoflavones Genistein and Daidzein: A Comparative Study in Bcrp1 −/− Mice, Pharm. Res. 27 (2010) 2098–2105. https://doi.org/10.1007/s11095-010-0208-5.

[110] W. Liu, Q. Meng, Y. Sun, C. Wang, X. Huo, Z. Liu, P. Sun, H. Sun, X. Ma, K. Liu, Targeting P-Glycoprotein: Nelfinavir Reverses Adriamycin Resistance in K562/ADR Cells., Cell. Physiol. Biochem. Int. J. Exp. Cell. Physiol. Biochem. Pharmacol. 51 (2018) 1616–1631. https://doi.org/10.1159/000495650.

[111] V. Székely, I. Patik, O. Ungvári, Á. Telbisz, G. Szakács, É. Bakos, C. Özvegy-Laczka, Fluorescent probes for the dual investigation of MRP2 and OATP1B1 function and drug interactions, Eur. J. Pharm. Sci. 151 (2020) 105395. https://doi.org/https://doi.org/10.1016/j.ejps.2020.105395.

[112] M.V. Razori, P.L. Martín, P.M. Maidagan, I.R. Barosso, N. Ciriaci, R.B. Andermatten, E.J. Sánchez Pozzi, C.L. Basiglio, M.L. Ruiz, M.G. Roma, Spironolactone ameliorates lipopolysaccharide-induced cholestasis in rats by improving Mrp2 function: Role of transcriptional and post-transcriptional mechanisms., Life Sci. 259 (2020) 118352. https://doi.org/10.1016/j.lfs.2020.118352.

[113] X.-Y. Liao, Q.-Q. Deng, L. Han, Z.-T. Wu, Z.-L. Peng, Y. Xie, G.-J. Wang, J.-Y. Aa, G.-Y. Pan, Leflunomide increased the renal exposure of acyclovir by inhibiting OAT1/3 and MRP2., Acta Pharmacol. Sin. 41 (2020) 129–137. https://doi.org/10.1038/s41401-019-0283-z.

[114] J.B. Koenderink, J.J.M.W. van den Heuvel, A. Bilos, G. Vredenburg, N.P.E. Vermeulen, F.G.M. Russel, Human multidrug resistance protein 4 (MRP4) is a cellular efflux transporter for paracetamol glutathione and cysteine conjugates., Arch. Toxicol. 94 (2020) 3027–3032. https://doi.org/10.1007/s00204-020-02793-4.

[115] H. Zhang, A. Patel, Y.-J. Wang, Y.-K. Zhang, R.J. Kathawala, L.-H. Qiu, B.A. Patel, L.-H. Huang, S. Shukla, D.-H. Yang, S. V Ambudkar, L.-W. Fu, Z.-S. Chen, The BTK Inhibitor Ibrutinib (PCI-32765) Overcomes Paclitaxel Resistance in ABCB1- and ABCC10-Overexpressing Cells and Tumors., Mol. Cancer Ther. 16 (2017) 1021–1030. https://doi.org/10.1158/1535-7163.MCT-16-0511.

[116] Y.-L. Sun, J.-J. Chen, P. Kumar, K. Chen, K. Sodani, A. Patel, Y.-L. Chen, S.-D. Chen, W.-Q. Jiang, Z.-S. Chen, Reversal of MRP7 (ABCC10)-mediated multidrug

resistance by tariquidar, PLoS One. 8 (2013) e55576–e55576. https://doi.org/10.1371/journal.pone.0055576.

[117] W. Tun-Yhong, C. Chinpaisal, P. Pamonsinlapatham, S. Kaewkitichai, Tenofovir Disoproxil Fumarate Is a New Substrate of ATP-Binding Cassette Subfamily C Member 11., Antimicrob. Agents Chemother. 61 (2017). https://doi.org/10.1128/AAC.01725-16.

[118] T. Funazo, T. Tsuji, H. Ozasa, K. Furugaki, Y. Yoshimura, T. Oguri, H. Ajimizu, Y. Yasuda, T. Nomizo, Y. Sakamori, H. Yoshida, Y.H. Kim, T. Hirai, Acquired Resistance to Alectinib in ALK-Rearranged Lung Cancer due to ABCC11/MRP8 Overexpression in a Clinically Paired Resistance Model., Mol. Cancer Ther. 19 (2020) 1320–1327. https://doi.org/10.1158/1535-7163.MCT-19-0649.

[119] B. Shi, F.-F. Xu, C.-P. Xiang, R. Jia, C.-H. Yan, S.-Q. Ma, N. Wang, A.-J. Wang, P. Fan, Effect of sodium butyrate on ABC transporters in lung cancer A549 and colorectal cancer HCT116 cells., Oncol. Lett. 20 (2020) 148. https://doi.org/10.3892/ol.2020.12011.

[120] K. Sawangrat, S. Yamashita, A. Tanaka, M. Morishita, K. Kusamori, H. Katsumi, T. Sakane, A. Yamamoto, Modulation of Intestinal Transport and Absorption of Topotecan, a BCRP Substrate, by Various Pharmaceutical Excipients and Their Inhibitory Mechanisms of BCRP Transporter., J. Pharm. Sci. 108 (2019) 1315–1325. https://doi.org/10.1016/j.xphs.2018.10.043.

[121] R.D. Harvey, N.R. Aransay, N. Isambert, J.-S. Lee, T. Arkenau, J. Vansteenkiste, P.A. Dickinson, K. Bui, D. Weilert, K. So, K. Thomas, K. Vishwanathan, Effect of multiple-dose osimertinib on the pharmacokinetics of simvastatin and rosuvastatin., Br. J. Clin. Pharmacol. 84 (2018) 2877–2888. https://doi.org/10.1111/bcp.13753.

[122] L.D. Weidner, K.L. Fung, P. Kannan, J.K. Moen, J.S. Kumar, J. Mulder, R.B. Innis, M.M. Gottesman, M.D. Hall, Tariquidar Is an Inhibitor and Not a Substrate of Human and Mouse P-glycoprotein., Drug Metab. Dispos. 44 (2016) 275–282. https://doi.org/10.1124/dmd.115.067785.

[123] X. Zhao, Y. Li, K. Du, Y. Wu, L. Liu, S. Cui, Y. Zhang, J. Gao, R.F. Keep, J. Xiang, Involvement of human and canine MRP1 and MRP4 in benzylpenicillin transport, PLoS One. 14 (2019) e0225702. https://doi.org/10.1371/journal.pone.0225702.

[124] M. Gameiro, R. Silva, C. Rocha-Pereira, H. Carmo, F. Carvalho, M. de L. Bastos, F. Remiao, Cellular Models and In Vitro Assays for the Screening of modulators of P-gp, MRP1 and BCRP., Molecules. 22 (2017). https://doi.org/10.3390/molecules22040600.

[125] E. Bakos, L. Homolya, Portrait of multifaceted transporter, the multidrug resistance-associated protein 1 (MRP1/ABCC1)., Pflugers Arch. 453 (2007) 621–641. https://doi.org/10.1007/s00424-006-0160-8.

[126] C. Willers, H. Svitina, M.J. Rossouw, R.A. Swanepoel, J.H. Hamman, C. Gouws,

Models used to screen for the treatment of multidrug resistant cancer facilitated by transporter-based efflux., J. Cancer Res. Clin. Oncol. 145 (2019) 1949–1976. https://doi.org/10.1007/s00432-019-02973-5.

[127] S. Mohana, M. Ganesan, N. Rajendra Prasad, D. Ananthakrishnan, D. Velmurugan, Flavonoids modulate multidrug resistance through wnt signaling in P-glycoprotein overexpressing cell lines, BMC Cancer. 18 (2018) 1168. https://doi.org/10.1186/s12885-018-5103-1.

[128] H. Li, S. Krstin, S. Wang, M. Wink, Capsaicin and Piperine Can Overcome Multidrug Resistance in Cancer Cells to Doxorubicin., Molecules. 23 (2018). https://doi.org/10.3390/molecules23030557.

[129] H. Li, S. Krstin, M. Wink, Modulation of multidrug resistant in cancer cells by EGCG, tannic acid and curcumin., Phytomedicine. 50 (2018) 213–222. https://doi.org/10.1016/j.phymed.2018.09.169.

[130] S. Fiala, S.A. Jones, M.B. Brown, A fundamental investigation into the effects of eutectic formation on transmembrane transport., Int. J. Pharm. 393 (2010) 68–73. https://doi.org/10.1016/j.ijpharm.2010.04.001.

[131] P.W. Stott, A.C. Williams, B.W. Barry, Transdermal delivery from eutectic systems: enhanced permeation of a model drug, ibuprofen, J. Control. Release. 50 (1998) 297–308. https://doi.org/https://doi.org/10.1016/S0168-3659(97)00153-3.

[132] S.E. Lu C, Cao J, Wang N, Significantly improving the solubility of non-steroidal antiinflammatory drugs in deep eutectic solvents for potential non-aqueous liquid administration, Medchemcomm. 7 (2016) 955–959. https://pubs.rsc.org/en/content/articlelanding/2016/md/c5md00551e/unauth.

[133] J.M. Silva, C. V Pereira, F. Mano, E. Silva, V.I.B. Castro, I. Sá-Nogueira, R.L. Reis, A. Paiva, A.A. Matias, A.R.C. Duarte, Therapeutic Role of Deep Eutectic Solvents Based on Menthol and Saturated Fatty Acids on Wound Healing, ACS Appl. Bio Mater. 2 (2019) 4346–4355. https://doi.org/10.1021/acsabm.9b00598.

[134] J.M. Silva, R.L. Reis, A. Paiva, A.R.C. Duarte, Design of Functional Therapeutic Deep Eutectic Solvents Based on Choline Chloride and Ascorbic Acid, ACS Sustain. Chem. Eng. 6 (2018) 10355–10363. https://doi.org/10.1021/acssuschemeng.8b01687.

[135] F. Al-Akayleh, S. Adwan, M. Khanfar, N. Idkaidek, M. Al-Remawi, A Novel Eutectic-Based Transdermal Delivery System for Risperidone, AAPS PharmSciTech. 22 (2020) 4. https://doi.org/10.1208/s12249-020-01844-4.

[136] B.G. Amsden, Biodegradable elastomers in drug delivery, Expert Opin. Drug Deliv. 5 (2008) 175–187. https://doi.org/10.1517/17425247.5.2.175.

[137] I.M. Aroso, R. Craveiro, Â. Rocha, M. Dionísio, S. Barreiros, R.L. Reis, A. Paiva, A.R.C. Duarte, Design of controlled release systems for THEDES-Therapeutic deep eutectic solvents, using supercritical fluid technology., Int. J. Pharm. 492 (2015) 73–79. https://doi.org/10.1016/j.ijpharm.2015.06.038.

[138] F. Mano, M. Martins, I. Sá-Nogueira, S. Barreiros, J.P. Borges, R.L. Reis, A.R.C. Duarte, A. Paiva, Production of Electrospun Fast-Dissolving Drug Delivery Systems with Therapeutic Eutectic Systems Encapsulated in Gelatin., AAPS PharmSciTech. 18 (2017) 2579–2585. https://doi.org/10.1208/s12249-016-0703-z.

[139] A. Gutiérrez, S. Aparicio, M. Atilhan, Design of arginine-based therapeutic deep eutectic solvents as drug solubilization vehicles for active pharmaceutical ingredients., Phys. Chem. Chem. Phys. 21 (2019) 10621–10634. https://doi.org/10.1039/c9cp01408j.

[140] M.A. Ali, M.S. Rahman, R. Roy, P. Gambill, D.E. Raynie, M.A. Halim, Structure Elucidation of Menthol-Based Deep Eutectic Solvent using Experimental and Computational Techniques, J. Phys. Chem. A. 125 (2021) 2402–2412. https://doi.org/10.1021/acs.jpca.0c10735.

[141] M.I. Rain, H. Iqbal, M. Saha, M.A. Ali, H.K. Chohan, M.S. Rahman, M.A. Halim, A comprehensive computational and principal component analysis on various choline chloride-based deep eutectic solvents to reveal their structural and spectroscopic properties., J. Chem. Phys. 155 (2021) 44308. https://doi.org/10.1063/5.0052569.

[142] J.A. Kist, H. Zhao, K.R. Mitchell-Koch, G.A. Baker, The study and application of biomolecules in deep eutectic solvents., J. Mater. Chem. B. 9 (2021) 536–566. https://doi.org/10.1039/d0tb01656j.

[143] W.A. Ahmed Arafa, Deep eutectic solvent for an expeditious sono-synthesis of novel series of bis-quinazolin-4-one derivatives as potential anti-cancer agents., R. Soc. Open Sci. 6 (2019) 182046. https://doi.org/10.1098/rsos.182046.

[144] Y.P. Mbous, M. Hayyan, A. Hayyan, W.F. Wong, M.A. Hashim, C.Y. Looi, Applications of deep eutectic solvents in biotechnology and bioengineering-Promises and challenges., Biotechnol. Adv. 35 (2017) 105–134. https://doi.org/10.1016/j.biotechadv.2016.11.006.

[145] V. Stepankova, P. Vanacek, J. Damborsky, R. Chaloupkova, Comparison of catalysis by haloalkane dehalogenases in aqueous solutions of deep eutectic and organic solvents, Green Chem. 16 (2014) 2754–2761. https://doi.org/10.1039/C4GC00117F.

[146] D. Mondal, J. Bhatt, M. Sharma, S. Chatterjee, K. Prasad, A facile approach to prepare a dual functionalized DNA based material in a bio-deep eutectic solvent, Chem. Commun. 50 (2014) 3989–3992. https://doi.org/10.1039/C4CC00145A.

[147] H. Zhao, DNA Stability in Ionic Liquids and Deep Eutectic Solvents., J. Chem. Technol. Biotechnol. 90 (2015) 19–25. https://doi.org/10.1002/jctb.4511.

[148] Z. Li, P.I. Lee, Investigation on drug solubility enhancement using deep eutectic solvents and their derivatives., Int. J. Pharm. 505 (2016) 283–288. https://doi.org/10.1016/j.ijpharm.2016.04.018.

[149] H.G. Morrison, C.C. Sun, S. Neervannan, Characterization of thermal behavior of

deep eutectic solvents and their potential as drug solubilization vehicles., Int. J. Pharm. 378 (2009) 136–139. https://doi.org/10.1016/j.ijpharm.2009.05.039.

[150] B. Olivares, F. Martínez, L. Rivas, C. Calderón, J. M Munita, P. R Campodonico, A Natural Deep Eutectic Solvent Formulated to Stabilize β-Lactam Antibiotics., Sci. Rep. 8 (2018) 14900. https://doi.org/10.1038/s41598-018-33148-w.

[151] Z. Xu, S. Liu, Y. Kang, M. Wang, Glutathione-Responsive Polymeric Micelles Formed by a Biodegradable Amphiphilic Triblock Copolymer for Anticancer Drug Delivery and Controlled Release, ACS Biomater. Sci. Eng. 1 (2015) 585–592. https://doi.org/10.1021/acsbiomaterials.5b00119.

[152] J. Mao, Y. Li, T. Wu, C. Yuan, B. Zeng, Y. Xu, L. Dai, A Simple Dual-pH Responsive Prodrug-Based Polymeric Micelles for Drug Delivery, ACS Appl. Mater. Interfaces. 8 (2016) 17109–17117. https://doi.org/10.1021/acsami.6b04247.

[153] I.P.E. Macário, H. Oliveira, A.C. Menezes, S.P.M. Ventura, J.L. Pereira, A.M.M. Gonçalves, J.A.P. Coutinho, F.J.M. Gonçalves, Cytotoxicity profiling of deep eutectic solvents to human skin cells, Sci. Rep. 9 (2019) 3932. https://doi.org/10.1038/s41598-019-39910-y.

CHAPTER TWO: CELL-BASED EFFLUX ASSAY TO IDENTIFY MRP1 SUBSTRATES

2.1. Introduction

Cell-based assays are more accurate and provide reliable result than membrane-based assays. It is possible to get a clear picture about the parameters involved in assessing whether the transported compounds are substrates or inhibitors. Although cell-based assays demand time and labor, these can give us clear idea about specific transporter protein activity in live conditions. On the other hand, membrane-based assays are complicated and needs sophisticated techniques. It is possible to grow the cells in a well plate and increase the expression of selective transporter proteins, which helps to determine specific substrates and modulators for overexpressed efflux pump.

2.1.1. Bidirectional transport assay

To measure the permeability and transport of the compounds across cell monolayer, transport assays have been widely used in the field of drug discovery to assess the property of the compounds as substrates or modulators. The cells overexpressing transporter proteins are grown on a trans- well filter and allowed to grow by forming tight junction among the cells. After growing a cell monolayer, the test compounds are loaded either in the apical side (known as the upper chamber) or basolateral side (known as the bottom chamber) and the experiment is initiated. Samples are collected from both chambers at different timepoints and quantified using LC-MSMS, HPLC-MS or HPLC-UV. The efflux radio (ER) can be calculated by measuring the permeability from either the apical to basolateral direction or from basolateral to apical direction. If the ER is greater than 2, the compounds are moved by transporter proteins across the cell monolayer. To test the inhibitory effect, probe substrates and the test compound are used. To perform this experiment the cell monolayer is incubated with test compound. Then the probe substrate

is added, and the ER is calculated for the substrate in the presence of test compounds. If the ER is less than 2 for the probe substrate in a concentration dependent manner, the test compound might work as an inhibitor. From the net flux, kinetics parameters such as Vmax and Km are also determined [1–3].

To perform this assay wild type, knocked out and ABC transporter overexpressed Caco-2 and MDCK cell lines are commonly used. Compounds having low or high permeability may give false result. Moreover, differences in cell lines, endogenous expression of the transporters and transfection with specific PGP, MRP1 or BCRP might give variable results. These factors might lead to difference in ER, K_m, and V_{max} [4,5].

2.1.2. Uptake assay/intracellular accumulation assay and efflux assay

Cell-based uptake and efflux assays are used to quantify the amount of drugs accumulated in the cells. Using analytical methods, flow cytometry, and radioactivity, the transport potential can be assessed for specific transporter proteins. Sometimes substrates might act as inhibitors. In some cases, it does not behave as an inhibitor. Therefore, the increased accumulation of the probe substrate in the presence of the test compound indicates that the test compound might work as inhibitor. While the opposite effect might happen due to an inducing effect of the test compound. The result is calculated based on the known inhibitor of specific transporter protein. Calcein AM, mitoxantrone, rhobdamine 123, and doxorubicin are widely used fluorescent substrates to assess the accumulation property in ABC-transporter overexpressed cell lines. Calcein AM is used to study MRP1 and P-gp. Mitoxantrone is used to study BCRP. Rhodamine 123 is used for Pgp. Calcein AM easily diffuses into the cell. After getting inside the cells, it gets cleaved by esterase enzymes to fluorescence-active acid calcein. Intracellular accumulation of fluorescent compounds has

an inverse relationship with ABC-efflux transporter activity. That is why this protocol is widely accepted for high-throughput inhibitor-screening assays. Confocal microscopy is also preferable and convenient to generate the map of localization of the fluorescent compounds in live or fixed cells. By this technique it is possible to get digital images of the distribution and the analysis [6–26].

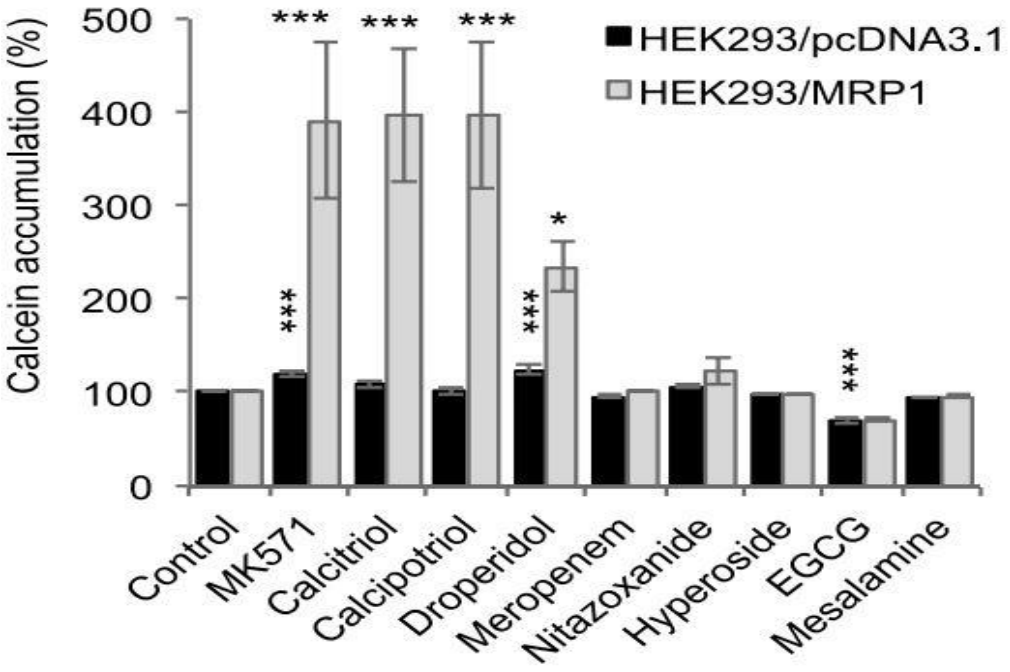

Figure 2.1. Effect on test compounds on Calcein AM accumulation assay. Image collected from the author with permission [18].

Tan et al showed in Figure 2.1 that in the presence of the MRP1 inhibitor MK-571, overexpressed HEK MRP1 cells have more accumulation of calcein than the respective parenteral control cell line. Calctriol and calcipotriol showed very high accumulation properties is similar to the inhibitor and so they can act as modulator. This calcein AM assay works to identify potential modulators [18].

For doxorubicin, normally people use H69 cancer cell line. Based on the provided data it proves feasibility for using doxorubicin-based fluorescence accumulation as a mean for development of the high-throughput screening assay.

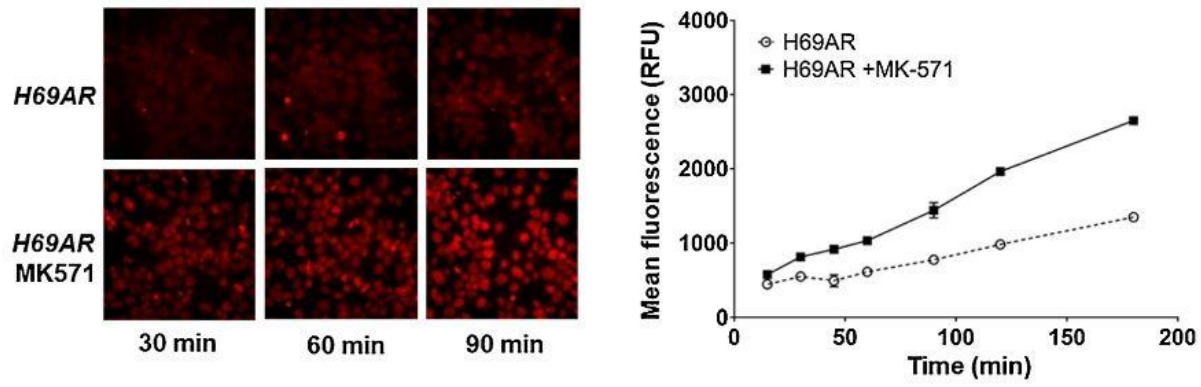

Figure 2.2. 10 μM doxorubicin was added in H69AR cells in the presence and absence of 50 μM MK571 for 15–180 min. Doxorubicin treatment at 30, 60, and 90 min are presented. Data are shown as mean ± SD (n = 3).

H69 AR cells overexpress MRP1 transporter. In case of overexpression and in presence of inhibitor MK-571, doxorubicin gets accumulated. This is indicated by high fluorescence intensity. It indicates the inhibitory potential of MK-571 (Figure 2.2). In this way we can characterize the inhibitory potential of the test compound using the doxorubicin-accumulation assay [21]. Some research groups worked on MRP1-mediated glutathione transport of the substrates. They found that MRP1 activity is directly related to glutathione conjugation. That is why it is imperative to conduct glutathione-content assay to ensure whether the drug is the MRP1 substrate or not [27]. Similarly drug-metabolizing enzyme, particularly CYP3A4 and GST, inhibition assays can confirm the potential to overcome drug resistance [28].

Analytical techniques can identify and quantify ABC transporter substrates based on the accumulation of drug inside the parental and overexpressed cells. LC-MS or HLPC techniques are normally followed to prove the activity of the test compounds as substrates or modulators. Sometimes inhibitors might or might not work as substrates of the transporter protein. For example, Amila et al performed the cellular-accumulation assay for Pgp inhibitors [29]. After treating the cells with inhibitors, the cells were collected and lysed. Supernatant from the centrifuged samples were injected into the mass spectrometer. Here different buffer solutions were used to sperate the inhibitors in the column chromatography. Gradient conditions were elected based on the polarity of the drug molecules. In the MRM mode of the spectrometer, compounds were detected with their suitable parent/daughter ions. Limit of detection (LOD) and limit of quantification (LOQ) were calculated. Concentrations of the inhibitors were normalized to the content of protein. In the LC-MSMS intracellular-content accumulation assay, the drugs 29, 34 and 45 did not show significant content difference between parental control and P-gp overexpressed cell lines. In a different experiment a simple technique identified and quantified P-gp substrates in an MDCK cell accumulation assay. Possible P-gp substrates are determined using intracellular accumulation of digitalis-like compounds in MDCK-Parental and MDCK-P-gp-overexpressing cell lines. The further effect of P-gp inhibitors elacridar and Ko143 of the possible substrates are assessed. The lipophilicity of the drugs might play a role in this transport assay. The amounts were quantified using LC-MS methods [9].

In cell-based efflux assay, after incubating the cells with drugs, the media is removed, and fresh media or buffer is added. The radiolabeled test compounds effluxed by the ABC

transporter get accumulated in the fresh medium. The amount of is measured using liquid scintillation counter [30].

2.1.3. 3D cell-based experiment

A recent advancement cell-based experiment research is three-dimensional cell-culture system with image analysis as the added dimension. Three-dimensional based cell cultures mimic the *in vivo* conditions. Three-dimensional 3D tumor spheroid is widely used to test the efficacy of new anticancer molecule because it resembles the structural features of solid tumor. This spheroid is used to check the drug resistance for anticancer agents [31,32]. For example, Nanayakkara et al performed calcein AM uptake assay in spheroids. Using prostate cancer cell line DU145TXR, spheroids were made following some minor modifications. Spheroids were treated with Pgp inhibitors followed by incubation with calcein AM. Fluorescence images were processed using the imageJ program and then three dimensional surface was analyzed based on pixel intensities [29].

2.1.4. Novel cell-based efflux assay

Though there are lots of assays for the identification of ABC-transporter substrates, inhibitors, or modulators, most of the experiments are complicated to perform technically. These assays are labor-intensive. Preparation of the cell lysate is complex. Intracellular drug content determination is time consuming and requires specialized equipment or expertise. Moreover, image-analysis platforms in substrate accumulation assays are generally costly. As an alternative approach, to identify substrates of ABC transporter, our goal was to develop simple HPLC-UV based cellular efflux assay using six selected compounds identified as modulators from previous experiments in our laboratory. To screen these compounds, we used a unique library of anticancer drugs [6,21,22]. Our aims

were as follows: i) determination of the drug content from extracellular, instead of measuring intracellular drug concentration, ii) evaluation of efflux activity of MRP1 on substrate drugs in overexpressing cell line and its parental (control) cell line, iii) comparison of efflux activity between known MRP1 substrate drug and experimental drug and iv) MTT colorimetric assay, to assess and validate the experiment.

We can hypothesize that cell-based efflux assay using HPLC-UV may identify the drugs on which MRP1 shows high efflux activity with an excellent efficiency. Further *in vitro* and *in vivo* models should be developed to validate and identify the possibility of these drugs to work as substrates of MRP1.

2.2. Materials and methods

2.2.1. Chemicals

Vincristine, alisertib, tozasertib, mesalamine, celecoxib, caboxantinib, and erlotinib were purchased from Cayman Chemical (Ann Arbor, MI). HBSS (Hank's Balanced Salt Solution with Ca and Mg added) and DMEM media were procured from GE Healthcare, Marlborough, MA.

2.2.2. Cell lines and cell culture

MDCKII cells were purchased from ATCC (Manassas, VA). For MDCKII-MRP1, parental cells were transfected with MRP1 vector. Cells were cultured in DMEM supplemented with 10 % fetal bovine serum. Cells were grown in a humidified incubator maintaining 5 % CO_2 at 37 °C. MDCKII-MRP1 was exposed to geneticin (0.2 mg/mL) once a month to induce the expression of MRP1.

2.2.3. Cell-based efflux assay

2.2.3.1. Optimization of incubation time

The initial time-point study was conducted to select optimal time for drug uptake and efflux. MDCKII-MRP1 cells were seeded at 1.5x 10^6 density/dish in small cell-culture dishes. After 24 hours, when the cell confluency was greater than 90 %, the media was removed and 50 μM of each drug prepared in 2-mL DMEM was added to the cells.

In the second timepoint experiment, after incubating for one hour, the media was removed, and cells were washed twice with 500 μL of HBSS buffer to remove residual media containing drug solution. Cells were then incubated with 1.5 mL HBSS buffer for two hours. Following incubation, buffer was collected from the cell-culture plate and

centrifuged at 12000 rpm for seven minutes to pelletize undissolved artifacts. The supernatants were collected into HPLC vials for analysis. To validate the results, sample blank, process blank, and spiked sample were run for each drug. Limit of quantification (LOQ) was quantified as 1 μM and limit of detection was 0.3 uM for the developed method. Vincristine was used as a control drug in this study [33].

2.2.3.2. Optimization of incubation dose

To select the optimum dose for treatment, we selected drug concentrations ranging from 50 to 150 μM and incubated with MRP1-overexpressed cells at 1.5x 10^6 cells/dish in small cell-culture dishes. After incubation, cellular morphology was considered for proper dose selection.

2.2.3.3. HPLC-UV instrumentation for selected modulators

HPLC preparation protocol was outlined below:

Vincristine and mesalamine were quantified using isocratic methods

Solvent composition:

a) Vincristine: Phosphate buffer/ACN (60:40), pH 3.8

b) Mesalamine: 0.1 % Formic acid in Milli-Q water/ACN (60:40)

⬇

For the rest of the drugs, linear gradient elution method was used.

(Solvent composition: 0.1 % Formic acid in Milli-Q water/ACN)

⬇

The injection volume was 20 μL for each drug sample.

⬇

Flow rate was 1.2 mL/min and temperature were controlled at 30 °C

Drug concentrations were measured using HPLC-UV (Thermo Scientific, San Jose, CA, USA).

The analytes were separated using C-18 column (Agilent Zoxbax, 4.6x75mm, 3.5 μm).

2.2.3.4. Experimental outline of cell-based efflux assay

MDCKII-MRP1 and MDCKII-P cells were seeded at 1.5x 10^6 density/1.5 mL in small cell-culture dishes

After 24 hours, when the cell confluency was greater than 90 %, the media was removed and 50 μM of each drug prepared in 2 mL DMEM was added to the cells

After incubating for one hour, the media was removed, and cells were washed twice with 500 μL of HBSS buffer

Cells were then incubated with 1.5-mL HBSS buffer for two hours.

Post incubation, buffer was collected and centrifuged at 12000 rpm for seven minutes to pelletize undissolved artifacts.

The supernatants were collected into HPLC vials for analysis. Vincristine was used as control.

2.2.3.4.1. Cell viability assay

MDCKII-P and MDCKII-MRP1 cells were plated into a 96-well plate at a density of 5x104 cells/well in 100-µL culture medium.

The next day, cells were treated with various concentrations (0.00064 µM to 50 µM) of drugs in 100 µL of DMEM media. Media only (untreated) was used as control

After 72 hours of incubation cells were treated with 10 µL of MTT dye (5 mg/ml in PBS) and incubated at 37 °C for four hours.

MTT formazan product was dissolved in 100 µL of 15 % SDS containing 10 mM HCl.

Cell viability was determined by measuring spectroscopic absorbance at 570 nm with a microplate reader.

2.2.3.5. Molecular Modeling Approach to identify substrate binding site

2.2.3.5.1. Drug and protein optimization and preparation

To identify the substrate-binding site in MRP1, we employed molecular docking. The protocol is outlined:

- Receptor and drug molecule preparation: Structure of drugs were collected from Pubchem compound server and MRP1 PDB code was collected (5UJ9) from RCSB databank.
- Optimization: After collecting the structures, these were optimized by ACD Chemsketch and PyMol. The optimized structures were saved in PDB format for further docking.

2.2.3.5.2. Molecular docking

- PyRx was used for molecular docking between optimized drug and protein.
- Docked poses of drug molecules were combined with protein using PyMol.
- Gridbox parameter selected:

  center_x = 86.22, center_y = 62.04, center_z = 57.96

  size_x = 67.70, size_y = 35.24, size_z = 35.97

- All docked posed were processed with Discovery studio used for visualization of ligand receptor nonbonding interaction analysis.

2.3. Data Analysis

Results are presented as mean±SD. All the experiments were performed at three independent times. Percent drug efflux of MRP1-overexpressed cell line was calculated in

terms of parental efflux control for each drug. The equation is (Efflux conc. of MRP1−Efflux conc. of Parental)/ Efflux conc. of Parental×100. For each drug we generated a standard curve to calculate the concentration effluxed drugs by MRP1 overexpressed and parental cell lines. For the MTT assay, we also conducted three independent experiments.

2.4. Result

2.4.1. Selection of incubation dose and time

Optimization of incubation dose

We selected three concentrations, 50, 100, and 150 μM, and incubated with the drugs to choose the suitable dose for conducting the experiment. For optimization we selected alisertib. We observed significant cell detachment from the culture dish for 100 uM and 150 uM drug concentrations. These concentrations were excluded from further assessment. Since 50 uM had maximum attachment of cells to the culture plates, this dose was selected. The cells showed no sign of mortality at the selected concentration.

Incubation time optimization

Two timepoint experiments were performed to select the optimum incubation time for absorption and efflux of drug molecules by MRP1. To select both incubation times, we proceeded with alisertib. According to the first timepoint experiment, after 1 hour in MRP1-overexpressed cell lines, maximum absorption was record by the cells. To see which one shows better absorption in the first-time dependent accumulation study, we

selected three time points ranges from 45 mins to 2 hours. As shown in **Figure 2.3**, we found that one hour shows maximum absorption.

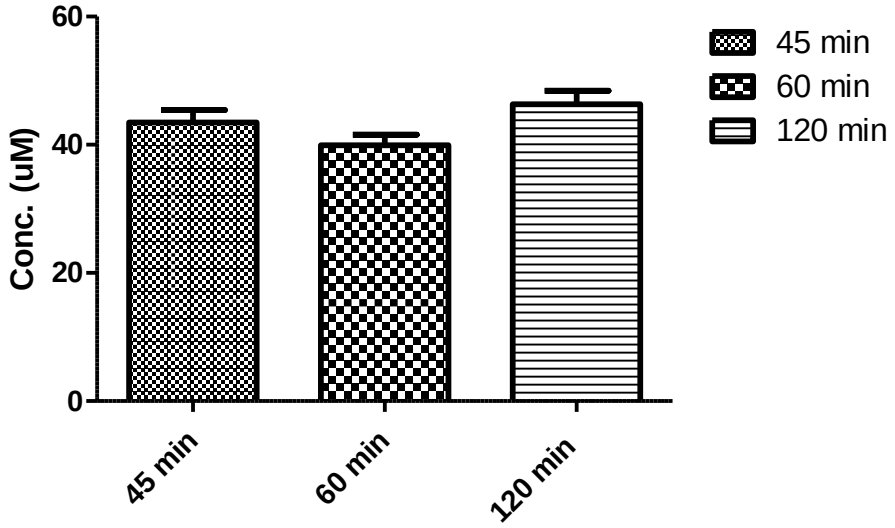

Figure 2.3. To choose first incubation time, three time points were selected. After incubating with MRP1-overexpressing cells at different times, aliquots of drug containing media was collected and injected in HPLC-UV. In the chromatograms, high absorption indicates low effluxed drug concentration in the extracellular media. Thus, the peak area and height will be small. One hour showed best response. After one hour, the cells showed most absorption of the drugs.

To conduct the second time experiment, we chose four points ranging from 0 hour to 4 hours. We observed the maximum efflux and we found that after two hours, MRP1 showed high efflux activity and drug concentration became maximum in the extracellular media

(Figure 2.3). From this study, two hours was selected based on efflux rate of MRP1-overexpressed cells.

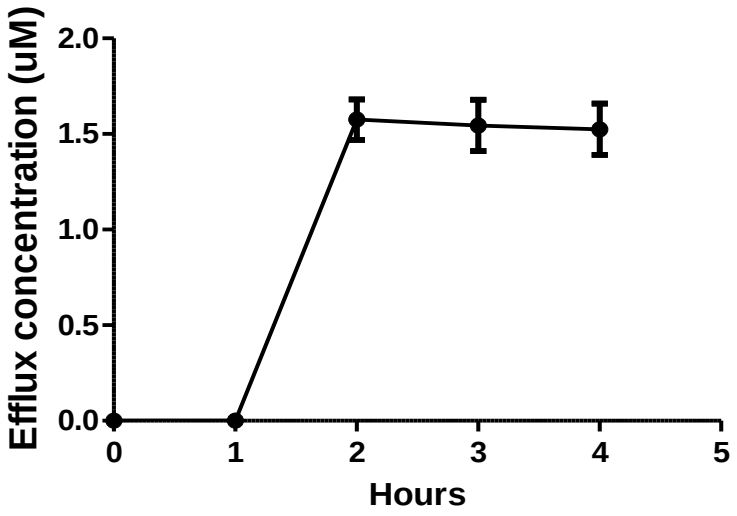

Figure 2.4. Experiment to determine the high efflux activity of MRP1 after adding fresh HBSS. Aliquots of extracellular media were collected at different times. Before adding the HBSS buffer, we removed-drug containing media. From the figure we can clearly see that after two hours the peak started becoming flat and going down until four hours. Two hours was selected for measuring efflux activity.

2.4.1.1. Optimized HPLC Parameters

Table 2.1. Optimized HPLC parameters such as calibration equation, wavelength of maximum absorbance and retention time for peak are given below.

Drugs	Calibration Equation	Wavelengths of maximum absorbance	Retention time in HPLC chromatogram
Alisertib	$y = 0.3326x - 0.6903$, $R^2 = 0.9971$	290 nm	6.37min

Tozasertib	y = 0.3884x - 0.7141, R^2 = 0.9932	254 nm	3.58min
Mesalamine	y = 0.6897x + 0.8723, R^2 = 0.9906	210 nm	0.62min
Celecoxib	y = 0.0566x - 0.1488, R^2 = 0.9999	254 nm	6.70min
Caboxantinib	y = 0.0052x + 0.098, R^2 = 0.9912	254 nm	6.92min
EGCG	y = 0.1252x - 0.4857, R^2 = 0.9979	280 nm	3.09min
Erlotinib	y = 0.0195x + 0.28, R^2 = 0.9941	254 nm	4.29min
Vincristine	y = 0.2497x + 2.1896, R^2 = 0.9952	210 nm	0.55min

For all the drugs R^2 values are ranged from 0.9906 to 1.0. Vincristine is used as a control drug in this experiment. It is a known MRP1 substrate.

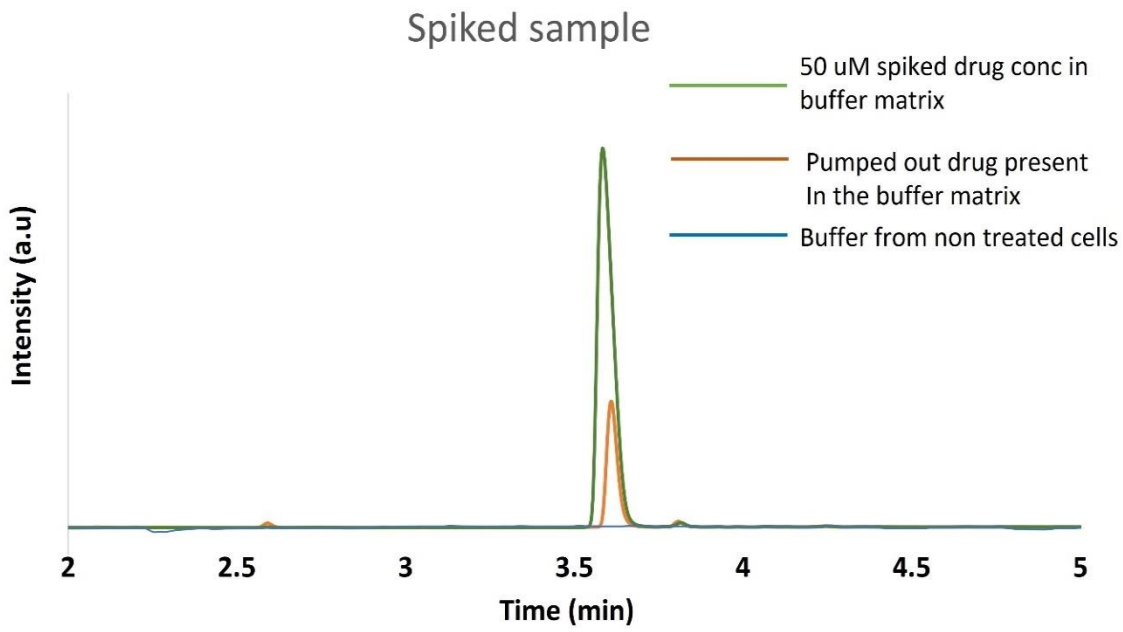

Figure 2.5. A sample chromatogram between 50 μM of spiked and cell treated concentrations of tozasertib and non-treated control. The chromatogram indicates that peak elution time was similar between the samples.

2.4.1.2. Assessment of efflux method using known substrates and modulator drugs

For incubation one hour was chosen and 50-μM concentration drug was selected for treatment. After incubation, drug containing extracellular media was removed and fresh HBSS buffer was added to the cell-culture plate. After two hours, the buffer sample was collected. The amount of drug pumped out from the cells was quantified using HPLC-UV. We calculated efflux concentrations from this experiment for all potential substrate drugs. **Table 2.2.** The results for seven drugs were as follows.

Drugs	Parental efflux	MRP1 efflux
Alisertib	3.52±0.292 μM	5.28±0.391 μM
Mesalamine	3.09±0.15 μM	4.17±0.357 μM
Celecoxib	11.34±0.969 μM	14.01±0.902 μM
Caboxantinib	11.28±2.93 μM	12.54±2.465 μM
Erlotinib	14.87±1.356 μM	16.58±1.630 μM
Tozasertib	15.53±2.062 μM	9.48±2.35 μM
Vincristine	16.51±1.294 μM	22.64±1.586 μM

Vincristine is a popular chemotherapeutic agent that is used to treat a variety of cancers. In this experiment we used vincristine as control because it is a known MRP1 substrate drug. MRP1-overexpressed cells will pump out most of the drugs. The amount of excreted drugs will be more than its parenteral control cells. The parental cells might show some efflux. This is due to endogenous expression of some MRP1 proteins and other ABC transporters in the parental cell line. If the drug is a substrate of MRP1, efflux concentration will be higher in MRP1-overexpressed cells. In MRP1-overexpressing cells, vincristine

(control) showed 37 % more efflux than parental cells. Alisertib shows around 50 % more efflux, mesalamine showed 35 % more efflux, and celecoxib showed 23 % more efflux in MRP1 overexpressed cells (Figure 2.6). The difference between both cell lines in terms of efflux were considered significant ($p<0.05$).

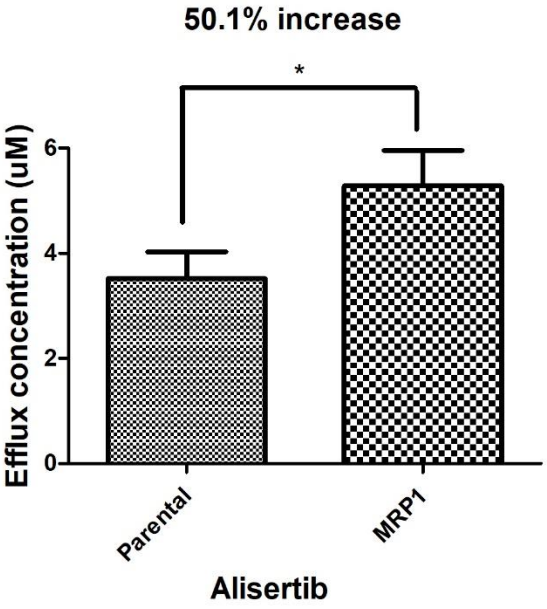
50.1% increase
*
Efflux concentration (uM)
0
2
4
6
Parental
MRP1
Alisertib

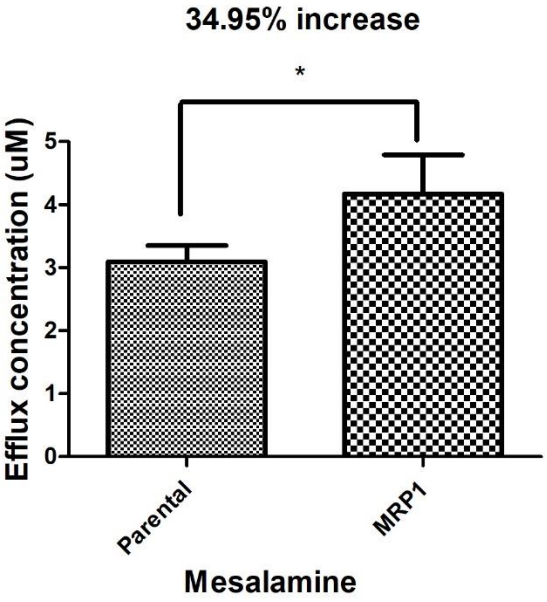
34.95% increase
*
Efflux concentration (uM)
0
1
2
3
4
5
Parental
MRP1
Mesalamine

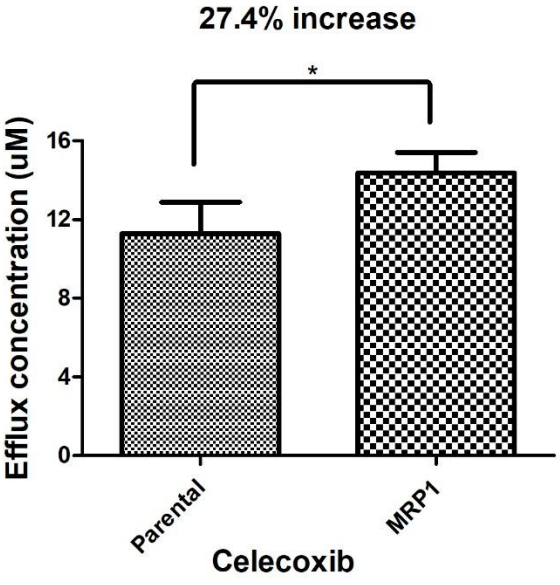
27.4% increase
*
Efflux concentration (uM)
0
4
8
12
16
Parental
MRP1
Celecoxib

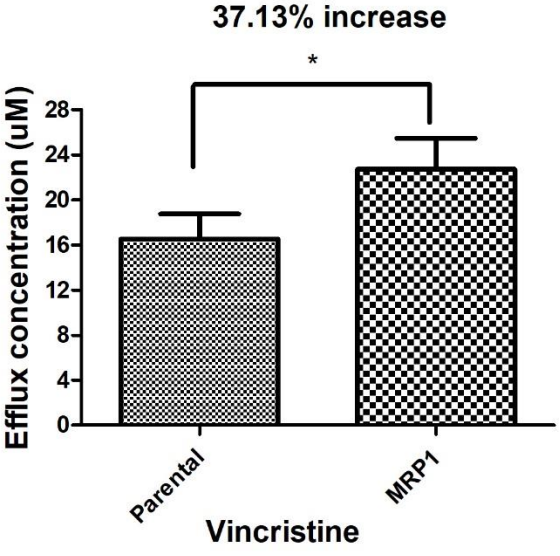
37.13% increase
*
Efflux concentration (uM)
0
4
8
12
16
20
24
28
Parental
MRP1
Vincristine

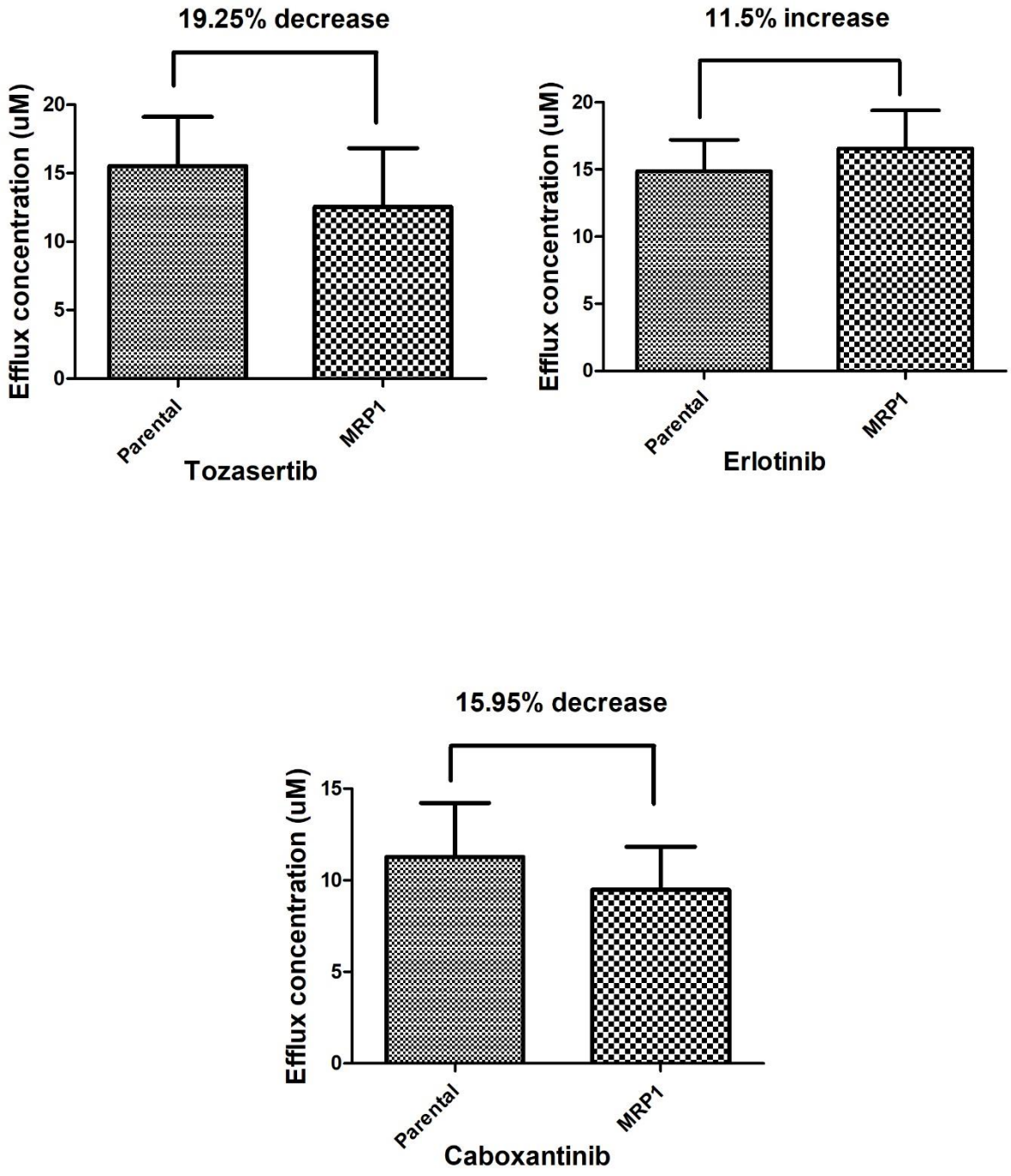

Figure 2.6. Efflux activity of MRP1-overexpressed and parental control cells on MRP1 modulators. Results are presented as average of three independent experiments. *P< 0.05 was considered statistically significant. Student's T test was performed to analyze the data.

2.4.1.3. MTT assay

To conduct an MTT assay, vincristine was used as control. The drug increased cell viability in MRP1-overexpressed cell line compared to parental cell line. Alisertib, mesalamine and celecoxib increased cell viability in MRP1-overexpressed cell lines. From the cell viability graph, difference in viability between two cell lines is clearly visible (Figure 2.7). For other drugs there is no considerable difference.

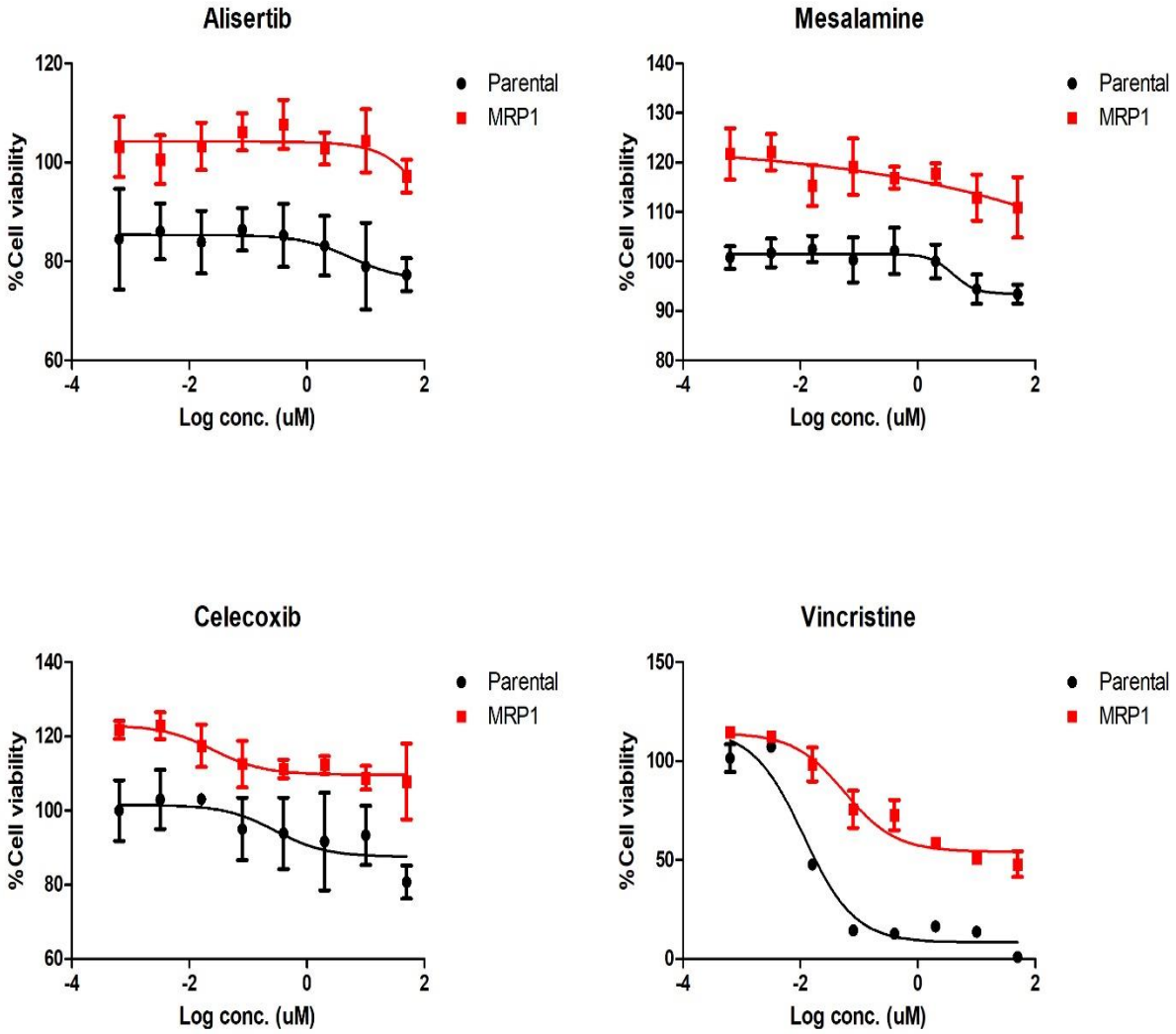

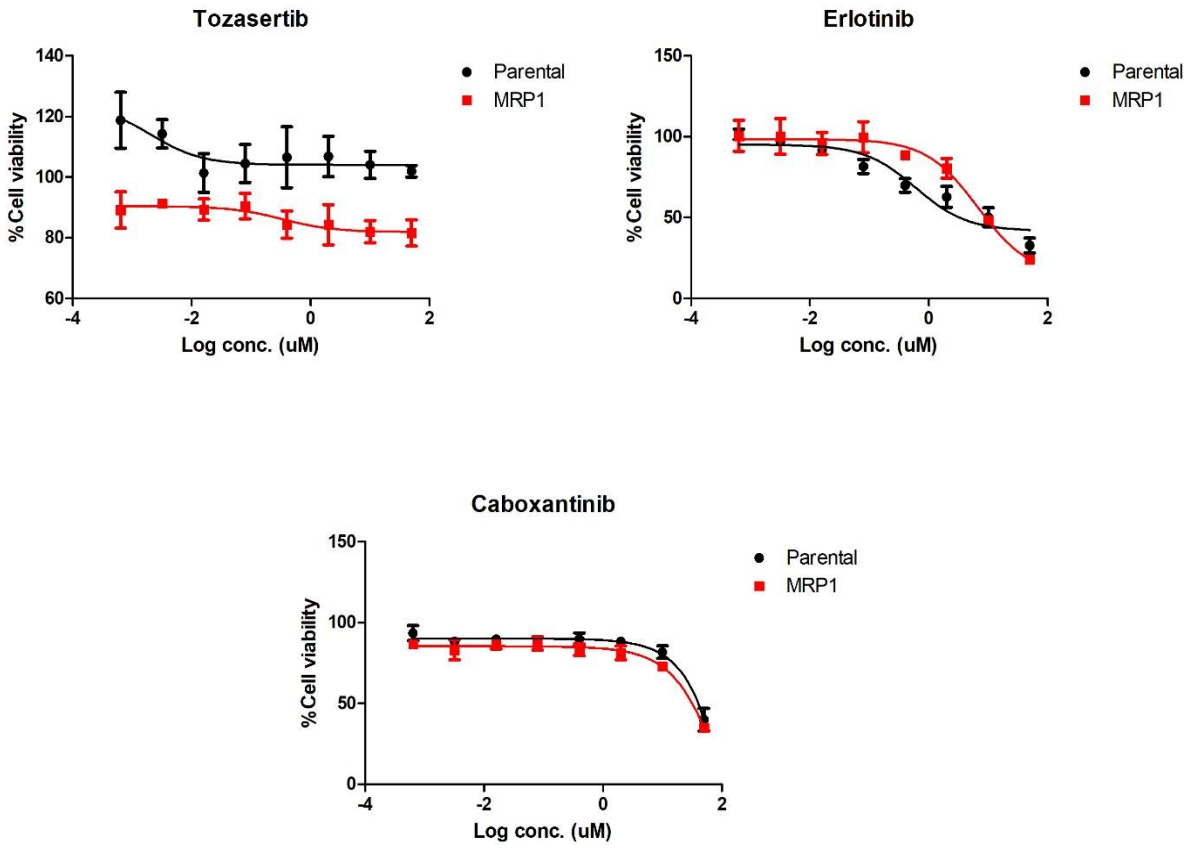

Figure 2.7. Cell viability in MRP1-overexpressed and parental cell line was determined using MTT assay. Results are presented as mean ± SD (n=3).

2.4.2. Substrate-MRP1 interaction using molecular modeling

Molecular modeling was performed for likely substrate drugs identified in the cell-based assays. We identified alisertib, mesalamine, and celecoxib as possible MRP1 substrates. It has been found that along with vincristine, three substrate likely drugs bind in the transmembrane region before being kicked out by MRP1 (Figure 2.8). In addition to evaluating the binding site using Discovery studio, we determined the possible amino acids that interact with the substrate drugs in the transmembrane binding site. All potential

substrate drugs, including vincristine, show hydrogen and hydrophobic type nonbonding interaction. The distance between nonbonding interaction between amino acids and different functional groups of drugs ranges from 2 to 5.5 angstrom (Figure 2.9-2.12, Table 2.3-2.6).

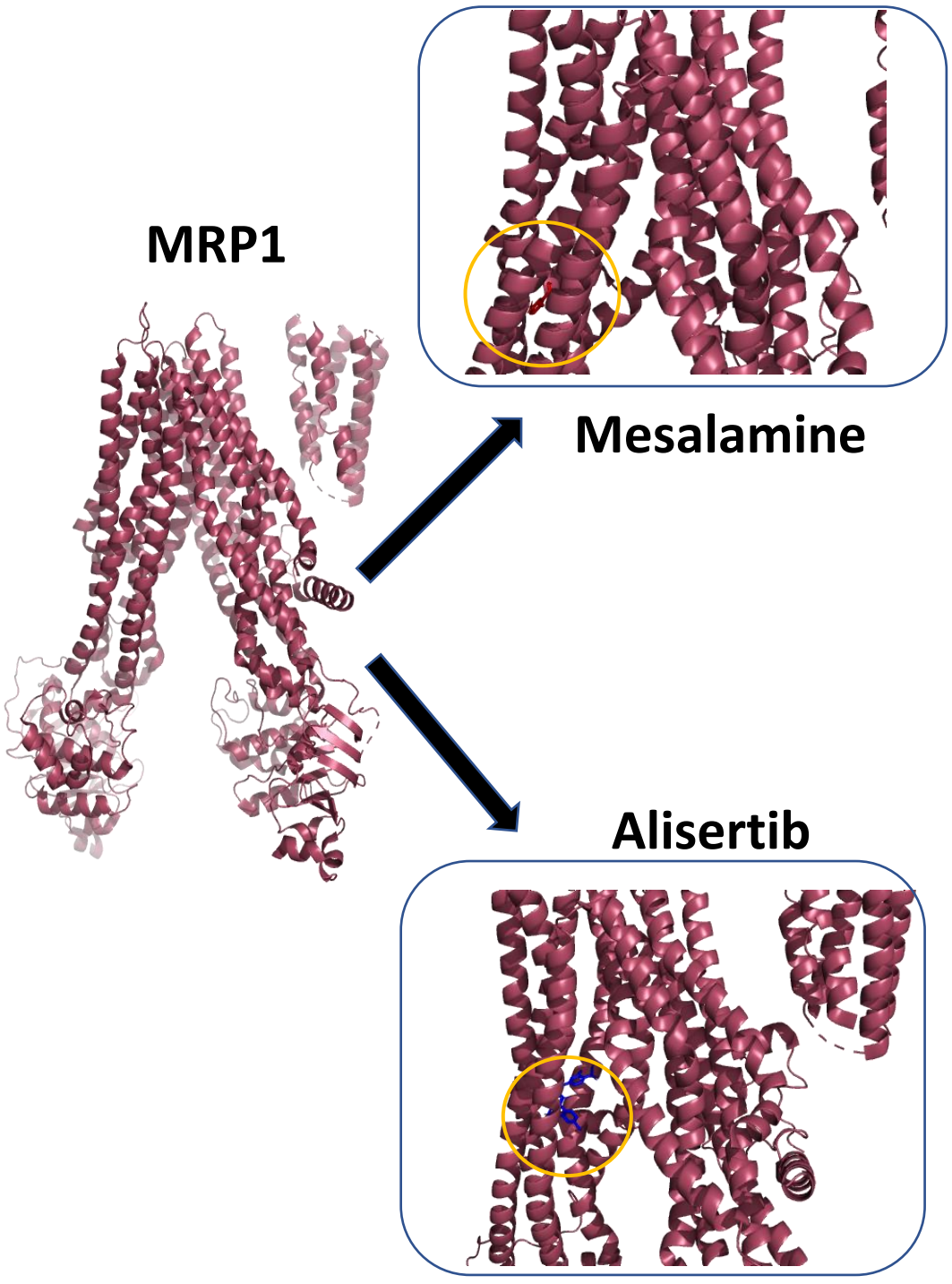

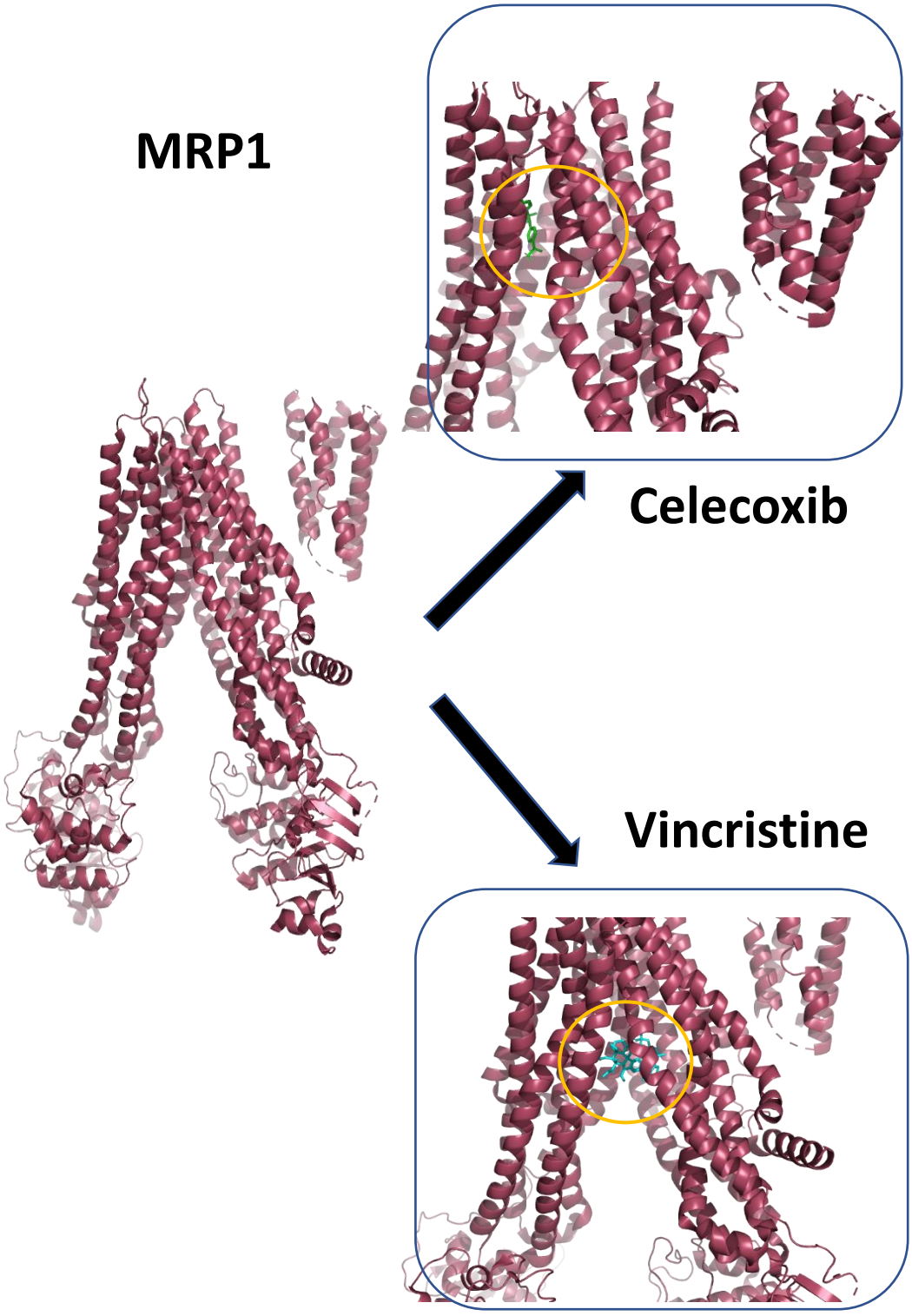

Figure 2.8. Binding site of alisertib, mesalamine, celecoxib, and vincristine in MRP1 (RCSB code: 5UJ9).

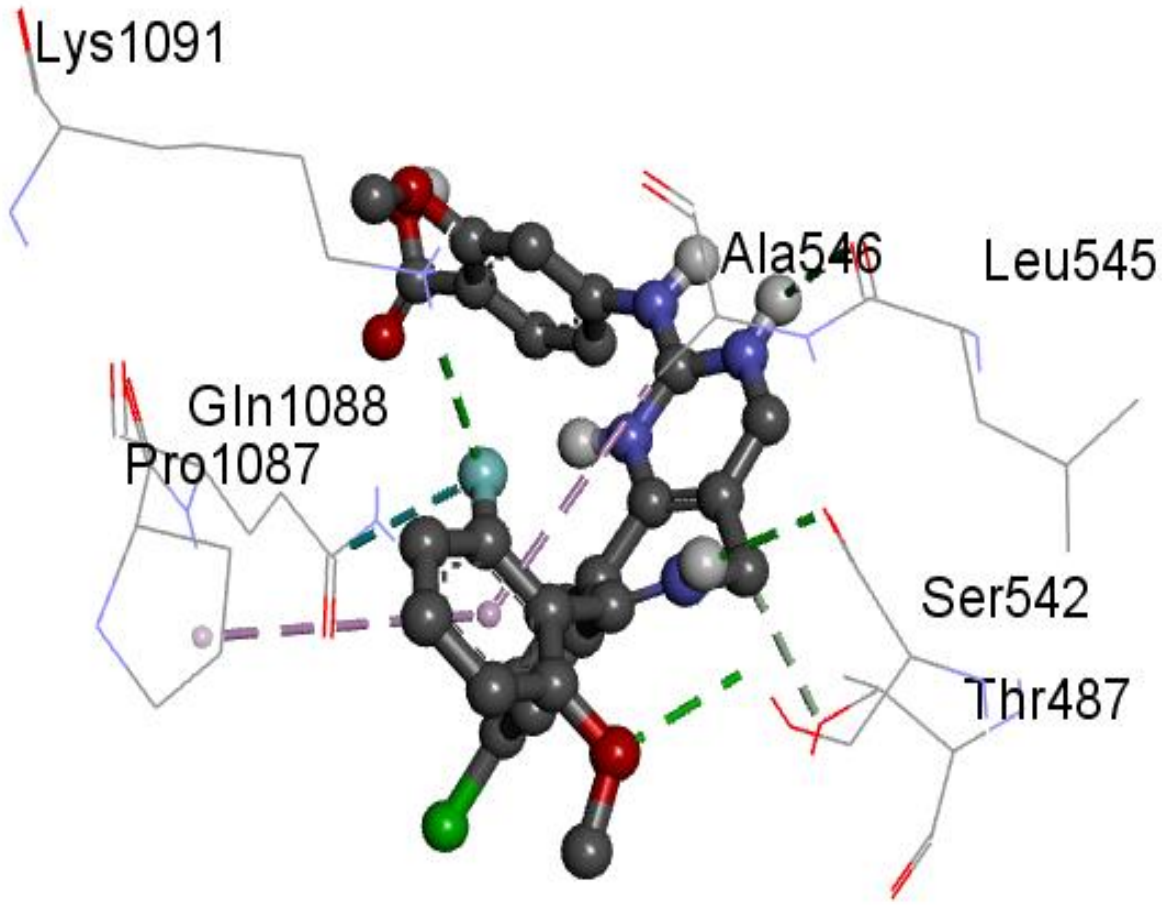

Figure 2.9. Ligand nonbonding interaction between alisertib and MRP1.

Table 2.3. List of amino acids, types of bonding interaction and bonding distance between MRP1 and alisertib.

Amino acids	**Bonding interaction**	**Distance**
Ser542	Hydrogen Bond	2.43837
Lys1091	Hydrogen Bond	2.65062
Leu545	Hydrogen Bond	2.97308
Thr487	Hydrogen Bond	2.87726
Gln1088	Electrostatic	3.64979

Ala546	Hydrophobic	4.26233
Pro1087	Hydrophobic	5.29246

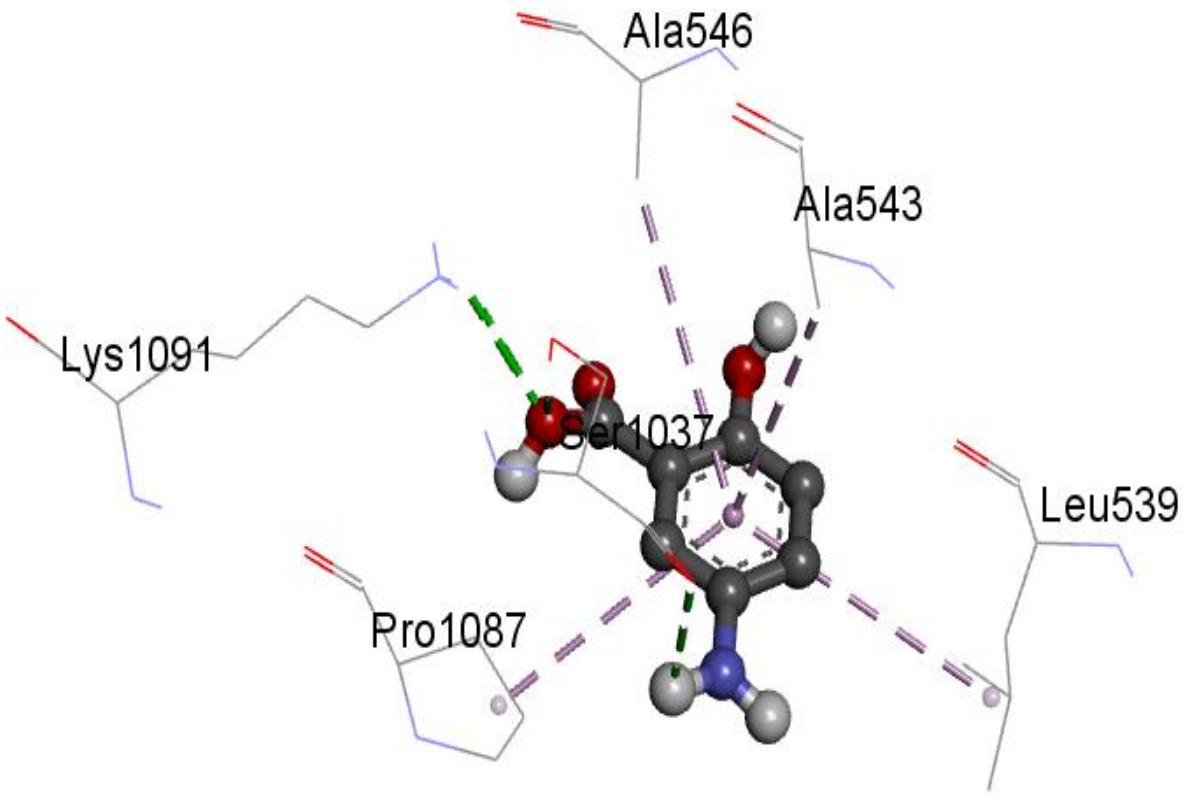

Figure 2.10. Ligand nonbonding interaction between mesalamine and MRP1.

Table 2.4. List of amino acids, types of bonding interaction and bonding distance between MRP1 and mesalamine.

Amino acids	**Bonding interaction**	**Distance**
Ser1037	Hydrogen Bond	1.68765
Lys1091	Hydrogen Bond	2.43794

Leu539	Hydrophobic	5.47189
Ala543	Hydrophobic	4.5404
Ala546	Hydrophobic	5.47976
Pro1087	Hydrophobic	5.07406

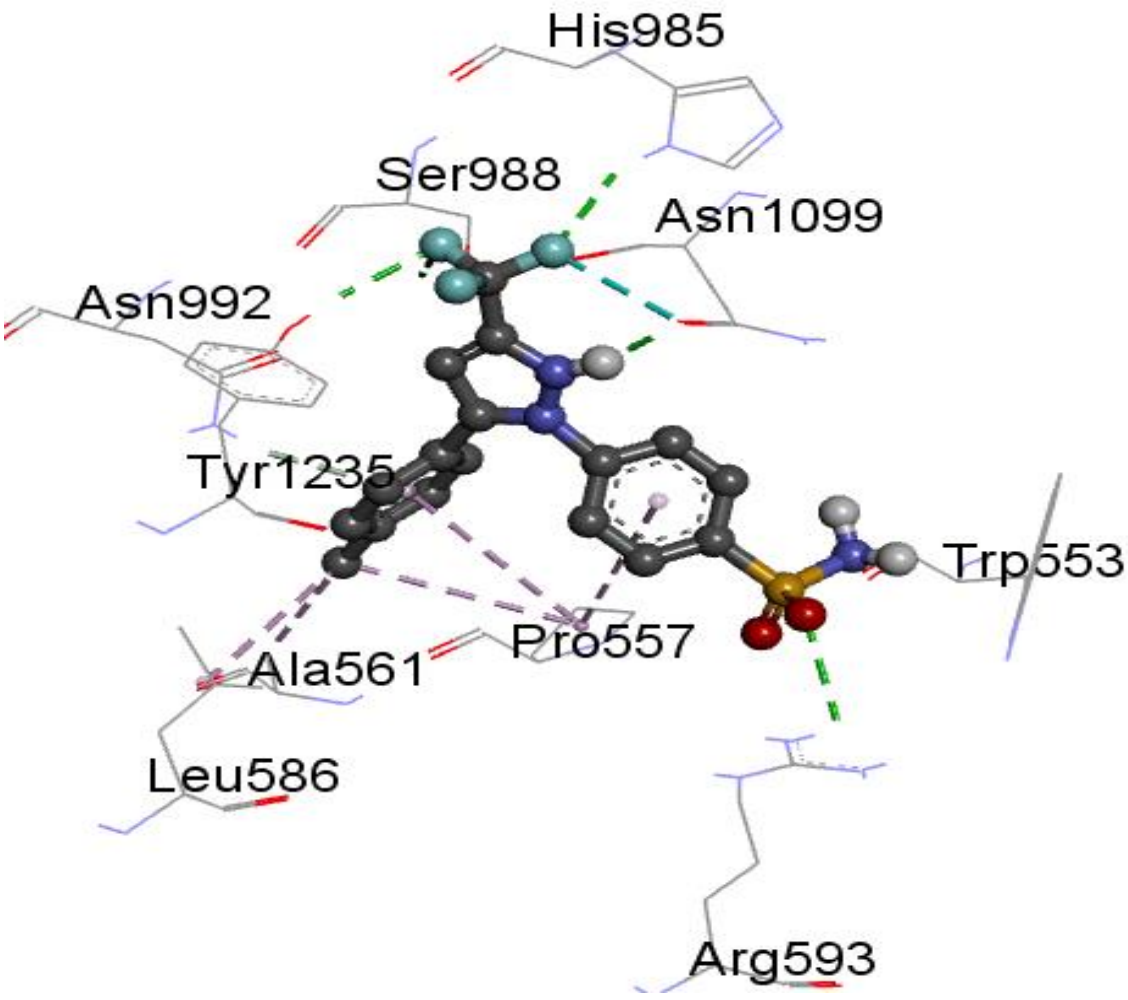

Figure 2.11. Ligand nonbonding interaction between celecoxib and MRP1.

Table 2.5. List of amino acids, types of bonding interaction and bonding distance between MRP1 and celecoxib.

Amino acids	**Bonds**	**Distance**
Arg593	Hydrogen Bond	2.68273
His985	Hydrogen Bond	2.54941
Ser988	Hydrogen Bond	2.52688
Tyr1235	Hydrogen Bond	2.38311
Asn1099	Hydrogen	2.95291
Asn992	Hydrogen Bond	3.0472
Ala561	Hydrophobic	3.86346
Pro557	Hydrophobic	4.96097
Leu586	Hydrophobic	4.34856
Trp553	Hydrophobic	4.94738

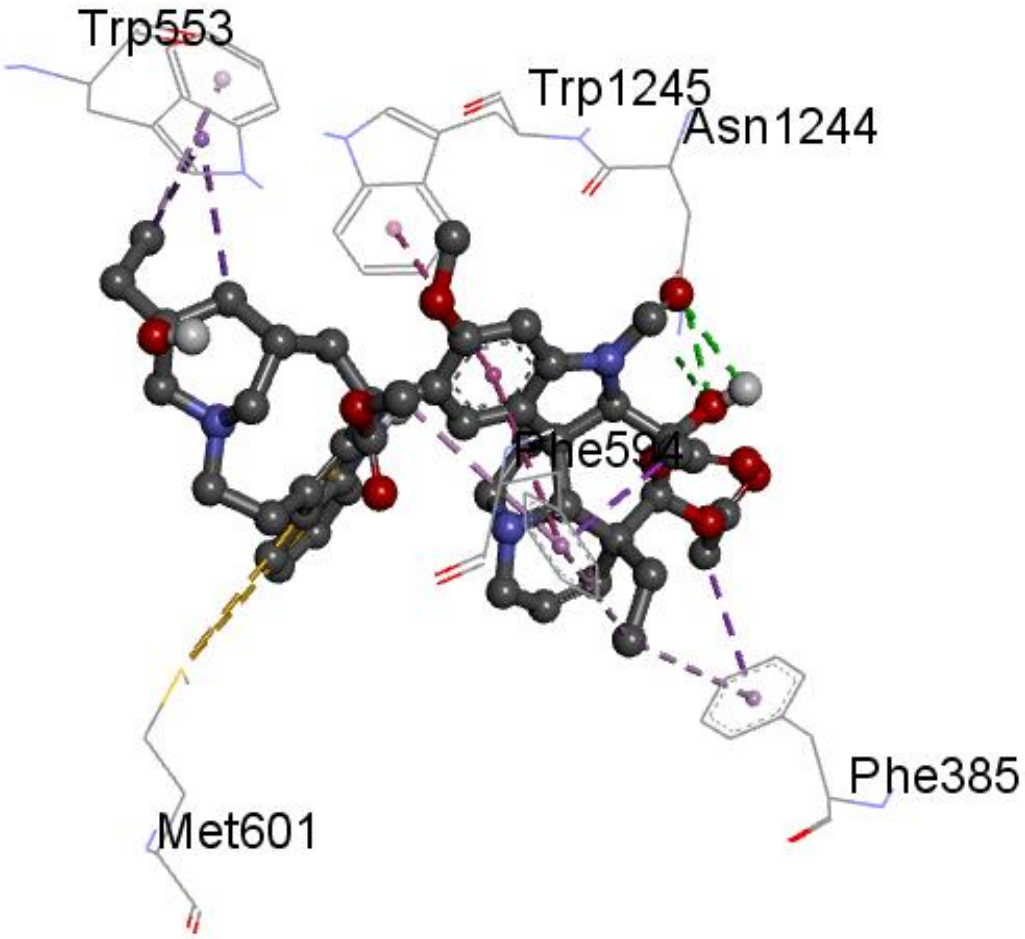

Figure 2.12. Ligand nonbonding interaction between vincristine and MRP1.

Table 2.6. List of amino acids, types of bonding interaction and bonding distance between MRP1 and vincristine.

Amino acids	**Bonding interaction**	**Distance**
Asn1244	Hydrogen Bond	2.52703
Trp553	Hydrophobic	3.63343

Phe594	Hydrophobic	3.50377
Phe385	Hydrophobic	3.80989
Trp1245	Hydrophobic	4.74317
Met601	Other	5.67833

2.4.3. Discussion

Here our main goal is to show direct efflux of potential substrate chemotherapeutic agents by MRP1-overexpressed cells. We developed a novel cell-based efflux assay using MDCKII MRP1 and its parental cell lines. After performing the experiment, we employed HPLC-UV to detect and quantify the amount of excreted drugs by both cell lines in fresh HBSS buffer. By using this method, we can directly determine the possible MRP1 substrates.

Using a known MRP1 substrate drug vincristine we found that our novel protocol shows efficacy in detecting difference of efflux between MRP1 overexpressed and parental cell line. The result is statistically significant. MRP1 considers vincristine as substrate and pumps out from the cancer cells [33]. Moreover, it has been found that beside being kicked out, vincristine also participate in overexpression of MRP1 [34]. For alisertib we found that MRP1 pumps out 50 % more in MRP1 overexpressed cells than parental control cells. The difference in terms of efflux is statistically significant. Alisertib is a known aurora kinase inhibitor and it is normally developed by Takeda Pharmaceuticals to treat T cell

lymphoma [35,36]. Iram et al conducted a screening study and found that it inhibited MRP1-mediated doxorubicin and $E_2$17βG efflux across the cellular membrane. The study provides substantial evidence of MRP1 interaction with alisertib and might behave as MRP1 inhibitor [21]. From the current experiment, it is clear that the drug it might work as a MRP1 substrate because the MRP1-overexpressed cells pump out statistically significant amounts of drug than control cells. Mesalamine is also sensitive to MRP1 efflux activity. Iram et al reported that mesalamine (hit molecule from National Clinical Collection) interacted with two color MRP1 in a screening assay. In that experiment structure changes during MRP1-mesalamine interaction were detected and recorded by fluorescence energy transfer [20]. For celecoxib, difference in efflux activity between MRP1-overexpressing cells and parental cells was found to be considerable. Iram et al reported celecoxib works as an MRP1 inhibitor. As a NSAID the drug selectively inhibits COX-2. Its primary function is to reduce and control gastrointestinal bleeding [21]. Based on the discussion above we can propose that compared to vincristine, these drugs are likely substrates of MRP1-mediated efflux. Tozasertib, erlotinib, and caboxantinib did not exhibit considerable variation in efflux rate between the two cell lines. To confirm and validate our novel protocol, we performed MTT cell viability assay. For alisertib, mesalamine, and tozasertib, cell viability was high in MRP1-overexpressed cells compared to parental cells and it produced a dose dependent curve. For other drugs, difference in cell viability was not considerable. We also demonstrated nonbonding interaction between substrate drugs and MRP1 before being pumped out from the cells (Table 2.3-2.6, Figure 2.8-2.12). Several reasons might influence the pumping activity of MRP1 on substrate likely drugs such as low affinity, hydrophilicity, hydrophobicity and single bipartite substrate-binding site of

MRP1 [8,9,37]. Further *in vivo* studies are warranted to justify the substrate relationship with MRP1 for alisertib, mesalamine, and celecoxib. The novel protocol will assist in the design and development of selective MRP1 inhibitors to overcome MRP1-mediated MDR for these substrate likely drugs.

Our newly developed protocol has several advantages over other traditional methods. It is simple, easy to follow, and avoids complexity to perform. We do not need any sophisticated or expensive instrument to detect MRP1 substrates. The protocol just needs two cell line to perform the experiment. In the last final step of experiment, drugs are detected and quantified by HPLC-UV. The difference in efflux rate between the two cell lines are expressed as statistically significant. Moreover, the experiment is validated by MTT assay. As this is a preliminary protocol and all the drugs have positive logP value, we used alisertib to optimize and select incubation time points. If someone wants to follow our protocol, we suggest optimizing incubation time points for each new drug. The novel protocol will assist drug discovery scientist to detect new substrates of MRP1, as well as substrates of other prominent ABC transporters. Moreover, it will aid in the development of novel ABC-transporter inhibitors.

2.5. Conclusion

We developed an easy-to-follow cell-based efflux method to detect MRP1 substates. Here we showed direct interaction of MRP1 with its substrate likely drugs. We found for some modulator drugs, MRP1 actively pump them out from the cells. We employed HPLC-UV to detect and quantify the drugs. One key feature of this protocol is that we exclusively focused on extracellular drug concentration pumped put by MRP1. This strategy avoids complex intracellular drug concentration measurement. The protocol will the pave the way

for development of advanced *in vitro* and *in vivo* substrate-selective MPR1-deficient and overexpressed efflux models. LCMS based identification and quantification will increase accuracy of the protocol. In a nutshell, the novel protocol will assist cancer scientist to detect resistance in chemotherapy, develop novel ABC transporter inhibitor and identify non substrate chemotherapeutic agents.

2.6. References

[1] K.E. Sampson, A. Brinker, J. Pratt, N. Venkatraman, Y. Xiao, J. Blasberg, T. Steiner, M. Bourner, D.C. Thompson, Zinc finger nuclease-mediated gene knockout results in loss of transport activity for P-glycoprotein, BCRP, and MRP2 in Caco-2 cells., Drug Metab. Dispos. 43 (2015) 199–207. https://doi.org/10.1124/dmd.114.057216.

[2] S.E.B. Ambjorner, M. Wiese, S.C. Kohler, J. Svindt, X.L. Lund, M. Gajhede, L. Saaby, B. Brodin, S. Rump, H. Weigt, N. Brunner, J. Stenvang, The Pyrazolo[3,4-d]pyrimidine Derivative, SCO-201, Reverses Multidrug Resistance Mediated by ABCG2/BCRP., Cells. 9 (2020). https://doi.org/10.3390/cells9030613.

[3] X. Ming, B.M. Knight, D.R. Thakker, Vectorial transport of fexofenadine across Caco-2 cells: involvement of apical uptake and basolateral efflux transporters., Mol. Pharm. 8 (2011) 1677–1686. https://doi.org/10.1021/mp200026v.

[4] K.L.R. Brouwer, D. Keppler, K.A. Hoffmaster, D.A.J. Bow, Y. Cheng, Y. Lai, J.E. Palm, B. Stieger, R. Evers, In vitro methods to support transporter evaluation in drug discovery and development., Clin. Pharmacol. Ther. 94 (2013) 95–112. https://doi.org/10.1038/clpt.2013.81.

[5] G. Pottier, S. Marie, S. Goutal, S. Auvity, M.-A. Peyronneau, S. Stute, R. Boisgard, F. Dolle, I. Buvat, F. Caille, N. Tournier, Imaging the Impact of the P-Glycoprotein (ABCB1) Function on the Brain Kinetics of Metoclopramide., J. Nucl. Med. 57 (2016) 309–314. https://doi.org/10.2967/jnumed.115.164350.

[6] B.G. Peterson, K.W. Tan, B. Osa-Andrews, S.H. Iram, High-content screening of clinically tested anticancer drugs identifies novel inhibitors of human MRP1 (ABCC1)., Pharmacol. Res. 119 (2017) 313–326. https://doi.org/10.1016/j.phrs.2017.02.024.

[7] S.H. Iram, S.P.C. Cole, Differential functional rescue of Lys(513) and Lys(516) processing mutants of MRP1 (ABCC1) by chemical chaperones reveals different domain-domain interactions of the transporter., Biochim. Biophys. Acta. 1838 (2014) 756–765. https://doi.org/10.1016/j.bbamem.2013.11.002.

[8] E. Gozalpour, R. Greupink, A. Bilos, V. Verweij, J.J.M.W. van den Heuvel, R. Masereeuw, F.G.M. Russel, J.B. Koenderink, Convallatoxin: a new P-glycoprotein substrate., Eur. J. Pharmacol. 744 (2014) 18–27. https://doi.org/10.1016/j.ejphar.2014.09.031.

[9] E. Gozalpour, M.J. Wilmer, A. Bilos, R. Masereeuw, F.G.M. Russel, J.B. Koenderink, Heterogeneous transport of digitalis-like compounds by P-glycoprotein in vesicular and cellular assays., Toxicol. In Vitro. 32 (2016) 138–145. https://doi.org/10.1016/j.tiv.2015.12.009.

[10] S. Shukla, H. Zaher, A. Hartz, B. Bauer, J.A. Ware, S. V Ambudkar, Curcumin inhibits the activity of ABCG2/BCRP1, a multidrug resistance-linked ABC drug

transporter in mice., Pharm. Res. 26 (2009) 480–487. https://doi.org/10.1007/s11095-008-9735-8.

[11] M. Patel, Y. Sheng, N.K. Mandava, D. Pal, A.K. Mitra, Dipeptide prodrug approach to evade efflux pumps and CYP3A4 metabolism of lopinavir., Int. J. Pharm. 476 (2014) 99–107. https://doi.org/10.1016/j.ijpharm.2014.09.035.

[12] K.L. Fung, A.K. Tepede, K.M. Pluchino, L.M. Pouliot, J.N. Pixley, M.D. Hall, M.M. Gottesman, Uptake of compounds that selectively kill multidrug-resistant cells: the copper transporter SLC31A1 (CTR1) increases cellular accumulation of the thiosemicarbazone NSC73306., Mol. Pharm. 11 (2014) 2692–2702. https://doi.org/10.1021/mp500114e.

[13] W. Zhou, X. Zhang, C. Cheng, F. Wang, X. Wang, Y. Liang, K.K.W. To, W. Zhou, H. Huang, L. Fu, Crizotinib (PF-02341066) reverses multidrug resistance in cancer cells by inhibiting the function of P-glycoprotein., Br. J. Pharmacol. 166 (2012) 1669–1683. https://doi.org/10.1111/j.1476-5381.2012.01849.x.

[14] G. Valdameri, L. Pereira Rangel, C. Spatafora, J. Guitton, C. Gauthier, O. Arnaud, A. Ferreira-Pereira, P. Falson, S.M.B. Winnischofer, M.E.M. Rocha, C. Tringali, A. Di Pietro, Methoxy stilbenes as potent, specific, untransported, and noncytotoxic inhibitors of breast cancer resistance protein., ACS Chem. Biol. 7 (2012) 322–330. https://doi.org/10.1021/cb200435y.

[15] Z. Duan, J. Zhang, S. Ye, J. Shen, E. Choy, G. Cote, D. Harmon, H. Mankin, Y. Hua, Y. Zhang, N.S. Gray, F.J. Hornicek, A-770041 reverses paclitaxel and doxorubicin resistance in osteosarcoma cells., BMC Cancer. 14 (2014) 681. https://doi.org/10.1186/1471-2407-14-681.

[16] F. Shen, S. Chu, A.K. Bence, B. Bailey, X. Xue, P.A. Erickson, M.H. Montrose, W.T. Beck, L.C. Erickson, Quantitation of doxorubicin uptake, efflux, and modulation of multidrug resistance (MDR) in MDR human cancer cells., J. Pharmacol. Exp. Ther. 324 (2008) 95–102. https://doi.org/10.1124/jpet.107.127704.

[17] D.A. Parasrampuria, M. V Lantz, L.Z. Benet, A human lymphocyte based ex vivo assay to study the effect of drugs on P-glycoprotein (P-gp) function., Pharm. Res. 18 (2001) 39–44. https://doi.org/10.1023/a:1011070509191.

[18] K.W. Tan, A. Sampson, B. Osa-Andrews, S.H. Iram, Calcitriol and Calcipotriol Modulate Transport Activity of ABC Transporters and Exhibit Selective Cytotoxicity in MRP1-overexpressing Cells., Drug Metab. Dispos. 46 (2018) 1856–1866. https://doi.org/10.1124/dmd.118.081612.

[19] A. Krishan, C.M. Fitz, I. Andritsch, Drug retention, efflux, and resistance in tumor cells., Cytometry. 29 (1997) 279–285.

[20] S.H. Iram, S.J. Gruber, O.N. Raguimova, D.D. Thomas, S.L. Robia, ATP-Binding Cassette Transporter Structure Changes Detected by Intramolecular Fluorescence Energy Transfer for High-Throughput Screening., Mol. Pharmacol. 88 (2015) 84–94. https://doi.org/10.1124/mol.114.096792.

[21] A. Sampson, B.G. Peterson, K.W. Tan, S.H. Iram, Doxorubicin as a fluorescent reporter identifies novel MRP1 (ABCC1) inhibitors missed by calcein-based high content screening of anticancer agents., Biomed. Pharmacother. 118 (2019) 109289. https://doi.org/10.1016/j.biopha.2019.109289.

[22] B. Osa-Andrews, K.W. Tan, A. Sampson, S.H. Iram, Development of Novel Intramolecular FRET-Based ABC Transporter Biosensors to Identify New Substrates and Modulators., Pharmaceutics. 10 (2018). https://doi.org/10.3390/pharmaceutics10040186.

[23] Y. Dong, H. Liao, J. Yu, H. Fu, D. Zhao, K. Gong, Q. Wang, Y. Duan, Incorporation of drug efflux inhibitor and chemotherapeutic agent into an inorganic/organic platform for the effective treatment of multidrug resistant breast cancer., J. Nanobiotechnology. 17 (2019) 125. https://doi.org/10.1186/s12951-019-0559-y.

[24] Z. Duan, E. Choy, F.J. Hornicek, NSC23925, identified in a high-throughput cell-based screen, reverses multidrug resistance., PLoS One. 4 (2009) e7415. https://doi.org/10.1371/journal.pone.0007415.

[25] D. Cihalova, F. Staud, M. Ceckova, Interactions of cyclin-dependent kinase inhibitors AT-7519, flavopiridol and SNS-032 with ABCB1, ABCG2 and ABCC1 transporters and their potential to overcome multidrug resistance in vitro., Cancer Chemother. Pharmacol. 76 (2015) 105–116. https://doi.org/10.1007/s00280-015-2772-1.

[26] J. Mo, M. Kang, J.-X. Ye, J.-B. Chen, H.-B. Zhang, C. Qing, Gibberellin derivative GA-13315 sensitizes multidrug-resistant cancer cells by antagonizing ABCB1 while agonizes ABCC1., Cancer Chemother. Pharmacol. 78 (2016) 51–61. https://doi.org/10.1007/s00280-016-3051-5.

[27] I. Akan, S. Akan, H. Akca, B. Savas, T. Ozben, Multidrug resistance-associated protein 1 (MRP1) mediated vincristine resistance: effects of N-acetylcysteine and Buthionine sulfoximine., Cancer Cell Int. 5 (2005) 22. https://doi.org/10.1186/1475-2867-5-22.

[28] S.Y. Eid, M.A. Althubiti, M.E. Abdallah, M. Wink, M.Z. El-Readi, The carotenoid fucoxanthin can sensitize multidrug resistant cancer cells to doxorubicin via induction of apoptosis, inhibition of multidrug resistance proteins and metabolic enzymes, Phytomedicine. 77 (2020) 153280. https://doi.org/https://doi.org/10.1016/j.phymed.2020.153280.

[29] A.K. Nanayakkara, C.A. Follit, G. Chen, N.S. Williams, P.D. Vogel, J.G. Wise, Targeted inhibitors of P-glycoprotein increase chemotherapeutic-induced mortality of multidrug resistant tumor cells., Sci. Rep. 8 (2018) 967. https://doi.org/10.1038/s41598-018-19325-x.

[30] R.J. Kathawala, K. Sodani, K. Chen, A. Patel, A.H. Abuznait, N. Anreddy, Y.-L. Sun, A. Kaddoumi, C.R.J. Ashby, Z.-S. Chen, Masitinib antagonizes ATP-binding cassette subfamily C member 10-mediated paclitaxel resistance: a preclinical

study., Mol. Cancer Ther. 13 (2014) 714–723. https://doi.org/10.1158/1535-7163.MCT-13-0743.

[31] M. Ravi, V. Paramesh, S.R. Kaviya, E. Anuradha, F.D.P. Solomon, 3D cell culture systems: advantages and applications., J. Cell. Physiol. 230 (2015) 16–26. https://doi.org/10.1002/jcp.24683.

[32] A.S. Nunes, A.S. Barros, E.C. Costa, A.F. Moreira, I.J. Correia, 3D tumor spheroids as in vitro models to mimic in vivo human solid tumors resistance to therapeutic drugs., Biotechnol. Bioeng. 116 (2019) 206–226. https://doi.org/10.1002/bit.26845.

[33] D.R. Hipfner, R.G. Deeley, S.P.C. Cole, Structural, mechanistic and clinical aspects of MRP1, Biochim. Biophys. Acta - Biomembr. 1461 (1999) 359–376. https://doi.org/https://doi.org/10.1016/S0005-2736(99)00168-6.

[34] C.A. Slapak, P.M. Fracasso, R.L. Martell, D.L. Toppmeyer, J.M. Lecerf, S.B. Levy, Overexpression of the multidrug resistance-associated protein (MRP) gene in vincristine but not doxorubicin-selected multidrug-resistant murine erythroleukemia cells., Cancer Res. 54 (1994) 5607–5613.

[35] V. Sehdev, D. Peng, M. Soutto, M.K. Washington, F. Revetta, J. Ecsedy, A. Zaika, T.T. Rau, R. Schneider-Stock, A. Belkhiri, W. El-Rifai, The aurora kinase A inhibitor MLN8237 enhances cisplatin-induced cell death in esophageal adenocarcinoma cells., Mol. Cancer Ther. 11 (2012) 763–774. https://doi.org/10.1158/1535-7163.MCT-11-0623.

[36] G. Görgün, E. Calabrese, T. Hideshima, J. Ecsedy, G. Perrone, M. Mani, H. Ikeda, G. Bianchi, Y. Hu, D. Cirstea, L. Santo, Y.-T. Tai, S. Nahar, M. Zheng, M. Bandi, R.D. Carrasco, N. Raje, N. Munshi, P. Richardson, K.C. Anderson, A novel Aurora-A kinase inhibitor MLN8237 induces cytotoxicity and cell-cycle arrest in multiple myeloma., Blood. 115 (2010) 5202–5213. https://doi.org/10.1182/blood-2009-12-259523.

[37] Z.L. Johnson, J. Chen, Structural Basis of Substrate Recognition by the Multidrug Resistance Protein MRP1., Cell. 168 (2017) 1075-1085.e9. https://doi.org/10.1016/j.cell.2017.01.041.

CHAPTER THREE: SPECTROSCOPIC AND BIOLOGICAL ACTIVITIES OF ETHYL GALLATE BASED THEDES

3.1. Introduction

Due to their low toxicity, straightforward manufacturing process, affordable starting material, and biodegradability, deep eutectic solvents (DES) are becoming a popular choice as an alternative of ionic liquid solvents. Lowering the melting point of a combination is a result of mixing two or more components. Tertiary DES mixing is less frequent than binary DES mixture. It is made by combining one hydrogen bond acceptor (quaternary salt) with another hydrogen bond donor in a specific molar ratio. The novel solvent has a low melting point, which is lower than the melting points of the raw materials needed to make DES.

Ionic liquids have become viable solvent systems in analytical chemistry over the past ten years. In the domains of biotechnology, pharmacology, environmental research, and medical science, it has a variety of uses. In order to improve transdermal permeability, the solubility of active pharmaceutical components, and the synthesis of drug candidates, ionic liquid is used in drug discovery and development research. Despite certain commendable qualities, it has drawbacks such as high synthesis costs, low biodegradability, poor biocompatibility, and toxic effects to vital cellular organelles. Due to its advantages over ionic liquids, DES is quickly becoming a highly promising class of green solvent. DES emerged as a desirable class among many deep eutectic solvent types. It became a crucial component in several scientific domains.

Another class of emerging practical deep eutectic solvents that achieved a breakthrough is therapeutic deep eutectic solvents. Active pharmaceutical ingredient (API) and another component are combined and then heated to create THEDES. It improves API's permeability, solubility, and stability. Additionally, THDES stops API from

recrystallizing. The API used in THEDES demonstrated potential for topical and transdermal drug delivery [1–5].

Correlation study between experimental studies and computational simulation employing molecular dynamics has recently received considerable interest, in addition to the numerous experimental results published on THEDES. It is feasible to explore in-depth atomic level interactive property between HBA and HBD using density functional theory, molecular dynamics, thermodynamics, PCA analysis, quantum calculation, favorable cluster analysis, and non-bonding interaction. [6] [7] [8].

Ethyl gallate (EG) is a plant metabolite and it is a naturally occurring antioxidant present is many plants sources [9]. The phytochemical has a diverse range of pharmacological properties. It is used as a food additive antioxidant [10,11]. It shows anti-atherosclerosis activity by blocking the early stage of the plaque formation. The mechanism underlying this activity might be due to the efflux of HDL cholesterol and suppression of cytokine activity [12]. Ethyl gallate rich *A. nilotica* leaf ethanolic extract showed as EC_{50} of 40 µg/mL against the human carcinoma cell line KB. The underlying mechanism of this therapeutic activity might be due to affecting the DNA and progressing to apoptosis [13]. Treatment with EG significantly inhibit histopathological changes in lung and attenuate edema formation in LPS-induced pulmonary injury in the rat model [14]. EG can bind with ERK1 and 2 and work as a novel inhibitor of both receptors. As a result it suppresses the growth of both anchorage dependent and independent growth of esophageal cancer cells [15]. It has been found that ethyl gallate decreases MDA-MB-231 and MCF-7 breast cancer cell proliferation in a dose dependent manner through Akt-

NF-κB signaling [16]. In terms of solubility EG is slightly water soluble [17]. It showed high solubility in ethanol and DMSO [18].

In this project our prime research interest is mainly focused on formulation of novel THDESs where ethyl gallate is used as primary ingredient and analysis of physicochemical, structural, and spectroscopic properties of the new formulations using experimental and computational approaches. After that cell-based assays will be conducted to assess biological activity. The new formulations will significantly increase the solubility and bioavailability of ethyl gallate. It will lead to breakthrough in pharmaceutical drug development and delivery research.

3.2. Materials and Methods

3.2.1. Chemicals

Acetonitrile (ACN) was purchased from Thermo-Fischer Scientific (Dubuque, IA, USA). Choline chloride (ChCl), Acetylcholine chloride (AChCl), PEG-400, and glcerol were purchased from Acros Organics (USA) and Tex Lab Supply. All of the chemicals had purity ≥ 98%. Chemicals used for the *in-vitro* assay will be discussed in the cell line and cell culture subsection. Double distilled (DD) water was used for the solubility study. Ethyl gallate was purchased from Cayman chemicals.

3.2.2. Preparation of THEDES

Ethyl gallate was mixed with different biomolecules in a different molar ratio in order to formulate the solvent. Overall process is outlined below:

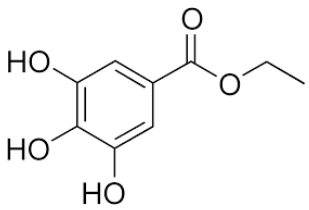

Ethyl gallate

Ethyl gallate was mixed with ChCl, AChCl, PEG 400 and glycerol in different molar ratios.

The mixtures were heated at 65°C with constant stirring (≤600 rpm) until ensuring the appearance of a homogeneous liquid mixture.

Observed for one day to ensure no possibility of crystal formation.

3.2.3. FTIR Spectroscopic Measurements

FTIR gives us necessary information about the major functional groups participated in nonbonding interactions. The flowchart given below describes the IR spectroscopic measurement process.

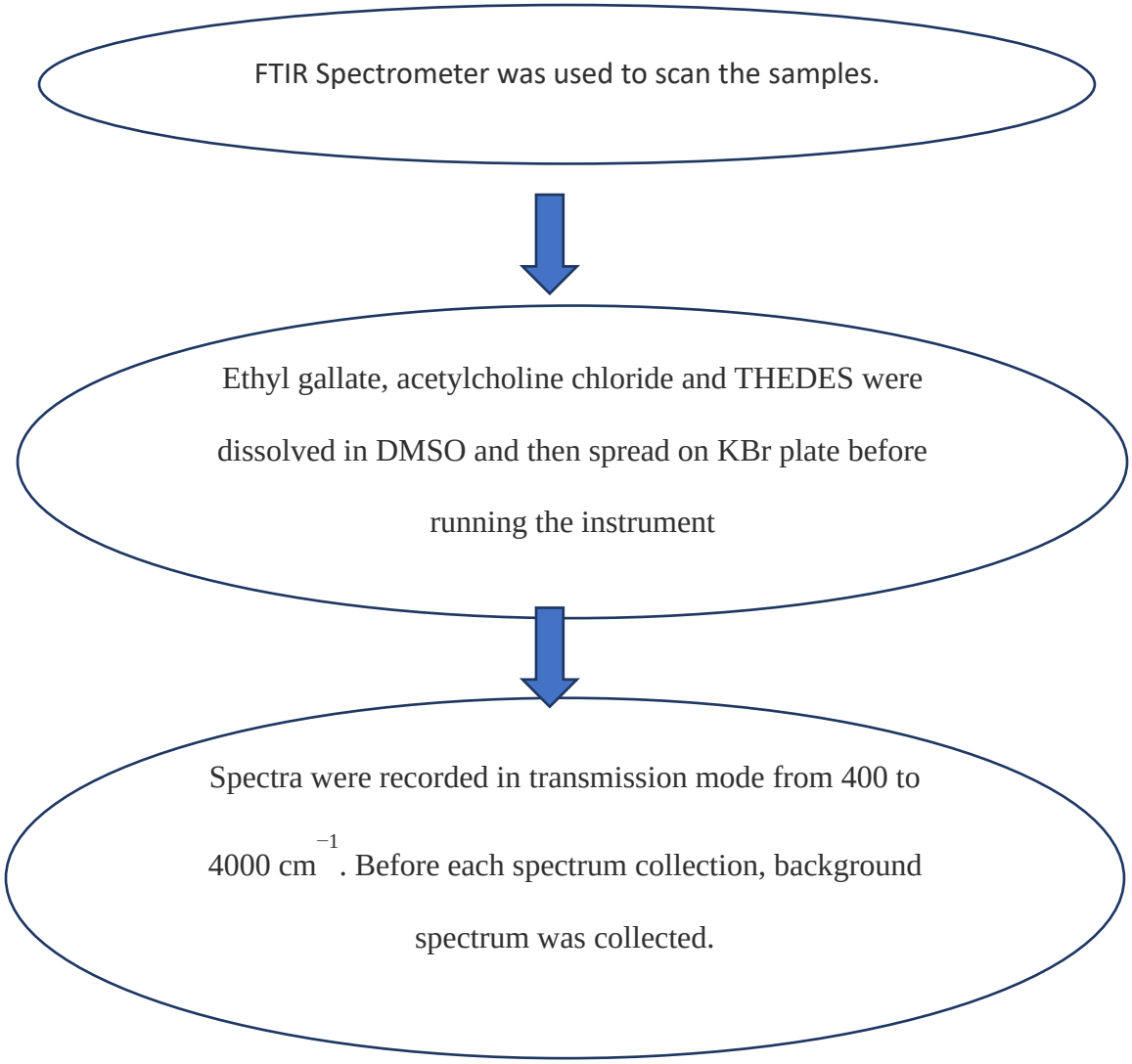

3.2.4. NMR Spectroscopic measurements

To conduct ^{1}H and ^{13}C NMR, the THEDES were dissolved in deuterated dimethyl sulfoxide and the chemical shift was measured in ppm (δ). The spectra were measured with a Bruker spectrometer (600 MHz). The outline is given below:

Samples were prepared by dissolving 200 mg in deuterated DMSO

Solution was transferred In NMR tubes

Proton and carbon NMR

Peak were analyzed using

BUKER 600MHz

3.2.5. Solubility Study

Saturated solution of EG and EG based THEDES were prepared in water. At first 1000 ppm solution of EG only was prepared to generate calibration curve. The EG powder and THEDES were added continuously in water until the disappearance of solute in the water. The solvation procedure continued until reaching the saturation point. It was observed for 48 hours to ensure that crystallization does not happen. All samples were filtered using a 0.2-µm filter and transferred to HPLC vials for further analysis (Figure 3.1).

Dionex UltiMate 3000 HPLC-UV was used to assess the solubility profiles of EG and EG-based THEDES in water. ZORBAX SB-C18 (4.6×75 mm i.d., particle size 3.5 µm) column was used to isolate peak. Injection volume was 5 µL.

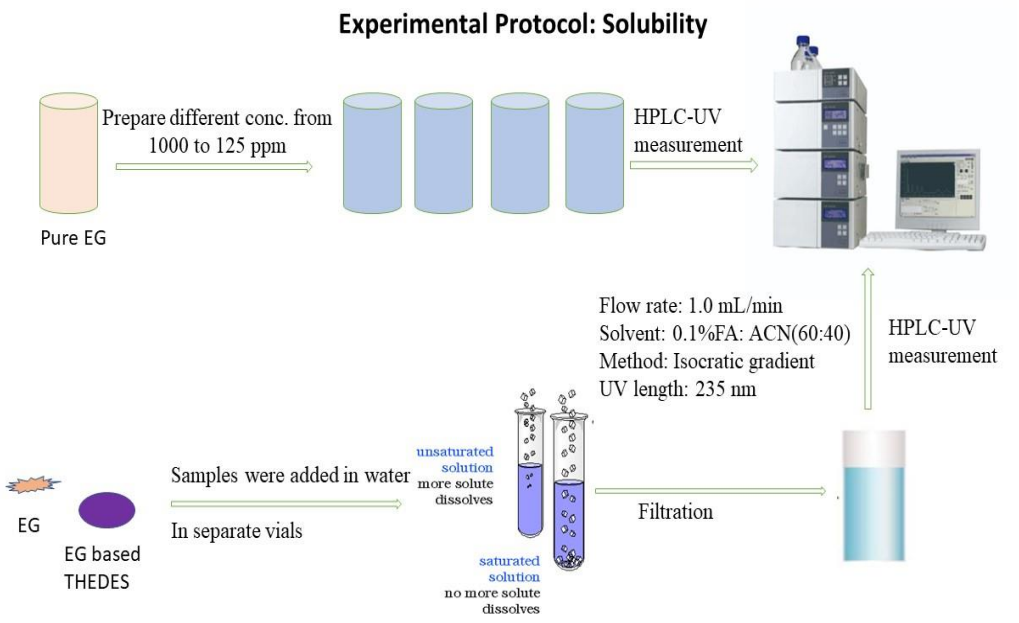

Figure 3.1. Outline of experimental procedure to measure solubility in water. Standard curve was generated by running pure ethyl gallate at different concentrations to calculate actual solubility of ethyl gallate based DES.

3.2.6. Computational Modeling

3.2.6.1. Molecular modeling calculations

The initial structures of ethyl gallate and acetylcholine chloride were optimized using molecular mechanics optimization tool in WebMO [19]. After optimization, electrostatic potential graph was generated, and energy parameters were calculated.

3.2.6.2. Molecular docking

Structure of ethyl gallate was collected from PubChem compound server. Structures of MRP1 (5UJ9), MUC1 (6BHB), HER2 (3PP0), and Akt (6HHG) were collected from RCSB databank and optimized using Swiss pdb viewer [20][21][22]. Finally docking was performed using PyRx. Docking pose were generated discovery studio and PyMol. Docking grid box parameters for MRP1 were as follows: (exhaustiveness = 8, center_x = 89.6944725892, center_y = 60.7344245156, center_z = 55.9919893333, size_x = 82.5463550749, size_y = 62.7802800506, size_z = 48.9755696918). Docking grid box parameters for Akt were as follows: (exhaustiveness = 8, center_x = 13.6093, center_y = -11.7637, center_z = -15.8331, size_x = 49.9149041843, size_y = 66.2937657166, size_z = 58.248783989). For mucin docking gridbox parameters were (exhaustiveness = 8, center_x = -2.4748, center_y = 25.6566, center_z = 4.0854, size_x = 39.6586597919, size_y = 42.2048911285, size_z = 32.259420166) and for HER2, docking parameters were (exhaustiveness = 8 center_x = 12.4648, center_y = 21.696, center_z = 34.0758, size_x = 59.7606887054, size_y = 47.3639290977, size_z = 57.6649198341).

3.2.7. Cell lines and cell culture

HEK-P, HEK-MRP1 and pancreatic cancer cells were cultured in Dulbecco’s modified Eagle’s medium (DMEM) (GE Healthcare Life Sciences, Logan, UT) complemented

with 10% v/v fetal bovine serum (FBS) (HycloneTM, GE Healthcare Life Sciences). Cell cultures were maintained at 37 °C in a humidified incubator supplied with 5 % CO_2.

3.2.7.1. Cell viability assay

Using MTT colorimetric assay the cytotoxic effect of THEDES was evaluated. In brief, HEK Parental and MRP1 overexpressed cells were plated into a 96-well plate (NEST®, Rahway, NJ) at a density of 5 x 10^4 cells/well in 100µL culture medium. For pancreatic cell line we plated 30,000 cells/well in 96-well plates. The next day, cells were treated with different concentrations (0.0084 µM to 1000 µM) of the DES and ethyl gallate in 100 µL of DMEM media. For pancreatic cancer cells we treated with 3.125 µM to 1000 µM. Cells incubated with media only were treated as control. Post-incubation for 72 h, 100 µL of culture medium was removed and cells were treated with 10 µL MTT dye (5 mg/ml in PBS) and incubated at 37°C for 4h. For pancreatic cell line we waited for two hours. The MTT formazan product was dissolved in 100 µL 15 % SDS containing 10mM HCl. For pancreatic cancer cell line 200 µL DMSO was added to each well to dissolve the formazan. Ethyl gallate was kept as the positive control to compare the effect of ethyl gallate DES. Before starting the experiment, 10mM pure ethyl gallate stock solution was prepared in DMSO. From this stock solution, working concentrations of the pure ethyl gallate was prepared. Working concentrations of therapeutic solvent were prepared directly from the ethyl gallate DES. Cell viability was determined by measuring spectroscopic absorbance at 570 nm with a microplate reader (Hidex Sense Beta Plus., Turku, Finland). Results were expressed as percentage of control values.

3.2.8. Cell cycle analysis

Cells were seeded into six-well plates at a concentration of 500,000 cells/well and allowed to attach in culture overnight. A total of three mL of culture media containing the test samples were added. The next day cells were treated with IC_{50} and 2x IC_{50} concentrations of ethyl gallate and ethyl gallate (positive control)-based THEDES and incubated for 48 h. The cells were washed twice with ice-cold 1X PBS (Hyclone™ L laboratories, Inc) and collected after trypsinization. Cell pellets were washed two times with ice-cold 1X PBS and fixed with one mL of ice-cold ethanol for 45min at 20 °C. After that, ethanol was removed, and cell pellet was resuspended in 500 µL propidium iodide (PI)/RNase staining solution (BD Biosciences) and incubated for 15 min at room temperature and stored in the dark. Cell suspension was collected in a flow cytometer tube and scanned with a BD Accuri™ C6 flow cytometer (BD Biosciences, San Jose, CA, USA) using BD Accuri™ C6 software, version 1.0.

3.2.9. Solvatochromism of ethyl gallate based THEDES

Solvatochrmsim was applied to measure solvent polarity in different temperatures.

Experiment was carried out using Nile red, 4 –nitroaniline, and N,N-diethyl-4-nitroaniline at conc. of 5×10^{-4} M. Regents were properly mixed with the solvent.

A 200 µL aliquot of each sample was loaded into a 96-well plate.

Maximum absorbance and corresponding wavelength were determined using UV-Vis spectrometer in different temperatures. UV spectral scanning was initially selected from 230 nm to 700 nm.

3.2.10. Melting point determination of ethyl gallate based THEDES

Melting point was determined using TA-Q2000 differential scanning calorimeter at a heating rate of 10 ℃ per min. Ten mg of sample was taken in an aluminum pan and an empty pan was used as reference. Before running the instrument, the sample holder was covered with aluminum lid. Temperature range was set from -100 to +200 ℃. To ensure no moisture contamination, nitrogen gas was purged at a rate of 20 ml/min. TA-60WS program was used to generate the thermal scan.

3.3. Result and discussion

3.3.1. Formulation of THEDES

To formulate THEDES, pure ethyl gallate was mixed with choline chloride, acetylcholine chloride, glycerol, or PEG 400 in different molar ratios. Initially we started from 1:1 molar ratio for all the DES. Then we increased the ratio until getting the successful formulation. Successful formulations are presented in Table 3.1. All liquid preparations were viscous and appeared transparent. No precipitates were observed after formulation. To conduct further experiments, we selected acetylcholine chloride-based DES because it was more clearer and transparent compared to other THEDES.

Table 3.1. Different formulations of ethyl gallate based THEDES

THEDES	Ratio	Appearance in room temperature
Ethyl gallate: Glycerol	1:6	Solid (behave as liquid at 37 ℃)
Ethyl gallate: Choline chloride	1:3	Liquid
Ethyl gallate: Acetylcholine	**1:2**	**Liquid**

chloride		
Ethyl gallate: PEG 400	1:1	Liquid

3.3.2. Solubility study

Solubility plays a vital role to achieve desired plasma concentrations in our body and to exert proper therapeutic response. Poorly water-soluble drugs need high doses to be administered to get optimum plasma concentration. Around 40 % of new chemical entities are found to be poorly soluble which becomes a major challenge for the pharmaceutical industry and formulation scientists. Solubility problems lead to inadequate bioavailability and, as a result, therapeutic potency decreases [23–25]. Improving drug solubility is, therefore, an urgent need for pharmaceutical scientists [23–25].

In this experiment, we tried to improve the water solubility of ethyl gallate:acetylcholine chloride-based DES. The results showed that in THEDES water solubility of ethyl gallate is 38 times higher than the slightly soluble ethyl gallate powder. The solubility data is displayed in Figure 3.2. The standard curve is linear ($y=0.1106x-2.9302$, $R^2 = 0.9988$) over the range of 0 to 1500 ppm.

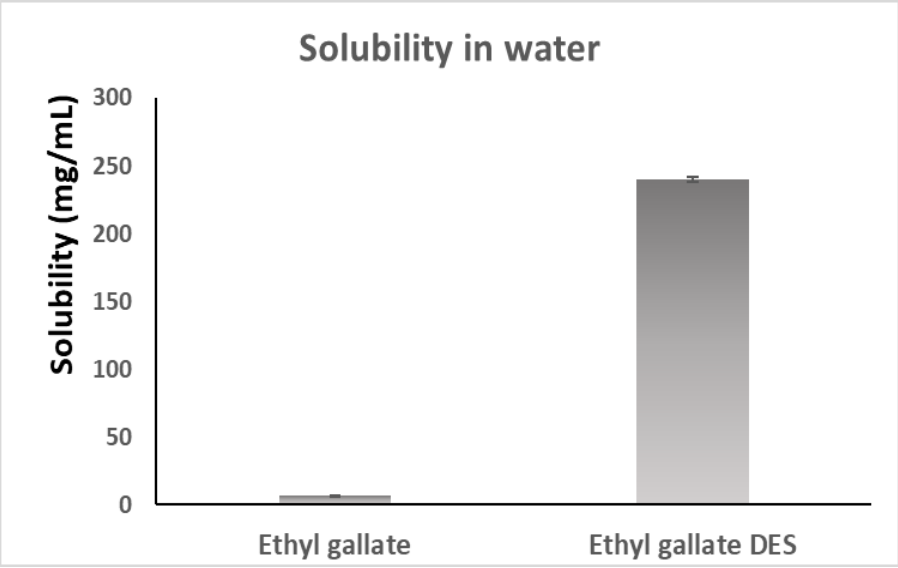

Figure 3.2. Solubility of ethyl gallate in API form and in THEDES form in water. Right image represents standard curve generated from pure ethyl gallate to calculate unknown concentration.

THEDES are versatile solvents to improve the solubility and efficacy of drug molecules. The new formulation is an emerging a new approach for drug delivery. It has been demonstrated that THEDES significantly reduces the solubility issue, which may improve drug delivery, and reduce the dose requirement to potentiate the therapeutic effect of the API. Extensive studies on improving solubility by THEDES has not been done yet. Various studies prove that THEDES can enhance the solubility and bioavailability. As a result, bioactivity increases [23,26,27]. Solubility is a major issue in the field of drug delivery research. Solubility limits drug development process. Poor water solubility significantly affects bioavailability and as a result drastically affect pharmacological action [23,28]. From the result it can be predicted that, pharmacological response might be improved due to the high solubility enhancement by THEDES (Figure 3.2).

3.3.3. IR spectroscopic analysis

IR analysis for THEDES including raw components were performed separately and spectra were overlapped to show the difference in peak intensity.

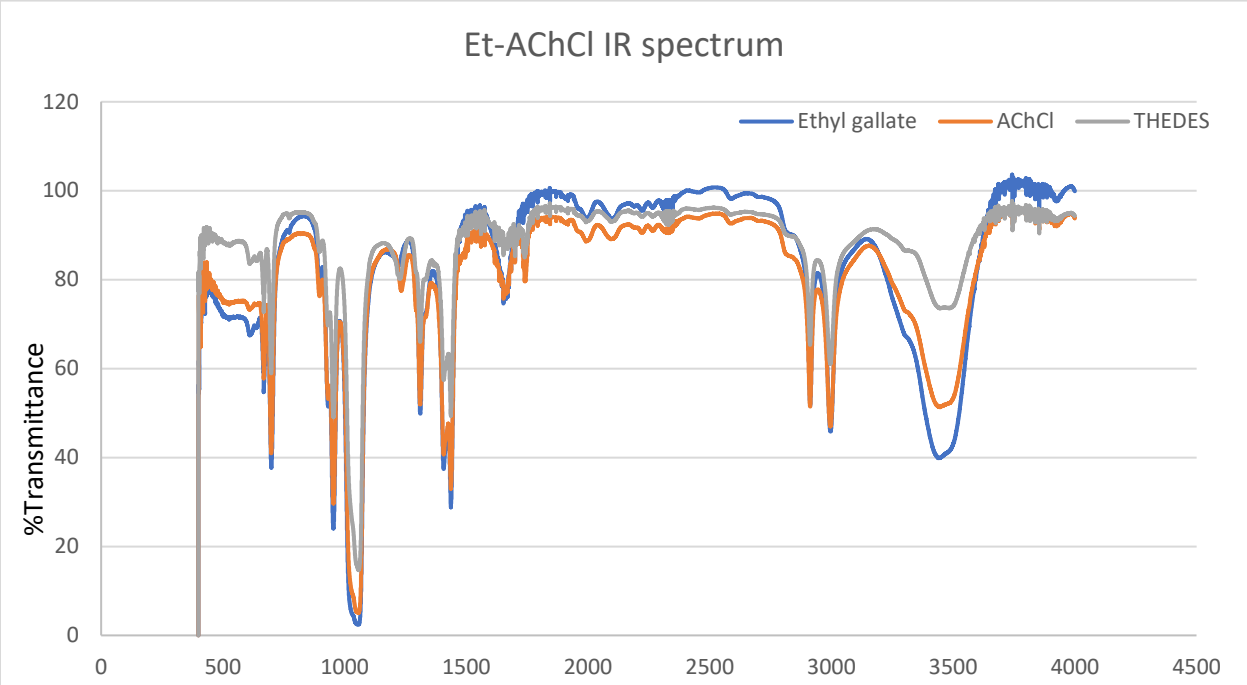

Samples	Functional group intensity ratio	Value
ETHYL GALLATE	-CO/-CH	0.418
	-OH/-CH	1.12
DES	-CO/-CH	0.428
	-OH/-CH	0.571

Figure 3.3. IR spectrum of pure ethyl gallate, acetylcholine chloride and ethyl gallate based DES.

The -OH group of ethyl gallate broadened between 3070 to 3700 cm^{-1}. In the same range peak for THEDES became narrow. It indicates that strong hydrogen bonding interaction between -OH of ethyl gallate and AChCl. The -CO stretching vibration for ethyl gallate is visible between 1616 to 1733 cm^{-1}. For THEDES it appears to be indistinguishable. The

distinctive -CH stretching vibration occurs around 2833 to 3076 cm^{-1}. In this region absorption band of THEDES decreases more than the parent compound ethyl gallate and AChCl (Figure 3.2). The spectral bands indicate possibly H bonding interaction happened. Change in peak intensity and peak deviation indicate possibility of nonbonding interaction between HBD and HBA in DES [29][30]. Peak intensity ratio was also calculated to add more insights in hydrogen bonding interaction. The eutectic interaction is predominantly between the -OH on the gallate to the AChCl (Figure 3.3). Intensity change was high (1.12, and 0.57 for -OH/-CH in ethyl gallate, and DES respectively).

3.3.4. NMR spectroscopic analysis

Both ^{13}CNMR and ^{1}HNMR were conducted for the DES components to assess potential intermolecular interactions.

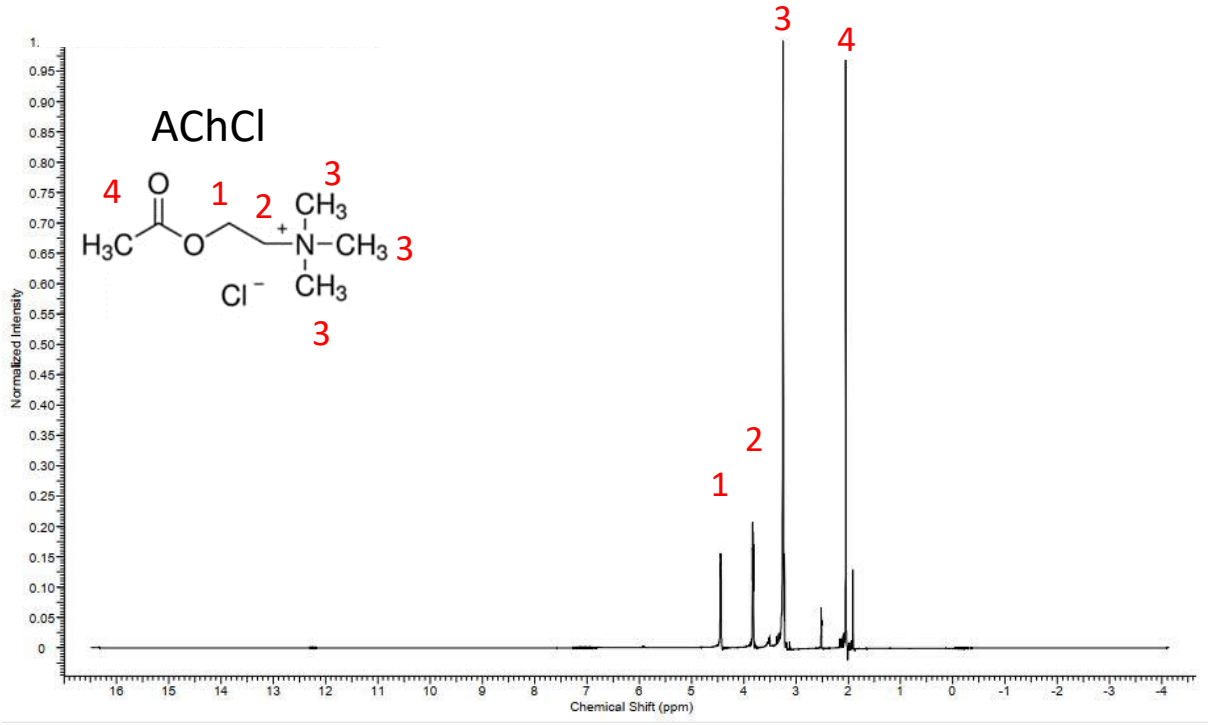

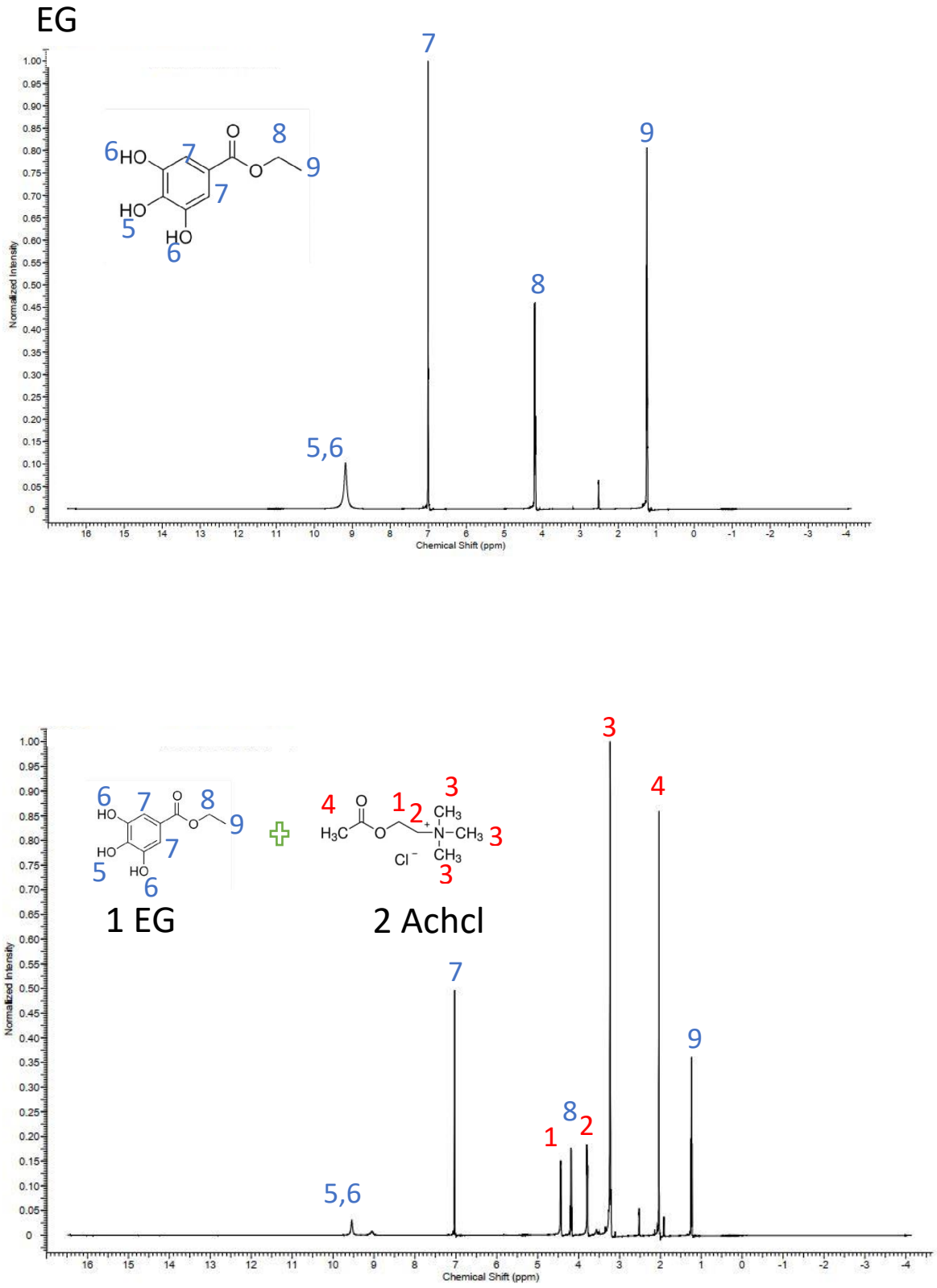

Figure 3.4. [1]HNMR of ethyl gallate and its DES.

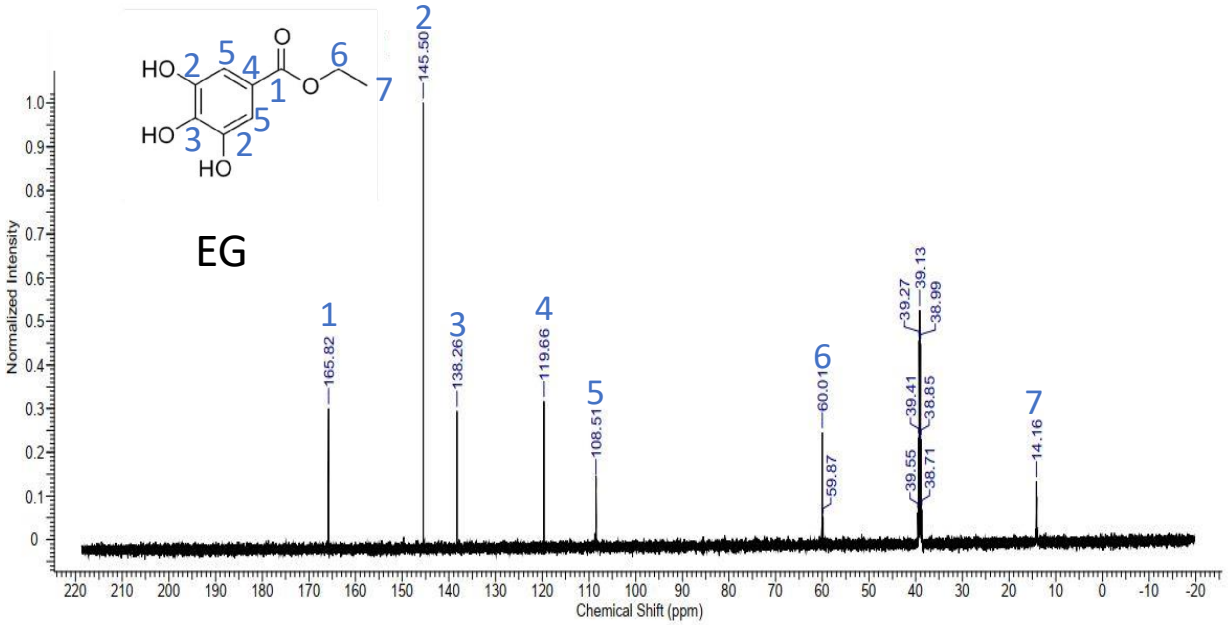
EG
Normalized Intensity
Chemical Shift (ppm)
165.82
145.50
138.26
119.66
108.51
60.01
59.87
39.27
39.13
38.99
39.41
38.85
39.55
38.71
14.16

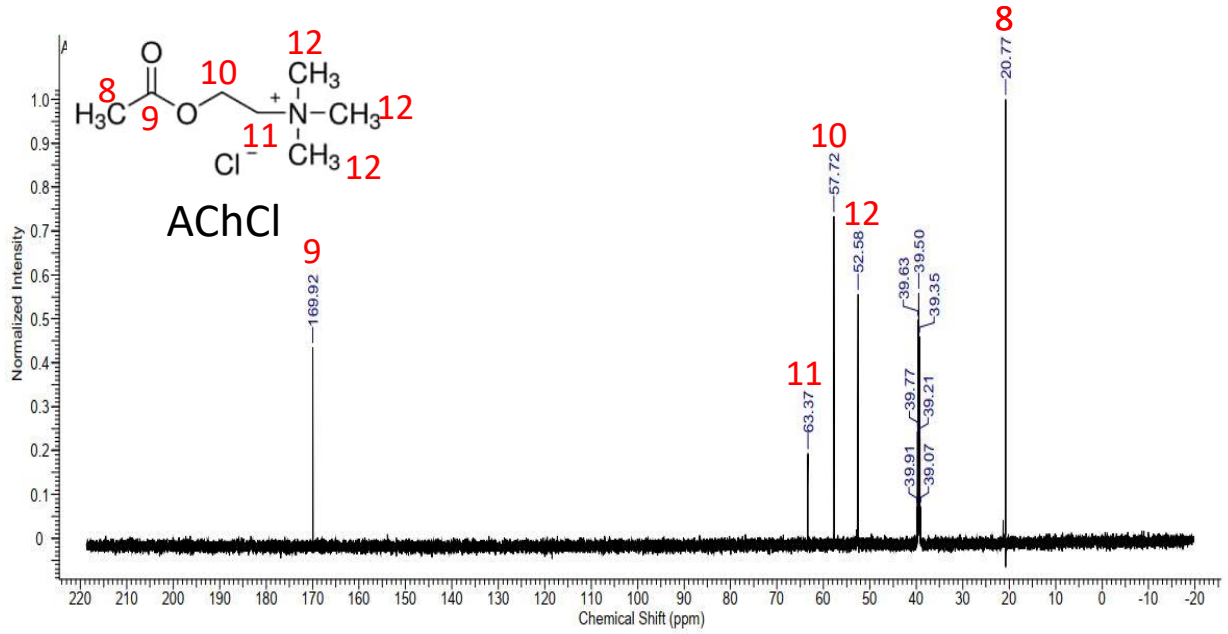
AChCl
Normalized Intensity
Chemical Shift (ppm)
169.92
63.37
57.72
52.58
39.63
39.50
39.35
39.77
39.21
39.91
39.07
20.77

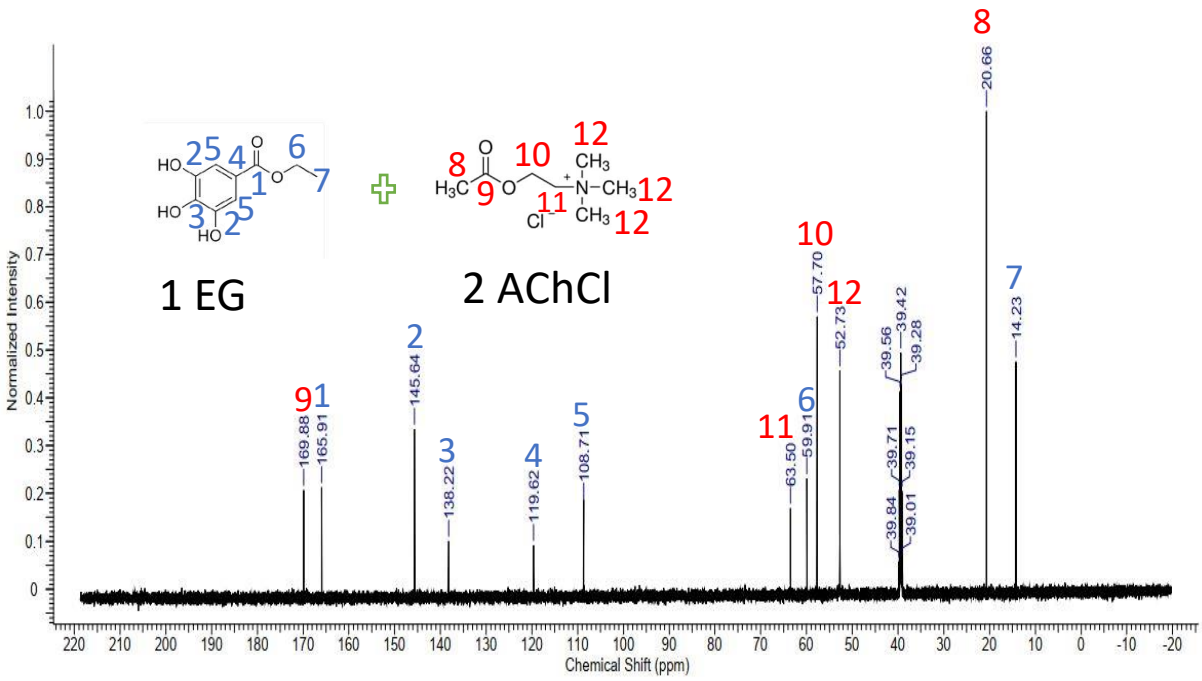

Figure 3.5. ^{13}C-NMR of ethyl gallate and its DES components.

Data was generated and acquired using the ACD-NMR software. For both NMR analysis we marked the number of carbons by position. Chemical shift was measured in δ ppm. For proton NMR the scale was 0 to 10 ppm and for carbon NMR 0 to 220 ppm. In proton NMR, for ethyl gallate and AChCl we observed four different types of protons respectively (Figure 3.4). Normalized intensity for protons in ethyl gallate decreases compared to AChCl in solvent formation. Moreover, chemical shift for the protons in ethyl gallate was observed in the solvent peaks (most intensely for -OH protons labeled as 4 and 5). In carbon NMR, peak intensity for carbons in ethyl gallate decreases in solvent compared with pure compound (Figure 3.5). Moreover, for carbons in ethyl gallate, we noticed chemical shift either up field or downfield in the solvent form. Similar

behavior was also observed for AChCl. Overall, change in chemical shift and peak intensity happened due to nonbonding interaction between components in DES.

3.3.5. Molecular modeling

Electrostatic potential graph and calculation of associated energy parameters were performed after molecule mechanistic optimization.

Table 3.2. Molecular properties of all DES components.

DES components	Total strain energy	Bond stretch	Angle bend	Stretch bend	OP bend	Torsion	Van der Waals	Electrostatic
Ethyl gallate	19.6796 kcal/mol	0.9899	4.189	-0.8553	0.0028	-8.3585	28.734	-5.0235
Acetylcholine chloride	15.8923 Kcal/mol	1.2625	3.9014	0.1125	0.0022	-1.4027	13.3395	-1.3230

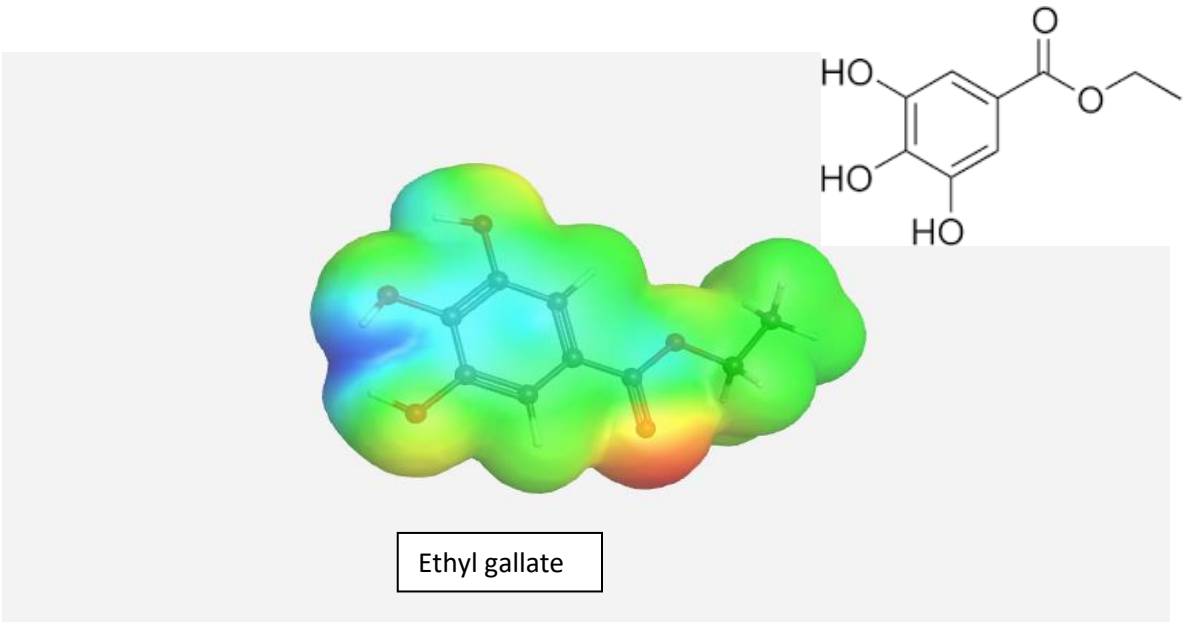

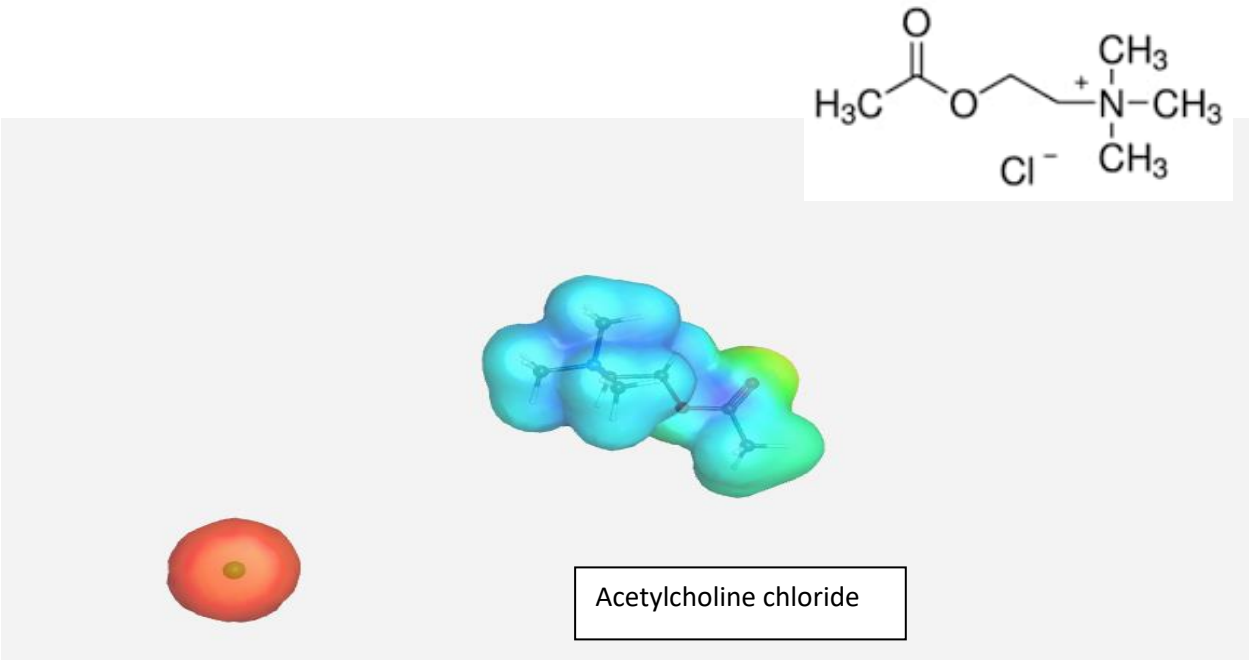

Figure 3.6. Electrostatic potential plots of ethyl gallate and acetylcholine chloride. The plots are generated from WebMO using extended Huckel molecular orbital theory.

Quantum parameters helps us to analyze nonbonding interaction (hydrogen bond) takes place between two DES components in ethyl gallate based DES. Table 3.2 represents thermodynamic properties of ethyl gallate and AChCl [19,31]. Electrostatic potential graph of ethyl gallate shows electrophilic and nucleophilic attack sites around oxygen and hydrogen. According to the electrostatic plot, red color is around oxygen of carbonyl group of ethyl gallate, and chloride ion of AChCl. It indicates electron rich area. Blue color is around hydrogen of hydroxyl groups of ethyl gallate and quaternary ammonium cation of AChCl. It indicates electron deficient area (Figure 3.6). Hydrogen bonding attraction may take place between red and blue marked areas and forms eutectic

interaction [19,32]. The above-mentioned information might explain the reasons behind forming deep eutectic solvent between ethyl gallate and acetylcholine chloride.

3.3.5.1. Molecular docking

Results of docking analysis between all possible proteins that are linked to pancreatic cancer pathogenesis and ethyl gallate are presented below:

Table 3.3. Binding affinity of ethyl gallate against proteins responsible for pancreatic cancer.

Protein	Dock score (Kcal/mol)
MRP1	-5.7
Akt	-6.4
MUC1	-4.9
HER2	-7.0

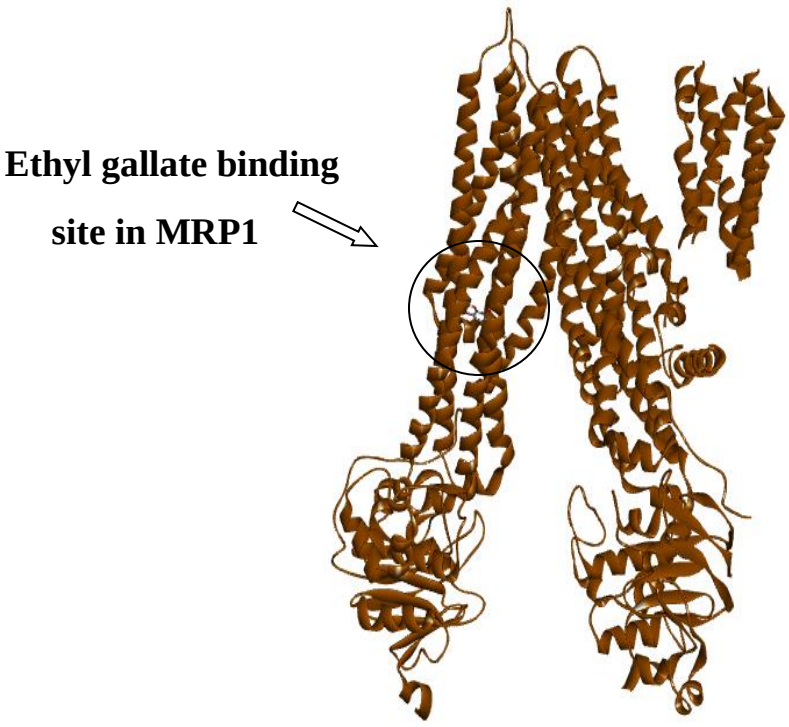

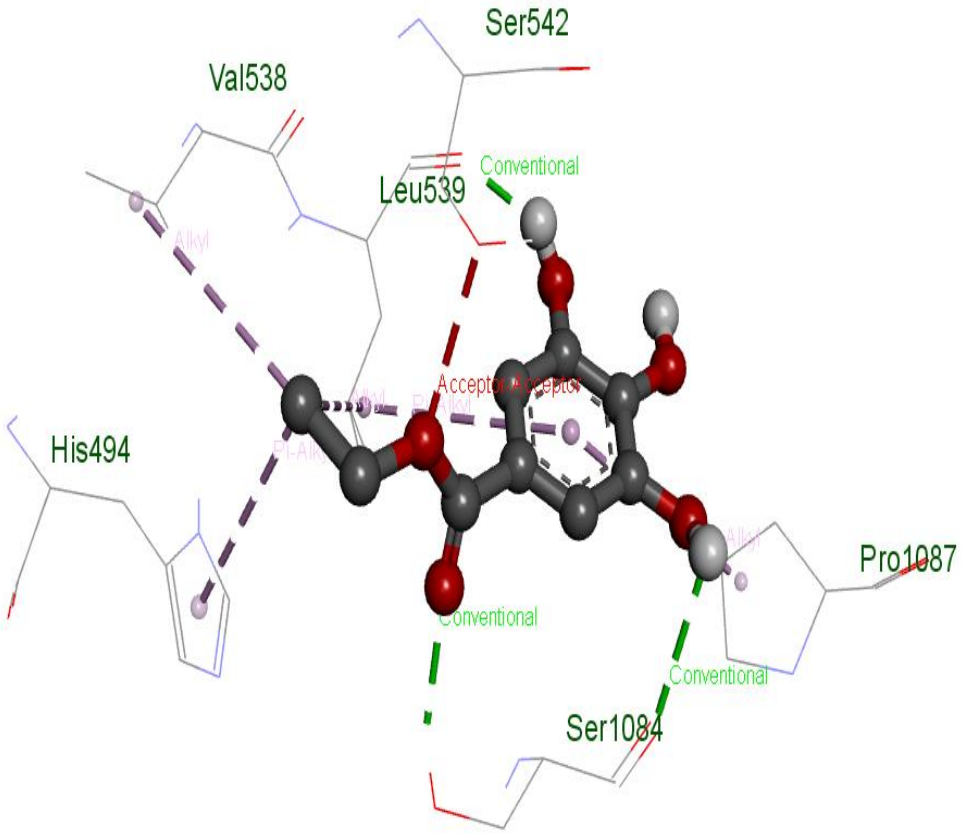

Figure 3.7. Ethyl gallate nonbonding interaction with MRP1. The top image shows drug binding site in the transmembrane region of MRP1 (circle).

Table 3.4. List of amino acids, types of bonding interaction and bonding distance between MRP1 and ethyl gallate

Amino acids	**Bonding interaction**	**Distance**
Ser1084	Hydrogen bond Hydrogen bond	2.15 2.68
Leu 539	Hydrogen bond Hydrophobic bond Hydrophobic bond	1.96 5.20 5.36
Val 538	Hydrophobic bond	5.28
His 494	Hydrophobic bond	4.83
Pro 1087	Hydrophobic bond	5.41

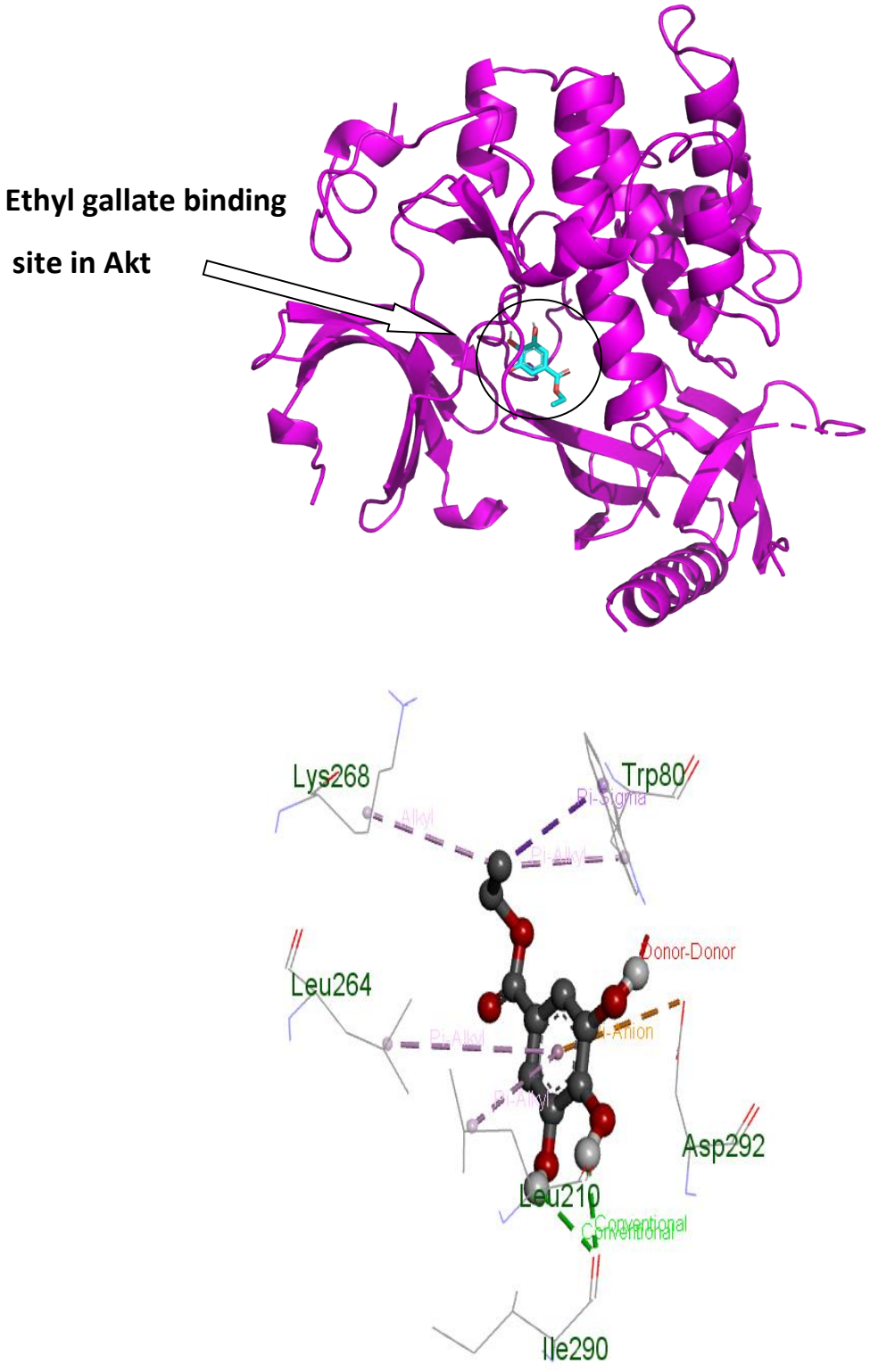

Figure 3.8. Ethyl gallate nonbonding interaction with protein kinase Akt. The top image shows drug binding site in Akt (circle).

Table 3.5. List of amino acids, types of bonding interaction and bonding distance between protein kinase Akt and ethyl gallate.

Amino acids	**Bonding interaction**	**Distance**
Ile 290	Hydrogen bond Hydrogen bond	2.55 2.41
Asp 292	Electrostatic	4.61
Trp 80	Hydrophobic bond Hydrophobic bond	3.88 4.00
Lys 268	Hydrophobic bond	4.39
Leu 210	Hydrophobic bond	4.49
Leu 264	Hydrophobic bond	5.47

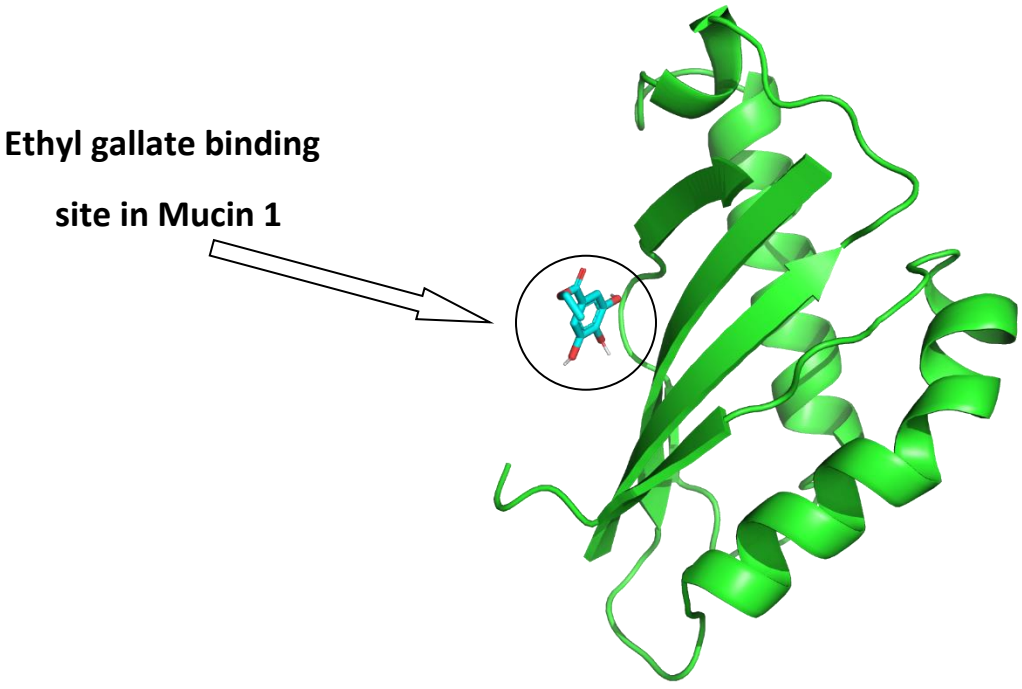

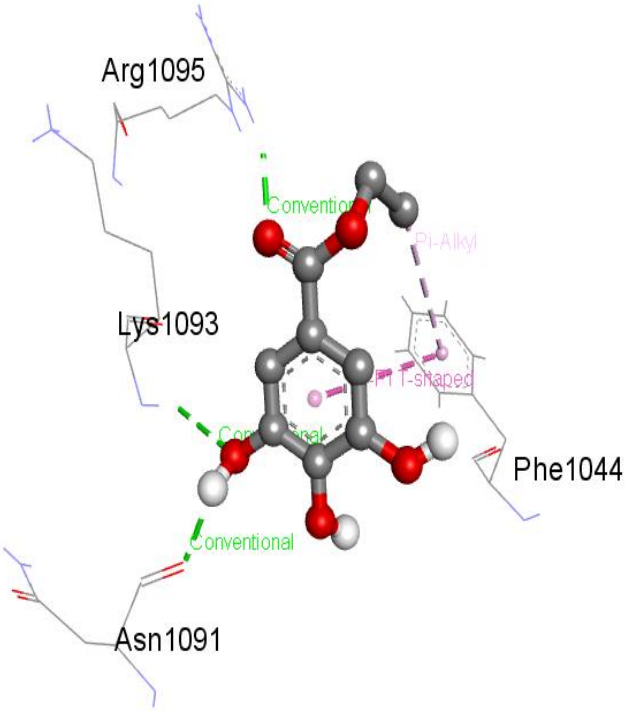

Figure 3.9. Ethyl gallate nonbonding interaction with Mucin 1 domain. The top image shows drug binding site in mucin 1 (circle).

Table 3.6. List of amino acids, types of bonding interaction and bonding distance between Mucin-1 domain and ethyl gallate.

Amino acids	**Bonding interaction**	**Distance**
Lys 1093	Hydrogen bond	2.92
Arg 1095	Hydrogen bond	2.00
Asn 1091	Hydrogen bond	2.24
Phe 1044	Hydrophobic bond Hydrophobic bond	4.86 5.37

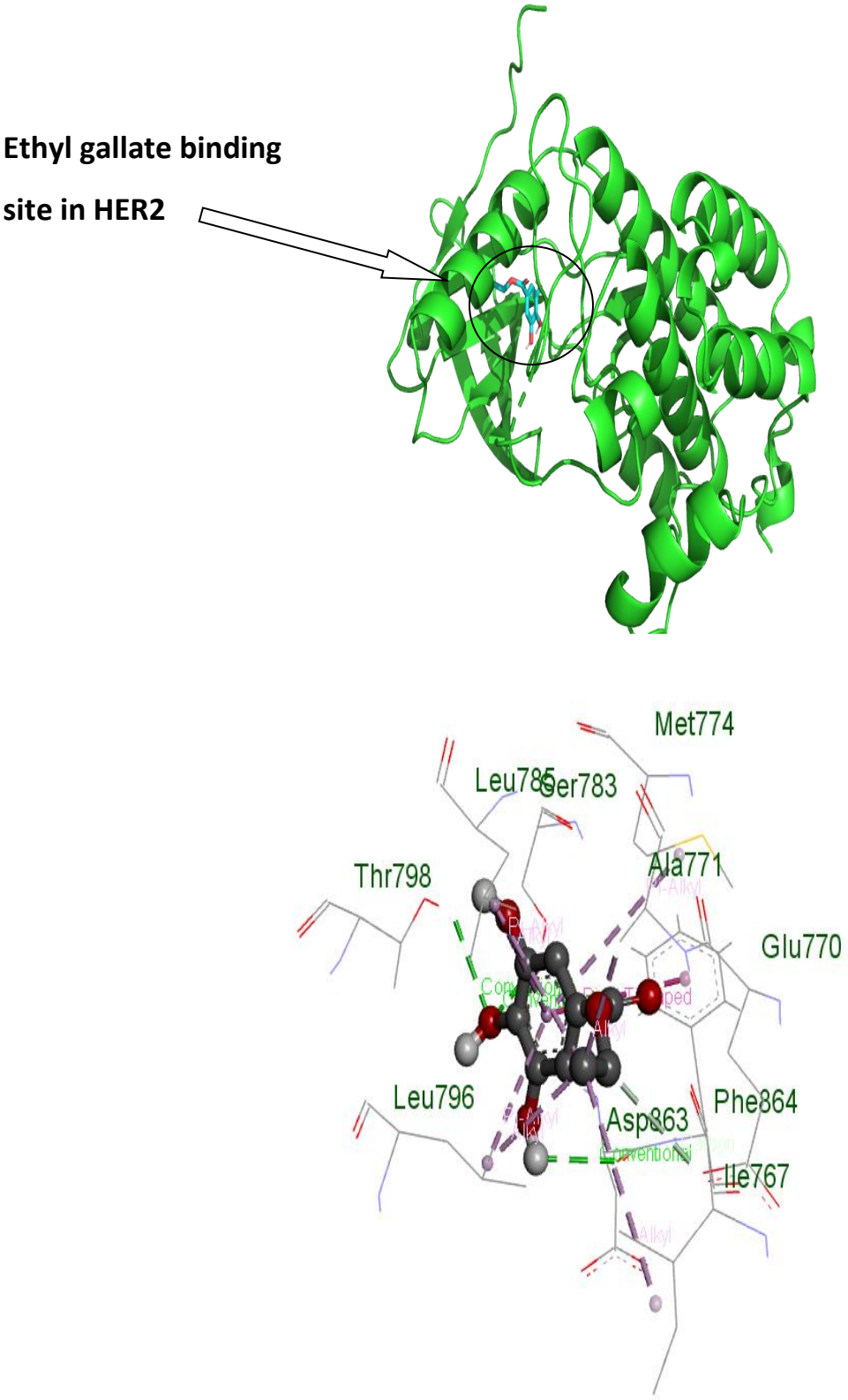

Figure 3.10. Ethyl gallate nonbonding interaction with HER2. The top image shows drug binding site of ethyl gallate in HER2 (circle).

Table 3.7. List of amino acids, types of bonding interaction and bonding distance between HER2 and ethyl gallate.

Amino acids	**Binding interaction**	**Distance in A^{o}**
Ser 783	Hydrogen bond	2.81
Thr 798	Hydrogen bond	2.85
Asp 863	Hydrogen bond	2.74
Glu 770	Hydrogen bond	3.69
Phe 864	Hydrophobic bond	5.07
Ala 771	Hydrophobic bond	3.31
Ile 767	Hydrophobic bond	5.36
Leu 785	Hydrophobic bond Hydrophobic bond	4.40 4.88
Leu 796	Hydrophobic bond Hydrophobic bond	3.36 5.43
Met 774	Hydrophobic bond	5.44

Pancreatic cancer is a major form of cancer. Abnormal tumor cells in the pancreas grow in an uncontrolled way and turn aggressive. Eventually it spreads to other parts of the body and affect the liver, abdomen, lung, bones, etc. Each year around 62,000 people in the USA are diagnosed with cancer. It is one of the ten most diagnosed types of cancer in the USA [33–35]. To treat aggressive pancreatic cancer, natural products-based drug candidates might be a suitable source of novel drug candidates. Ethyl gallate has a rich history of treating different cancer cell lines [16,36][37]. As a natural product, it has diverse pharmacological activities [38][39]. That is why we decided to see whether it shows potential in treating pancreatic cancer or not. From an MTT assay we found that DES prepared from ethyl gallate showed better activity than pure ethyl gallate. Moreover, in cell cycle analysis it has been observed that DES showed better activity than pure molecule. Based on this observation we conducted a molecular modeling approach against proteins that are mainly responsible for pancreatic cancer pathogenesis. We tried to investigate probable inhibitory mechanism. Akt is one of most activated

protein kinases that induce cancer cell growth and proliferation. Mucin 1 is aberrantly overexpressed in 90% pancreatic cancer metastasis. Overexpression of the receptor tyrosine kinase HER2 is significantly associated with poor treatment outcomes in pancreatic cancer patients [33-35]. These proteins collectively worsen the disease condition. In addition to pancreatic cancer, we also tested whether the drug works against MRP1 overexpressed cells or not. Molecular modeling assessment provides insight about the ethyl gallate-protein interaction. All 3D protein codes were collected from the RCSB data bank and optimized with Swiss PDB viewer. From docking scores, we can see that except MUC1 the drug shows good docking score against other three proteins. Good docking score means more negative value and high binding affinity between protein and drug [40]. HER2 showed the highest activity (-7.0 kcal/mol). We can assume that ethyl gallate showcases anticancer potential through inhibiting activity of Akt and HER2. In addition to pancreatic cancer inhibitory potential the drug molecule might hold potential to work against drug resistant protein (Figure 3.7---Figure 3.10, Table 3.3 ---Table 3.7).

Docking with MRP1 shows that the drug binds in the transmembrane region of MRP1. Probably by binding in that active site it inhibits efflux activity of MRP1. Nonbonding interaction analysis proves that majority of bonding interactions were hydrophobic. Bonding interaction distance ranges from 2.15 to 5.41 Å. Docking with protein kinase Akt shows the binding site is in the middle of the protein. Participating amino acids are mainly nonpolar and only two amino acids are polar. Majority of nonbonding interaction was hydrophobic type. Bonding distance ranges from 2.41 to 5.47 Å. The drug showed the greatest docking activity against HER2. Similarly, as other proteins, hydrophobic interaction is the major driving force behind nonbonding interaction with ethyl gallate.

Bonding distance ranges from 2.81 to 5.44 Å. Most of amino acids participated in nonbonding interactions are nonpolar. Rest of the amino acids are polar. Ethyl gallate binds in the left upper groove of the protein and probably inhibits its activity (Figure 3.7---Figure 3.10, Table 3.3 ---Table 3.7).

3.3.6. Cell viability: Drug resistant cell line

Using MTT assay cell proliferation inhibition was assessed in both parental and MRP1 overexpressed cells.

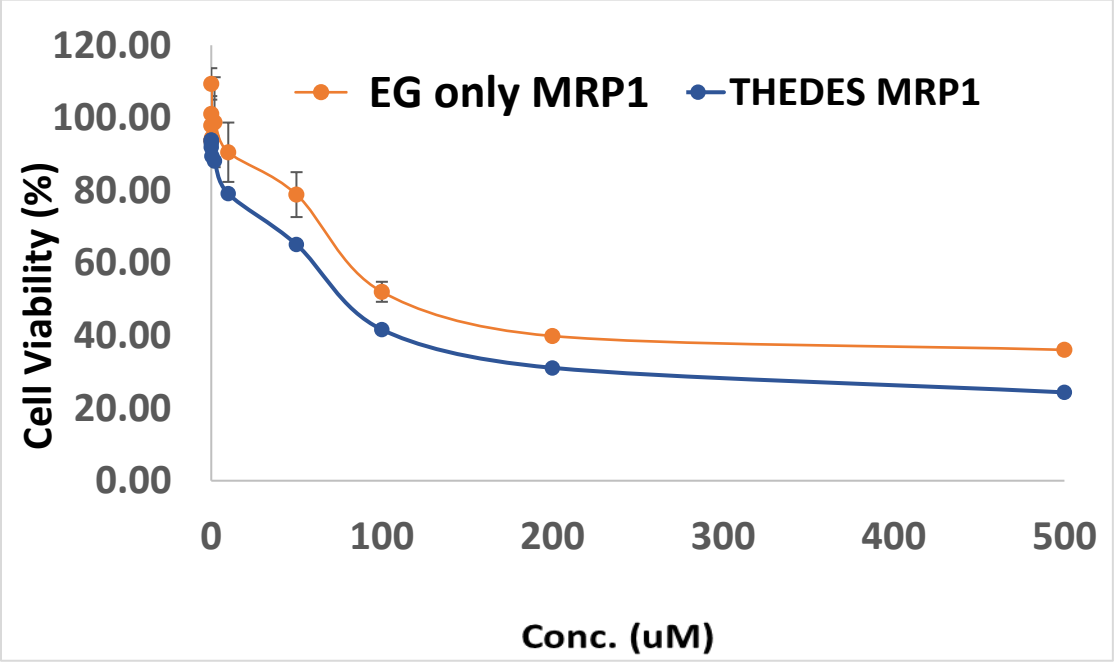

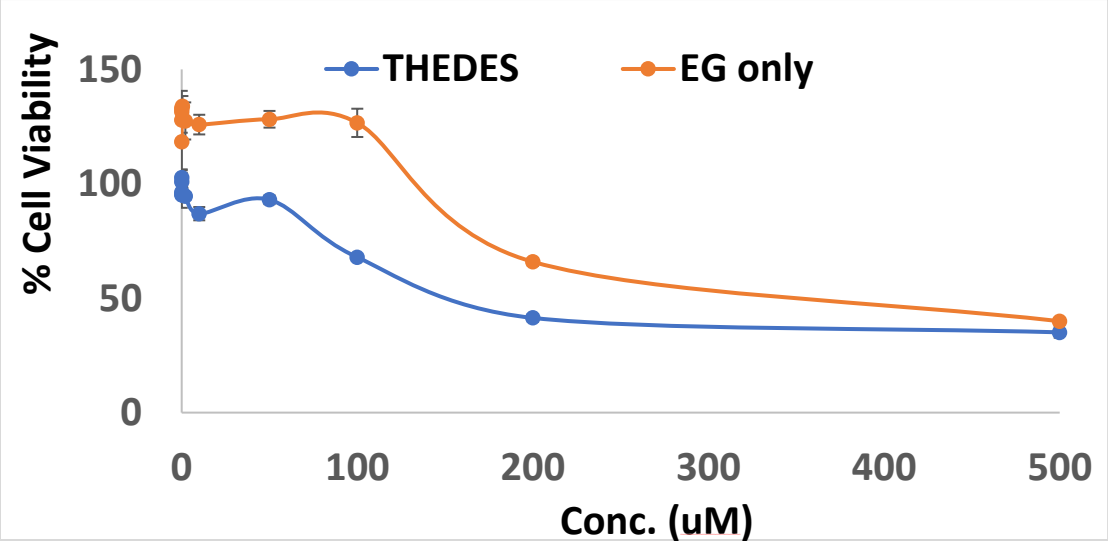

Figure 3.11. Top graph is MTT on HEK-MRP1 cells and bottom graph is on HEK-P cells. Pure ethyl gallate and DES were administered in the 96 well plate. Cell viability was calculated in Hidex microplate reader.

To get insight about the feasibility of THEDES behavior in biological systems, we conducted initial cell-based viability assays to assess the activity of ethyl gallate as THEDES. Both HEK-P and HEK-MRP1 are widely accepted cell lines for checking the drug resistance associated with many types of cancer. The assay reflects a potential bioactivity of ethyl gallate in THEDES formulation.

Pure ethyl gallate and ethyl gallate in THEDES formulation showed almost similar patterns but compared to pure ethyl gallate, DES showed better pharmacological activities in both parental and MRP1-drug resistant cells. Overall, after 100 μM concentration, cell viability started decreasing (Figure 3.11). It can be anticipated that ethyl gallate in DES format retains comparatively better therapeutic potential than pure ethyl gallate treatment. Excellent pharmacological activity and safety features of the DES potentiate the biological use of ethyl gallate based THEDES in different forms of cancer.

The reason is DES might deliver more ethyl gallate compared to pure ethyl gallate in the sight of action. From solubility experiments we found that DES significantly improves solubility of ethyl gallate. This phenomenon might be correlated with better therapeutic potential in the MTT assay. Further studies are needed to assess the mechanism in animal-based models.

3.3.7. Cell viability: Pancreatic cancer cell line

Pure ethyl gallate and ethyl gallate-based THEDES were applied on pancreatic cancer cell line.

Table 3.8. IC_{50} value of both DES and pure compounds

Samples	IC_{50} values in μM (mean+/−SD)
DES	640.3+/−59.99
Ethyl gallate pure	784.68+/−15.85

Ethyl gallate-based DES showed better IC_{50} value than pure compound (Table 3.8). We conducted MTT assay on pancreatic cancer cells to assess anticancer potential. Both samples show anticancer activity but ethyl gallate based DES was better compared to pure ethyl gallate. The reason may be DES delivers more ethyl gallate in the site of action. From solubility experiments, we found that DES tremendously improve solubility of poorly water-soluble ethyl gallate compared to the pure compound. It substantiates the better pharmacological potential of DES.

3.3.8. Cell cycle analysis

Cell cycle assessment was conducted in a flow cytometer to see which stage of cell growth are retarded by the drug and DES.

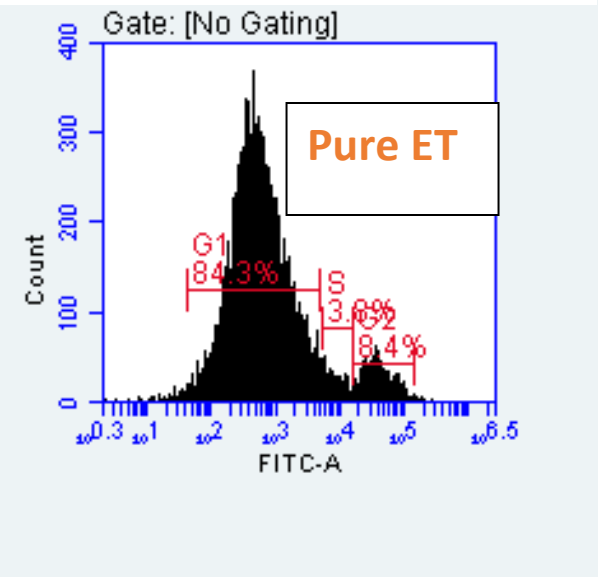

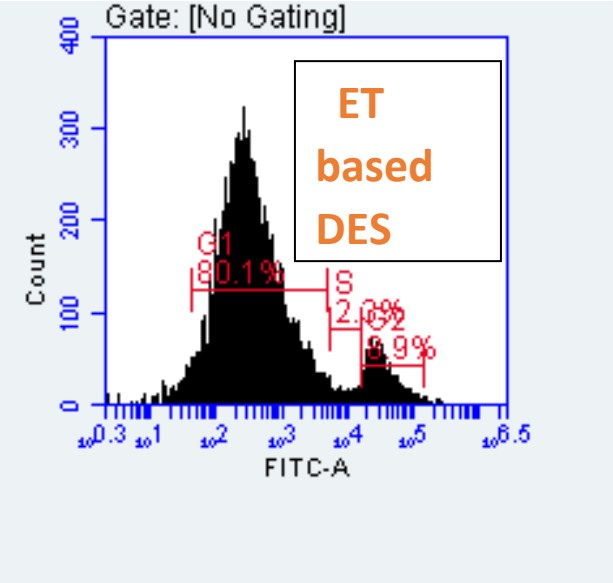

Trial 1

IC_{50} concentrations for pure ethyl gallate and ethyl gallate based DES

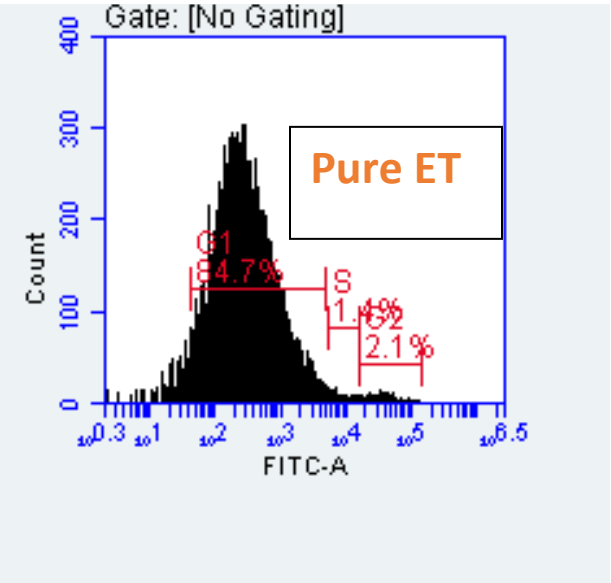

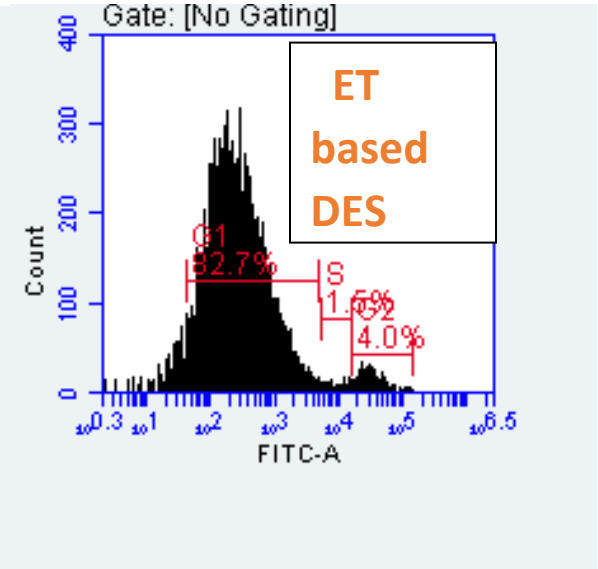

Trial 1

2IC_{50} concentrations for pure ethyl gallate and ethyl gallate based DES

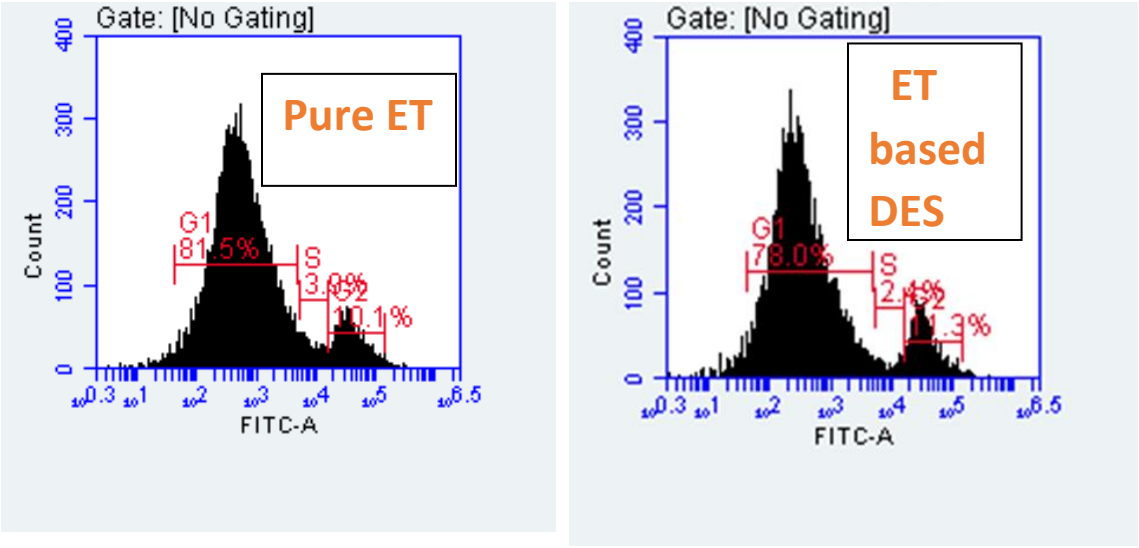

Trial 2

IC_{50} concentrations for pure ethyl gallate and ethyl gallate based DES

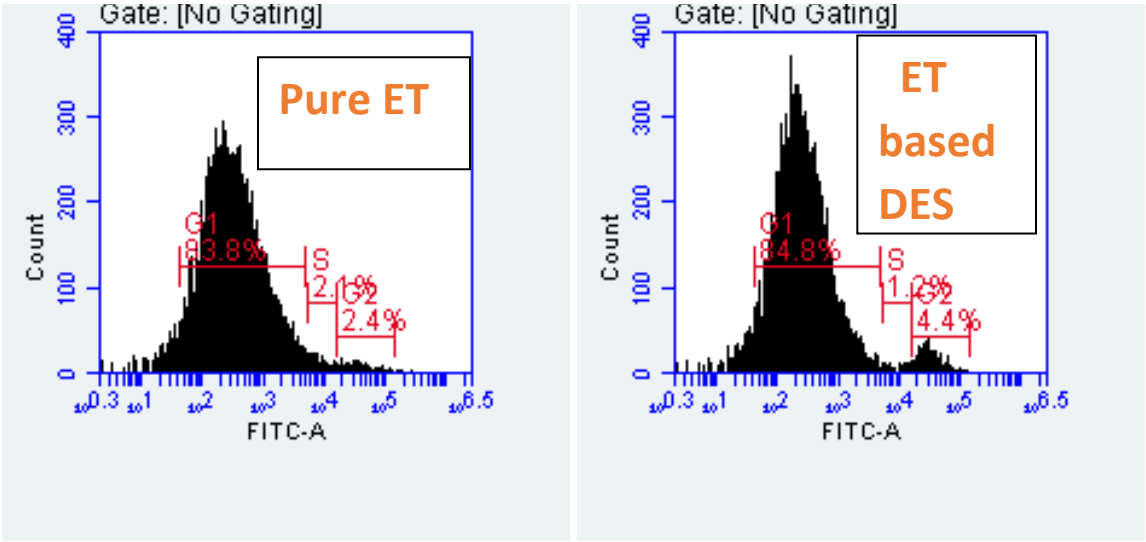

Trial 2

$2IC_{50}$ concentrations for pure ethyl gallate and ethyl gallate based DES

Figure 3.12. Cell cycle assessment of pure ethyl gallate and ethyl gallate based DES in pancreatic cancer cell line. IC_{50} and $2IC_{50}$ concentrations were administered to assess the potential. Results are shown as trial 1 and trial 2.

Cell cycle analysis provides critical information about cell proliferation and cell death. In eukaryotic cells, it consists of four phases: G1, S, G2 and M. Cell cycle arrest is a viral marker of excellent anticancer activity of new drug candidates. To investigate effect of novel DES in inhibiting pancreatic cancer growth at first, we conducted an MTT assay. Based on the MTT, we chose two doses (IC_{50} and $2XIC_{50}$) and incubated with pancreatic cells. We then investigated effect of the samples in cell cycle arrest. Propidium iodide was used as DNA staining reagent. Using flow cytometry-based analysis we quantified percent of cells in each phase of the cell cycle. Incubation with both pure ethyl gallate and ethyl gallate based DES showed arrest in cell growth in G1 phase of cell cycle (Figure 3.12). For pure ethyl gallate, population of arrested cells were similar in both doses of administration. For DES we noticed that preincubation with ethyl gallate-based DES led to increase in percentage of arrested cells in high concentration compared to pure drug (78 % to 85 %). Based on the observation, it can be postulated that DES holds promise in delivering poorly water-soluble anticancer agents like ethyl gallate to the site of action and exerts anticancer activity by stopping cell cycle transition from G1 to S phase (Figure 3.12). Further research is warranted to design novel pancreatic cancer drug and incorporate in DES for better delivery and maximize pharmacological activity. Some key proteins such as protein kinase Akt, Mucin-family protein MUC1, and Receptor tyrosine-protein kinase 2 play significant roles in invasion and metastasis of pancreatic cancer. We conducted a molecular molding study in these proteins and found that ethyl

gallate might inhibit activities of HER2 and Akt (high binding affinity). Thus, it probably inhibits progression of pancreatic cell growth [34,41,42].

3.3.9. Solvatochromism parameters

Solvatochromic parameters were measured at different temperatures. At room temperature (25 °C) polarizability value is 0.91, hydrogen bond acidity is 0.71 and hydrogen bond basicity is 0.43 (Figure 3.13). Due to dielectric effects, DES maintains these values. We observed different polarity values of all three parameters at different temperatures (25 to 45 °C). For polarizability we noticed an increasing trend in elevated temperature and decreasing trend in high temperature for hydrogen bond acidity and basicity (Figure 3.13). Variations in polarity values arise due to reorientation of dipole values in increasing temperature [43,44]. Moreover, depending on polarity of DES and its components in different temperatures red shift and blue shift were evident in UV spectroscopy [44].

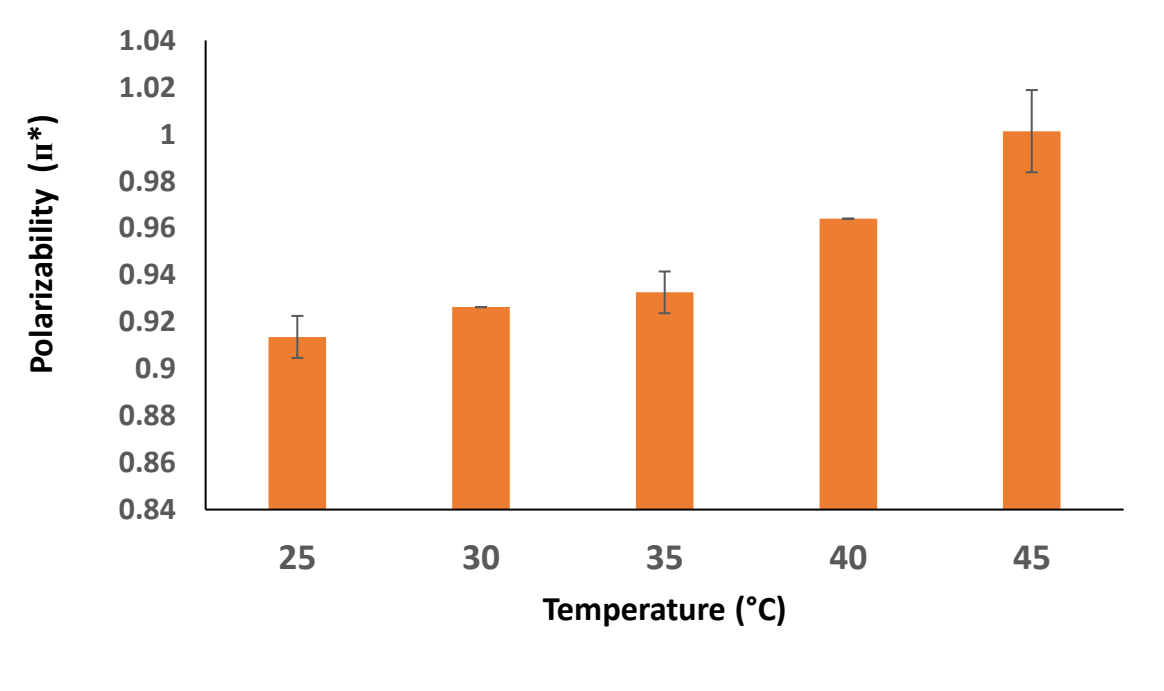

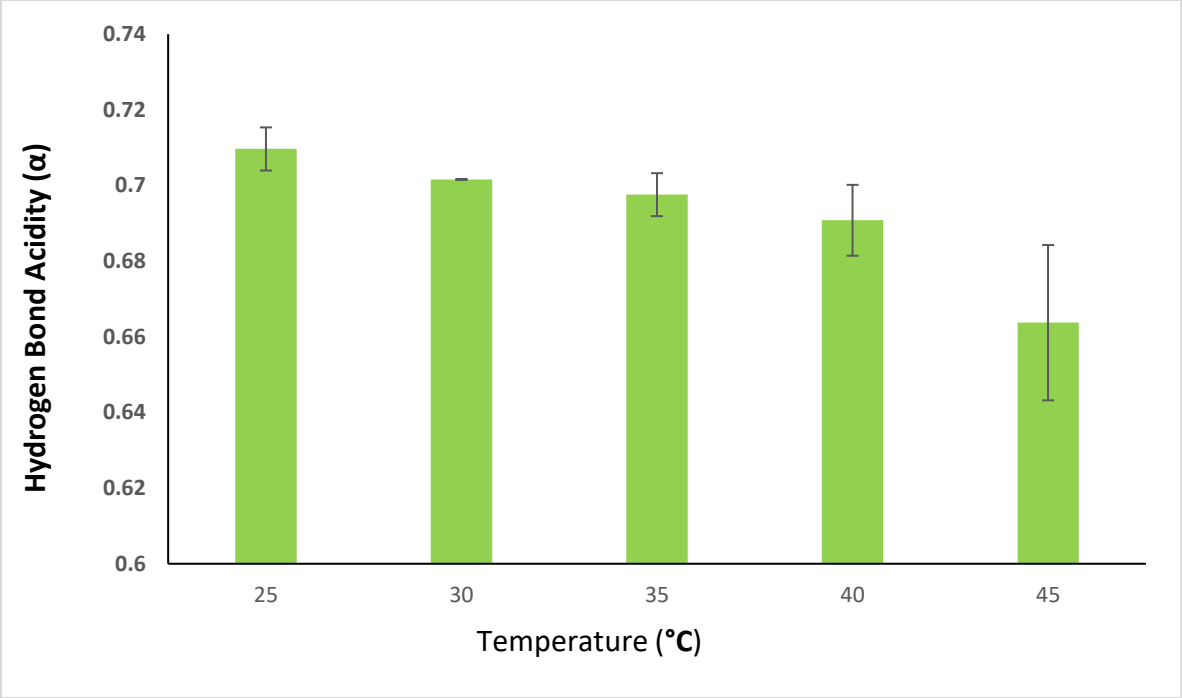

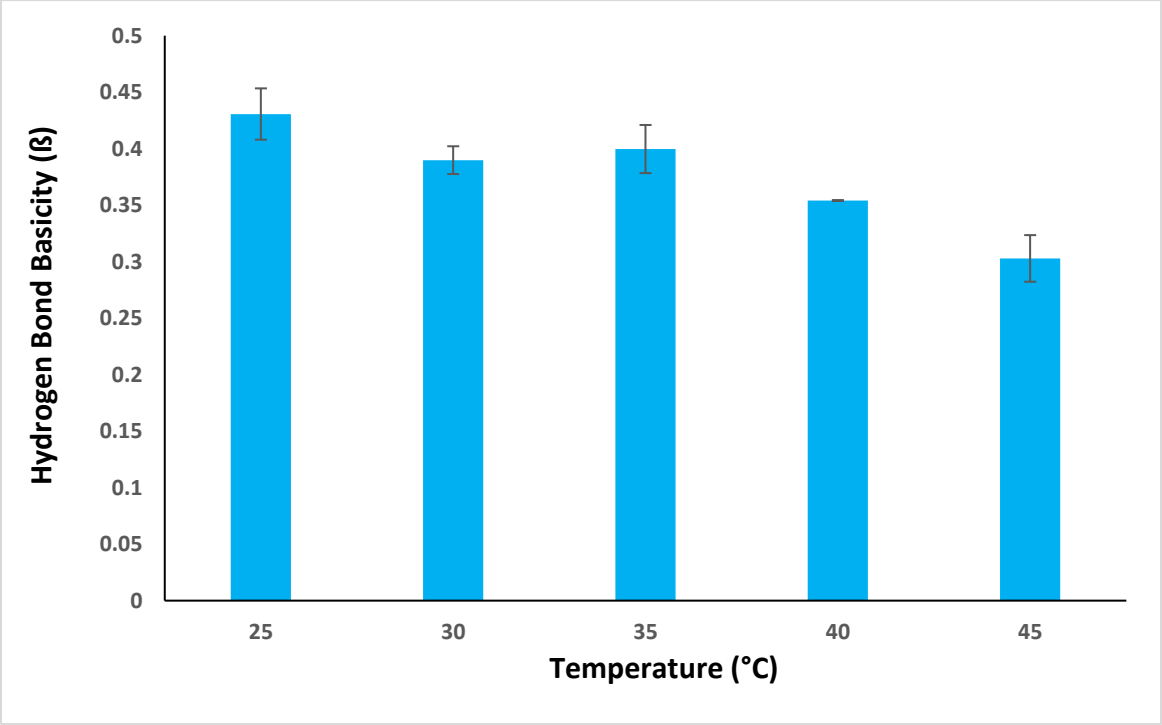

Figure 3.13. Polarity, hydrogen bond acidity and hydrogen bond basicity of ethyl gallate based DES in different temperatures.

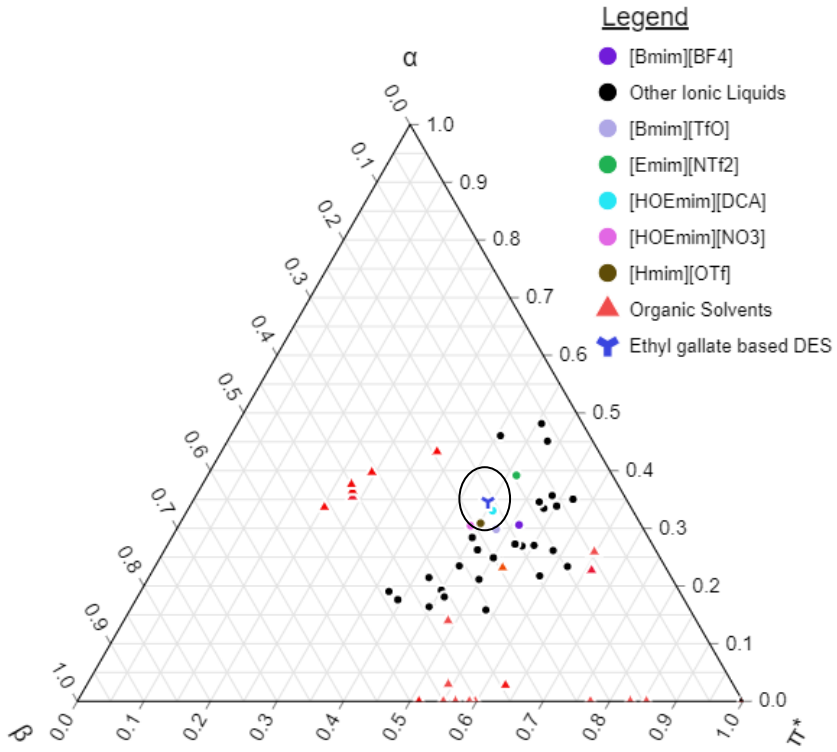

Figure 3.14. Ternary plot of ethyl gallate based DESs, ionic liquids, and organic solvents generated based on Kamlet-Taft parameters (α, β, and π*). Solvatochromism parameters were collected from previously published literature and plotted in ternary plot [45,46]. Ionic liquids closely related to DESs are highlighted in different colors to provide understanding about probable polar nature of formulated DES. Position of DES in the plot is shown inside the circle.

To get deep insight about solvatochromic behavior, Kamlet-Taft parameters of DES was compared with parameters of selected ionic liquids and organic solvents. Solvent selectivity triangle plot was generated from Kamlet-Taft parameters to describe polarity of test samples. Ethyl gallate based DES is mostly closed to polarity of ionic liquids. To produce the plot, polarity parameters at ambient temperature were selected. DES share similar properties with ionic liquids namely [Bmim][TfO], [HOEmim][DCA],

[HOEmim][NO3], [Emim][NTf2], [Hmim][OTf], and [Bmim][BF4] (Figure 3.13). Majority of ionic liquids that show similar properties contain 1-hexyl-3-methyl-imidazolium (Hmim) and 1-(2-hydroxylethyl)-3-methylimidazolium ([HOEMIm]), and 1-Butyl-3-methylimidazolium (Bmim) cations (Figure 3.14). Ionic liquids are used routinely as catalytic agents in drug synthesis, drug delivery, extraction, and separation of varieties of compounds [47,48].

3.3.10. Melting point determination using differential scanning calorimetry

Differential scanning calorimetry measures thermal transition of DES samples. Melting point was analyzed for spike in heat flow.

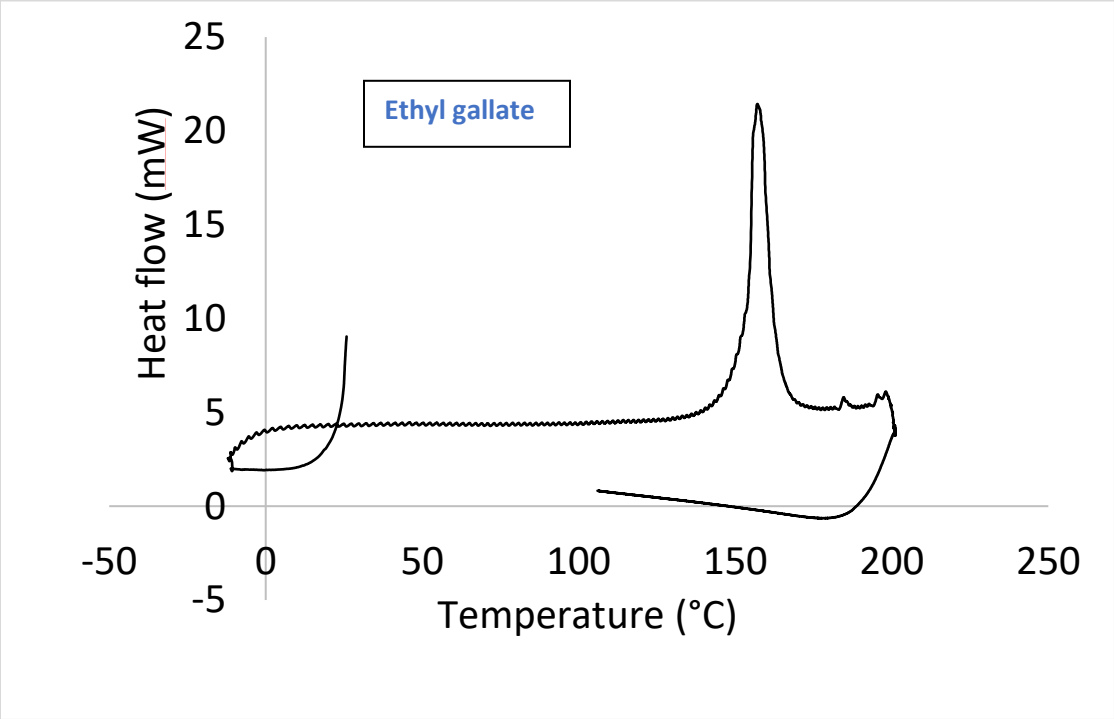

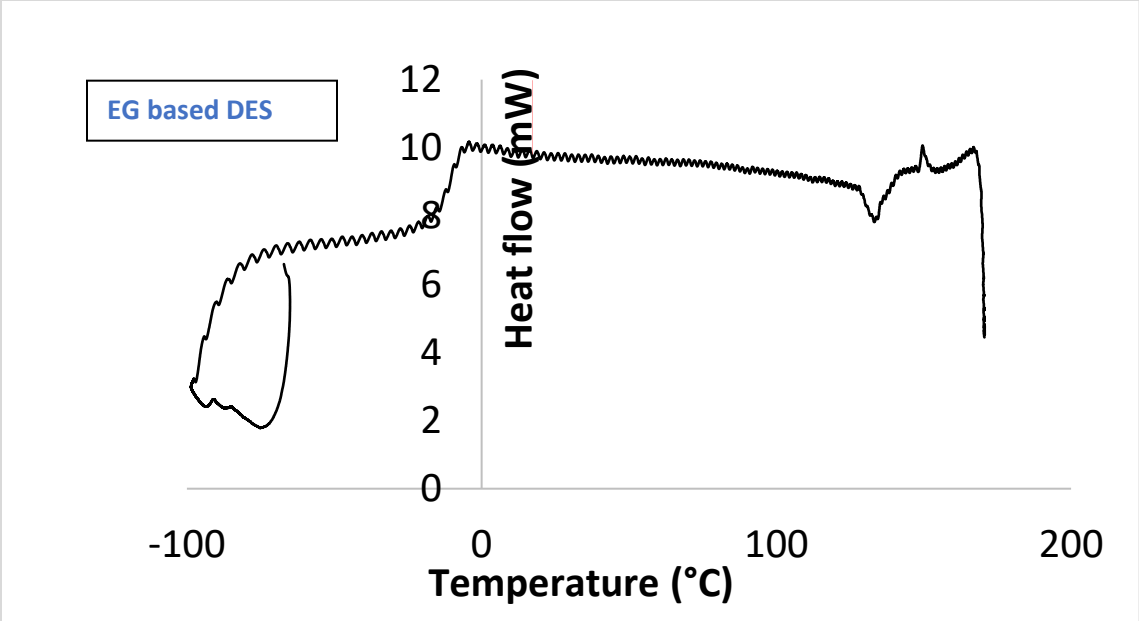

Figure 3.15. DSC curve of ethyl gallate based DES and individual components.

From the graph we can see that ethyl gallate shows a melting point around 150 °C (Figure 3.15). On the other hand, ethyl gallate based-THEDES showed melting point around below 0 °C. Reduction of melting point is considered significant. DES is constituted by HBD and HBA. Due to nonbonding interaction between HBA and HBD, depression of melting point might arise [49]. Depression of melting point might also be due to other types of bonding interactions, such as halogen bond, electrostatic forces, and van der Waals interaction [30,50]. Melting point depression is the core physicochemical property of forming DES. The above mentioned result (Figure 3.15) confirms formation of DES between ethyl gallate and acetylcholine chloride [30].

3.4. Conclusion

The Study proposes formulation of ethyl gallate based novel therapeutic solvent and that demonstrated excellent pharmacological properties in biological assays. Hydrogen bonding interaction between DES components was assessed using different spectroscopic

techniques. Molecular modeling provides deep understanding for formation of hydrogen bonding and inhibition of key proteins responsible for disease pathogenesis. Melting point determination justified successful DES formation. DES significantly improves water solubility of ethyl gallate compared to pure form. The DES shares similar polarity with some commonly available ionic liquids. Due to improved physicochemical and biological properties, DES will play key role in drug delivery applications.

3.5. References

[1] P.W. Stott, A.C. Williams, B.W. Barry, Transdermal delivery from eutectic systems: enhanced permeation of a model drug, ibuprofen, J. Control. Release. 50 (1998) 297–308. https://doi.org/https://doi.org/10.1016/S0168-3659(97)00153-3.

[2] S. Fiala, S.A. Jones, M.B. Brown, A fundamental investigation into the effects of eutectic formation on transmembrane transport., Int. J. Pharm. 393 (2010) 68–73. https://doi.org/10.1016/j.ijpharm.2010.04.001.

[3] B.G. Amsden, Biodegradable elastomers in drug delivery, Expert Opin. Drug Deliv. 5 (2008) 175–187. https://doi.org/10.1517/17425247.5.2.175.

[4] I.M. Aroso, R. Craveiro, Â. Rocha, M. Dionísio, S. Barreiros, R.L. Reis, A. Paiva, A.R.C. Duarte, Design of controlled release systems for THEDES-Therapeutic deep eutectic solvents, using supercritical fluid technology., Int. J. Pharm. 492 (2015) 73–79. https://doi.org/10.1016/j.ijpharm.2015.06.038.

[5] F. Mano, M. Martins, I. Sá-Nogueira, S. Barreiros, J.P. Borges, R.L. Reis, A.R.C. Duarte, A. Paiva, Production of Electrospun Fast-Dissolving Drug Delivery Systems with Therapeutic Eutectic Systems Encapsulated in Gelatin., AAPS PharmSciTech. 18 (2017) 2579–2585. https://doi.org/10.1208/s12249-016-0703-z.

[6] A. Gutiérrez, S. Aparicio, M. Atilhan, Design of arginine-based therapeutic deep eutectic solvents as drug solubilization vehicles for active pharmaceutical ingredients., Phys. Chem. Chem. Phys. 21 (2019) 10621–10634. https://doi.org/10.1039/c9cp01408j.

[7] M.A. Ali, M.S. Rahman, R. Roy, P. Gambill, D.E. Raynie, M.A. Halim, Structure Elucidation of Menthol-Based Deep Eutectic Solvent using Experimental and Computational Techniques, J. Phys. Chem. A. 125 (2021) 2402–2412. https://doi.org/10.1021/acs.jpca.0c10735.

[8] M.I. Rain, H. Iqbal, M. Saha, M.A. Ali, H.K. Chohan, M.S. Rahman, M.A. Halim, A comprehensive computational and principal component analysis on various choline chloride-based deep eutectic solvents to reveal their structural and spectroscopic properties., J. Chem. Phys. 155 (2021) 44308. https://doi.org/10.1063/5.0052569.

[9] Y.-Y. Tang, X.-M. He, J. Sun, C.-B. Li, L. Li, J.-F. Sheng, M. Xin, Z.-C. Li, F.-J. Zheng, G.-M. Liu, J.-M. Li, D.-N. Ling, Polyphenols and Alkaloids in Byproducts of Longan Fruits (Dimocarpus Longan Lour.) and Their Bioactivities, Mol. . 24 (2019). https://doi.org/10.3390/molecules24061186.

[10] O. Aldulaimi, F.I. Uche, H. Hameed, H. Mbye, I. Ullah, F. Drijfhout, T.D.W. Claridge, P. Horrocks, W.-W. Li, A characterization of the antimalarial activity of the bark of Cylicodiscus gabunensis Harms, J. Ethnopharmacol. 198 (2017) 221–225. https://doi.org/https://doi.org/10.1016/j.jep.2017.01.014.

[11] T. Kalaivani, C. Rajasekaran, L. Mathew, Free Radical Scavenging, Cytotoxic, and Hemolytic Activities of an Active Antioxidant Compound Ethyl Gallate from

Leaves of Acacia Nilotica (L.) Wild. Ex. Delile Subsp. Indica (Benth.) Brenan, J. Food Sci. 76 (2011) T144–T149. https://doi.org/https://doi.org/10.1111/j.1750-3841.2011.02243.x.

[12] W. Liu, J. Liu, S. Xing, X. Pan, S. Wei, M. Zhou, Z. Li, L. Wang, J.K. Bielicki, The benzoate plant metabolite ethyl gallate prevents cellular- and vascular-lipid accumulation in experimental models of atherosclerosis., Biochem. Biophys. Res. Commun. 556 (2021) 65–71. https://doi.org/10.1016/j.bbrc.2021.03.158.

[13] K. Thiagarajan, S. Mohan, T.K. Roy, R. Chandrasekaran, Antiproliferative effect of Acacia nilotica (L.) leaf extract rich in ethyl gallate against human carcinoma cell line KB., Indian J. Pharmacol. 52 (2020) 488–494. https://doi.org/10.4103/ijp.IJP_223_17.

[14] Q. Zhang, J. Nie, S.-J. Chen, Q. Li, Protective effects of ethyl gallate and pentagalloylglucose, the active components of Qingwen Baidu Decoction, against lipopolysaccharide-induced acute lung injury in rats., Drug Des. Devel. Ther. 13 (2019) 71–77. https://doi.org/10.2147/DDDT.S186029.

[15] F. Liu, X. Zu, X. Xie, K. Liu, H. Chen, T. Wang, F. Liu, A.M. Bode, Y. Zheng, Z. Dong, D.J. Kim, Ethyl gallate as a novel ERK1/2 inhibitor suppresses patient-derived esophageal tumor growth., Mol. Carcinog. 58 (2019) 533–543. https://doi.org/10.1002/mc.22948.

[16] H. Cui, J. Yuan, X. Du, M. Wang, L. Yue, J. Liu, Ethyl gallate suppresses proliferation and invasion in human breast cancer cells via Akt-NF-κB signaling., Oncol. Rep. 33 (2015) 1284–1290. https://doi.org/10.3892/or.2014.3682.

[17] TCI AMERICA, (n.d.). https://www.tcichemicals.com/US/en/p/G0016 (accessed July 2, 2020).

[18] No Title, (n.d.). https://www.caymanchem.com/product/34193/ethyl-gallate (accessed May 2, 2021).

[19] W.F. Polik, J.R. Schmidt, WebMO: Web-based computational chemistry calculations in education and research, WIREs Comput. Mol. Sci. 12 (2022) e1554. https://doi.org/https://doi.org/10.1002/wcms.1554.

[20] Z.L. Johnson, J. Chen, Structural Basis of Substrate Recognition by the Multidrug Resistance Protein MRP1., Cell. 168 (2017) 1075-1085.e9. https://doi.org/10.1016/j.cell.2017.01.041.

[21] N. Uhlenbrock, S. Smith, J. Weisner, I. Landel, M. Lindemann, T.A. Le, J. Hardick, R. Gontla, R. Scheinpflug, P. Czodrowski, P. Janning, L. Depta, L. Quambusch, M.P. Müller, B. Engels, D. Rauh, Structural and chemical insights into the covalent-allosteric inhibition of the protein kinase Akt., Chem. Sci. 10 (2019) 3573–3585. https://doi.org/10.1039/c8sc05212c.

[22] K. Aertgeerts, R. Skene, J. Yano, B.-C. Sang, H. Zou, G. Snell, A. Jennings, K. Iwamoto, N. Habuka, A. Hirokawa, T. Ishikawa, T. Tanaka, H. Miki, Y. Ohta, S. Sogabe, Structural analysis of the mechanism of inhibition and allosteric activation

of the kinase domain of HER2 protein., J. Biol. Chem. 286 (2011) 18756–18765. https://doi.org/10.1074/jbc.M110.206193.

[23] K.T. Savjani, A.K. Gajjar, J.K. Savjani, Drug solubility: importance and enhancement techniques., ISRN Pharm. 2012 (2012) 195727. https://doi.org/10.5402/2012/195727.

[24] S. Kalepu, V. Nekkanti, Insoluble drug delivery strategies: review of recent advances and business prospects., Acta Pharm. Sin. B. 5 (2015) 442–453. https://doi.org/10.1016/j.apsb.2015.07.003.

[25] C. Fink, D. Sun, K. Wagner, M. Schneider, H. Bauer, H. Dolgos, K. Mäder, S.-A. Peters, Evaluating the Role of Solubility in Oral Absorption of Poorly Water-Soluble Drugs Using Physiologically-Based Pharmacokinetic Modeling, Clin. Pharmacol. Ther. 107 (2020) 650–661. https://doi.org/https://doi.org/10.1002/cpt.1672.

[26] S. Trombino, C. Siciliano, D. Procopio, F. Curcio, A.S. Laganà, M.L. Di Gioia, R. Cassano, Deep Eutectic Solvents for Improving the Solubilization and Delivery of Dapsone., Pharmaceutics. 14 (2022). https://doi.org/10.3390/pharmaceutics14020333.

[27] M. Mokhtarpour, H. Shekaari, M.T. Zafarani-Moattar, S. Golgoun, Solubility and solvation behavior of some drugs in choline based deep eutectic solvents at different temperatures, J. Mol. Liq. 297 (2020) 111799. https://doi.org/https://doi.org/10.1016/j.molliq.2019.111799.

[28] S. Sareen, G. Mathew, L. Joseph, Improvement in solubility of poor water-soluble drugs by solid dispersion., Int. J. Pharm. Investig. 2 (2012) 12–17. https://doi.org/10.4103/2230-973X.96921.

[29] M. Liu, Z. Lai, L. Zhu, X. Ding, X. Tong, Z. Wang, Q. Bi, N. Tan, Novel amorphous solid dispersion based on natural deep eutectic solvent for enhancing delivery of anti-tumor RA-XII by oral administration in rats., Eur. J. Pharm. Sci. Off. J. Eur. Fed. Pharm. Sci. 166 (2021) 105931. https://doi.org/10.1016/j.ejps.2021.105931.

[30] B.B. Hansen, S. Spittle, B. Chen, D. Poe, Y. Zhang, J.M. Klein, A. Horton, L. Adhikari, T. Zelovich, B.W. Doherty, B. Gurkan, E.J. Maginn, A. Ragauskas, M. Dadmun, T.A. Zawodzinski, G.A. Baker, M.E. Tuckerman, R.F. Savinell, J.R. Sangoro, Deep Eutectic Solvents: A Review of Fundamentals and Applications, Chem. Rev. 121 (2021) 1232–1285. https://doi.org/10.1021/acs.chemrev.0c00385.

[31] S. Sevvanthi, S. Muthu, M. Raja, S. Aayisha, S. Janani, PES, molecular structure, spectroscopic (FT-IR, FT-Raman), electronic (UV-Vis, HOMO-LUMO), quantum chemical and biological (docking) studies on a potent membrane permeable inhibitor: dibenzoxepine derivative, Heliyon. 6 (2020) e04724. https://doi.org/https://doi.org/10.1016/j.heliyon.2020.e04724.

[32] H. Wang, S. Liu, Y. Zhao, J. Wang, Z. Yu, Insights into the Hydrogen Bond Interactions in Deep Eutectic Solvents Composed of Choline Chloride and Polyols,

ACS Sustain. Chem. Eng. 7 (2019) 7760–7767. https://doi.org/10.1021/acssuschemeng.8b06676.

[33] A.A. Connor, S. Gallinger, Pancreatic cancer evolution and heterogeneity: integrating omics and clinical data, Nat. Rev. Cancer. 22 (2022) 131–142. https://doi.org/10.1038/s41568-021-00418-1.

[34] S. Khan, N. Chauhan, M.M. Yallapu, M.C. Ebeling, S. Balakrishna, R.T. Ellis, P.A. Thompson, P. Balabathula, S.W. Behrman, N. Zafar, M.M. Singh, F.T. Halaweish, M. Jaggi, S.C. Chauhan, Nanoparticle formulation of ormeloxifene for pancreatic cancer., Biomaterials. 53 (2015) 731–743. https://doi.org/10.1016/j.biomaterials.2015.02.082.

[35] J. Kleeff, M. Korc, M. Apte, C. La Vecchia, C.D. Johnson, A. V Biankin, R.E. Neale, M. Tempero, D.A. Tuveson, R.H. Hruban, J.P. Neoptolemos, Pancreatic cancer, Nat. Rev. Dis. Prim. 2 (2016) 16022. https://doi.org/10.1038/nrdp.2016.22.

[36] S. Mohan, K. Thiagarajan, R. Chandrasekaran, In vitro evaluation of antiproliferative effect of ethyl gallate against human oral squamous carcinoma cell line KB, Nat. Prod. Res. 29 (2015) 366–369. https://doi.org/10.1080/14786419.2014.942303.

[37] S. Mohan, K. Thiagarajan, R. Chandrasekaran, Evaluation of ethyl gallate for its antioxidant and anticancer properties against chemical-induced tongue carcinogenesis in mice., Biochem. J. 474 (2017) 3011–3025. https://doi.org/10.1042/BCJ20170316.

[38] S. Mushtaq, B.H. Abbasi, B. Uzair, R. Abbasi, Natural products as reservoirs of novel therapeutic agents., EXCLI J. 17 (2018) 420–451. https://doi.org/10.17179/excli2018-1174.

[39] D.J. Newman, G.M. Cragg, Natural Products as Sources of New Drugs over the Nearly Four Decades from 01/1981 to 09/2019, J. Nat. Prod. 83 (2020) 770–803. https://doi.org/10.1021/acs.jnatprod.9b01285.

[40] O. Trott, A.J. Olson, AutoDock Vina: improving the speed and accuracy of docking with a new scoring function, efficient optimization, and multithreading, J Comput Chem. 31 (2010) 455–461. https://doi.org/10.1002/jcc.21334.

[41] S.-H. Han, K.H. Ryu, A.-Y. Kwon, The Prognostic Impact of HER2 Genetic and Protein Expression in Pancreatic Carcinoma-HER2 Protein and Gene in Pancreatic Cancer., Diagnostics (Basel, Switzerland). 11 (2021). https://doi.org/10.3390/diagnostics11040653.

[42] C.M. Parsons, D. Muilenburg, T.L. Bowles, S. Virudachalam, R.J. Bold, The role of Akt activation in the response to chemotherapy in pancreatic cancer., Anticancer Res. 30 (2010) 3279–3289.

[43] M.J. Kamlet, J.L. Abboud, R.W. Taft, The solvatochromic comparison method. 6. The .pi.* scale of solvent polarities, J. Am. Chem. Soc. 99 (1977) 6027–6038. https://doi.org/10.1021/ja00460a031.

[44] A.K. Dwamena, D.E. Raynie, Solvatochromic Parameters of Deep Eutectic Solvents: Effect of Different Carboxylic Acids as Hydrogen Bond Donor, J. Chem. Eng. Data. 65 (2020) 640–646. https://doi.org/10.1021/acs.jced.9b00872.

[45] M.S. Rahman, D.E. Raynie, Thermal behavior, solvatochromic parameters, and metal halide solvation of the novel water-based deep eutectic solvents, J. Mol. Liq. 324 (2021) 114779. https://doi.org/https://doi.org/10.1016/j.molliq.2020.114779.

[46] Ternary Plot, (n.d.). https://www.ternaryplot.com/.

[47] S.K. Singh, A.W. Savoy, Ionic liquids synthesis and applications: An overview, J. Mol. Liq. 297 (2020) 112038. https://doi.org/https://doi.org/10.1016/j.molliq.2019.112038.

[48] K.S. Egorova, E.G. Gordeev, V.P. Ananikov, Biological Activity of Ionic Liquids and Their Application in Pharmaceutics and Medicine, Chem. Rev. 117 (2017) 7132–7189. https://doi.org/10.1021/acs.chemrev.6b00562.

[49] G. García, S. Aparicio, R. Ullah, M. Atilhan, Deep Eutectic Solvents: Physicochemical Properties and Gas Separation Applications, Energy & Fuels. 29 (2015) 2616–2644. https://doi.org/10.1021/ef5028873.

[50] A. Alhadid, L. Mokrushina, M. Minceva, Design of Deep Eutectic Systems: A Simple Approach for Preselecting Eutectic Mixture Constituents., Molecules. 25 (2020). https://doi.org/10.3390/molecules25051077.

CHAPTER FOUR

A COMPARATIVE STUDY BETWEEN TWO DODECYL GALLATE BASED THEDESs

4.1. Introduction

Dodecyl gallate is a natural product. It is a derivative of dodecanol and gallic acid. As an antioxidant compound, it shows diverse biological activities, such as antiproliferative, antibacterial, antifungal, etc. Cheng et al conducted a study on the anticancer potential of dodecyl gallate in a human osteosarcoma cell line. Apoptotic and antiproliferative mechanisms were explored using MG-63 cell line. IC_{50} value was found decreasing over 72 hour long treatment. Flow cytometry revealed cell growth arrest in the G1 and S phases. It has been found that increase in Bax/Bcl-2 ratio, decrease in IAP, and increase in apoptotic protein activity of caspase 3 and 8 indicates probable signaling of anticancer activity of dodecyl gallate in osteosarcoma [1]. Dodecyl gallate has been found to work against drug resistant bacteria. Kim et al showed that as a novel adjuvant, dodecyl gallate increases the efficiency of antimicrobial peptide bacitracin in treating community-associated MRSA (CA-MRSA) strain of bacteria [2]. Eddy et al conducted bacterial DNA gyrase inhibition study on a series of plant polyphenols. Interestingly it has been found that as a food additive, dodecyl gallate significantly inhibits activity of the enzyme. The drug might behave as an ATP competitive inhibitor of the enzyme. It could work against DNA topoisomerase enzyme of *E. coli* [3]. In a different study liver protection property of dodecyl gallate was shown in carbon tetrachloride-induced hepatic toxic rat model. In combination with gallic acid, the molecule significantly increased level of hepatic protective enzymes. Moreover, increase in P53 level confirms clearance of damaged hepatocytes to prevent lifelong failure of liver [4]. Dodecyl gallate improves oxidation stability of tribal insert to treat knee arthroplasty. It significantly protects oxidation state of highly crosslinked polymer polyethylene and enhance performance of surgical treatment for knee malfunction [5].

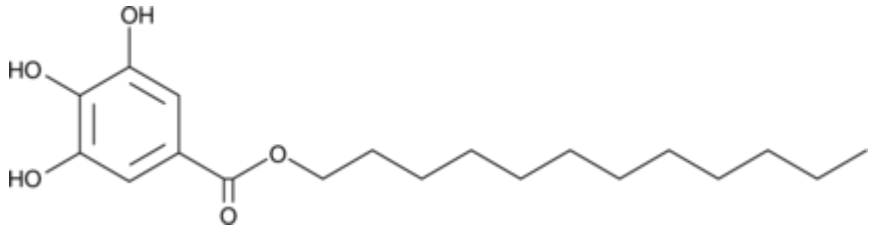

Figure 4.1. Chemical structure of dodecyl gallate.

In room temperature it exists as a crystalline solid. Its molar mass is 338.4 daltons. The molecular formula is $C_{19}H_{30}O_5$ (Figure 4.1). The molecule is insoluble in water but soluble in ether and ethanol. Due to nonpolarity, logP value is very high. That is why in this project our goal was to improve solubility of the drug like molecule. If the solubility is improved, it may further accelerate drug delivery and optimize other pharmacokinetic parameters. To improve solubility, we formulated two therapeutic deep eutectic solvents with TBABR and PEG 400. These compounds were selected based on screening with a series of biomolecules. It has been shown that therapeutic deep eutectic solvent holds great promise for improving drug solubility and delivery. As a result, bioavailability, permeability, stability, etc. are enhanced. We performed thermal stability, polarity, and structural property measurements. Deep eutectic solvent is formed due to nonbonding interactions. Using IR spectroscopy, we assessed the property. By utilizing solvatochromism, we assessed the polarity of the solvents. Thermal stability tests were performed using TGA. Molecular modeling analysis provides information about noncovalent interaction between components of THEDES. The goal of this project was to compare structural and spectroscopic properties of THEDES prepared from dodecyl gallate.

4.2. Experimental outline

4.2.1. Materials and Methods

Dodecyl gallate was purchased from Cayman Chemical (Ann Arbor, Michigan). TBABR (tetra-butyl ammonium bromide) was obtained from Sigma Aldrich. Polyethylene glycol (PEG 400) was purchased from Tex Lab Supply, Amarillo, Texas. Purity of these purchased chemicals was more than 90 %. We proceeded without further purification.

4.2.2. Formulation of the dodecyl gallate based THEDES

Dodecyl gallate-based deep eutectic solvent was formulated by mixing with a series of biomolecules at different molar ratios. Components were mixed properly and covered in a small glass container with magnetic stir bar. The glass containers were kept on a hot plate (80 °C) with continuous stirring (≤600 rpm) for 30 mins to 1.3 hours at normal atmospheric pressure. The mixing was continued until homogenous liquids were obtained. The solvents were kept under observation further for 24 hours to ensure no crystal formation. We observed dodecyl gallate forms DES with TBABR and PEG400 at 1:1 molar ratios (Figure 4.2).

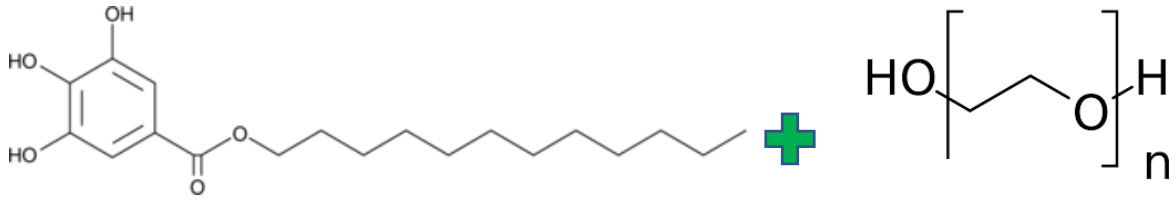

1 mole **1 mole**

Dodecyl gallate: PEG400 (1:1)

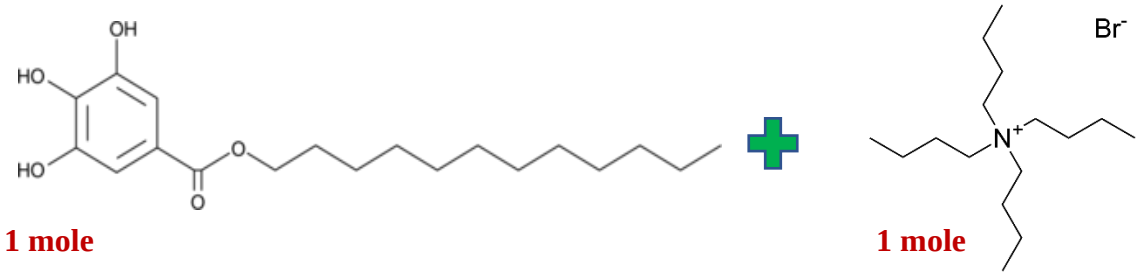

Dodecyl gallate: TBABR (1:1)

Figure 4.2. DES formulation between dodecyl gallate and other components at 1:1 molar ratios.

4.2.3. Thermal degradation analysis using Thermogravimetry

Thermogravimetric analyses of THEDESs were performed using TG/DTA 220 Seiko Instruments, Japan. Approximately, 10 mg of each DES sample was collected on a TGA aluminum pan and placed in the hot chamber with an empty aluminum pan as blank. The oven temperature range was set from 25 °C to 400 °C at constant rate of 10 °C/min. To maintain an inert atmospheric condition, nitrogen gas was used at a flow of 50 mL/min (Figure 4.3). Nitrogen removes pyrolysis gases, such as CH_4, C_2H_2, H_2, CO, CO_2, and water vapor, from the instrument to avoid possibility of contamination.

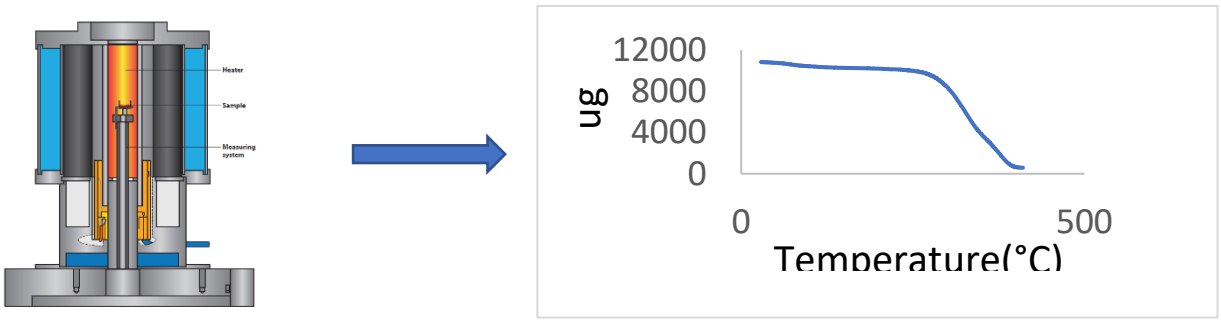

Figure 4.3. Thermogravimetric analysis describes degradation of DES with increase in temperature.

4.2.4. Water solubility experiment

To determine solubility of dodecyl gallate incorporated in DES, both dodecyl gallate based DES and the pure powder were added in water in a small, closed glass containers. The containers were then stirred for about 24 hours. The solutions were observed further for crystal formation. After observing the solution for crystal formation, solution was filtered using 0.22 μm filter paper before performing UV scan. Biotek UV microplate reader was utilized to produce absorption spectra. Range of wavelength was chosen from 230 nm to 700 nm. Wavelength of maximum absorption was selected, and spectral the interval was set at 10 nm. 250 μL of aliquot of test sample was loaded in a 96-well plate (Figure 4.4).

The outline below describes the solubility measurement of two deep eutectic solvents prepared from Dod. In this case at first standard curve was generated using pure dodecyl gallate. Then solubility of DES was measured by utilizing the standard curve equation.

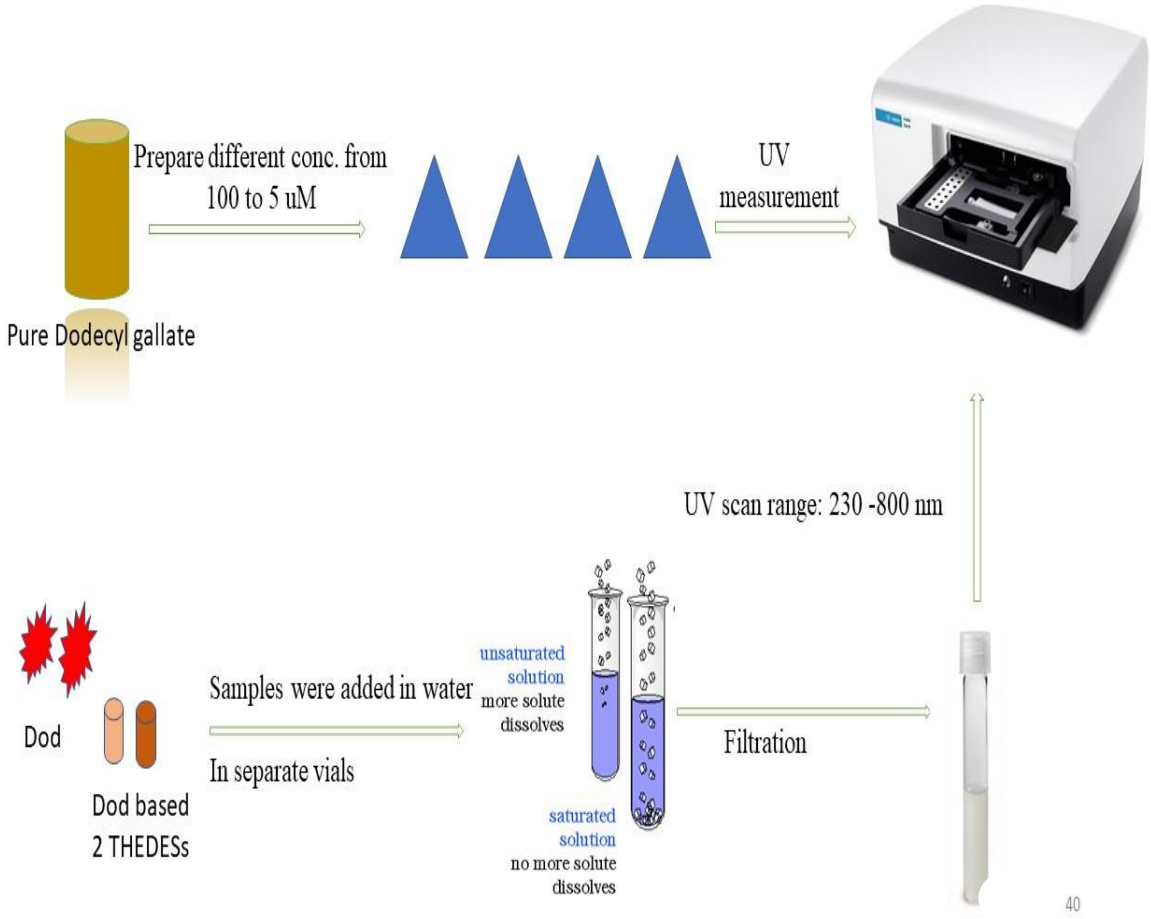

Figure 4.4. The flow diagram shows systematic outline of solubility experiment to determine solubility of dodecyl gallate.

4.2.5. FR-IR spectroscopic measurement

Infrared spectroscopic assessment is an excellent tool to investigate nonbonding interaction between components of therapeutic deep eutectic solvent. The outline of performing IR analysis is given below. Before running the experiment, each sample was prepared freshly.

FT-IR Spectrometer was used to scan the samples

Dodecyl gallate, PEG400, Dod-PEG400, Dod-TBABR were dissolved in DMSO and then spread on KBR plate before running the instrument

Spectra were recorded in transmission mode from 400 to 4000 cm^{-1}. Before each spectrum collection, background spectrum was collected.

4.2.6. Solvatochromism of THEDES

Experient was carried out using Nile red, 4–nitroaniline and N,N-diethyl -4-nitroaniline at conc. of 5×10^{-4} M

A 200 µL aliquot of each sample was loaded into a 96-well plate

Appropriate amount of dye was micro pipetted and mixed with DES sample and control solvent

Maximum absorbance and corresponding wavelength were determined using UV-Vis spectrometer in different temperatures

Transfer in 96 well plate

THEDES mixed with dyes

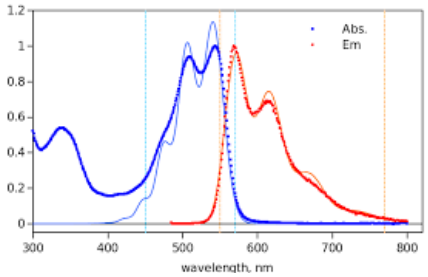

Scan in 96 UV spectrometer

4.2.7. Molecular modeling

Electrostatic potential graphs were generated for all the DES components including dodecyl gallate, tetra butyl ammonium bromide and polyethylene glycol 400. With the help of electron density location, we can get idea about electronic charge distribution of all atoms across the molecule, chemical reactivity and reveal charge transfer between noncovalent bonds, and lone pair electrons [6,7]. WebMO server was mainly followed to generate the data. In WebMO, blue/red indicates electron poor/electron rich and green/yellow means intermediate region [8].

4.3. Results and discussion

TBABR and PEG400 based deep eutectic solvent were formulated by mixing with dodecyl gallate at 1:1 molar ratio. Samples were heated at 80 °C for about one hour until a homogeneous mixture was obtained. The samples were further observed for 24 hours to exclude possibility of crystal formation.

4.3.1. Thermal stability of two dodecyl gallate based THEDES

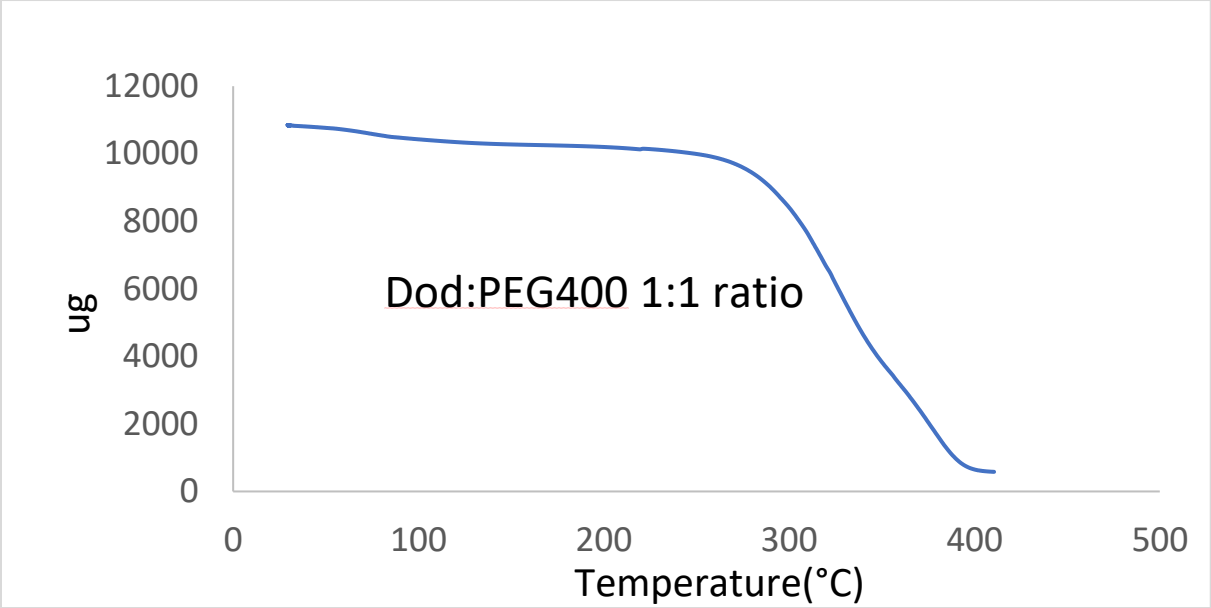

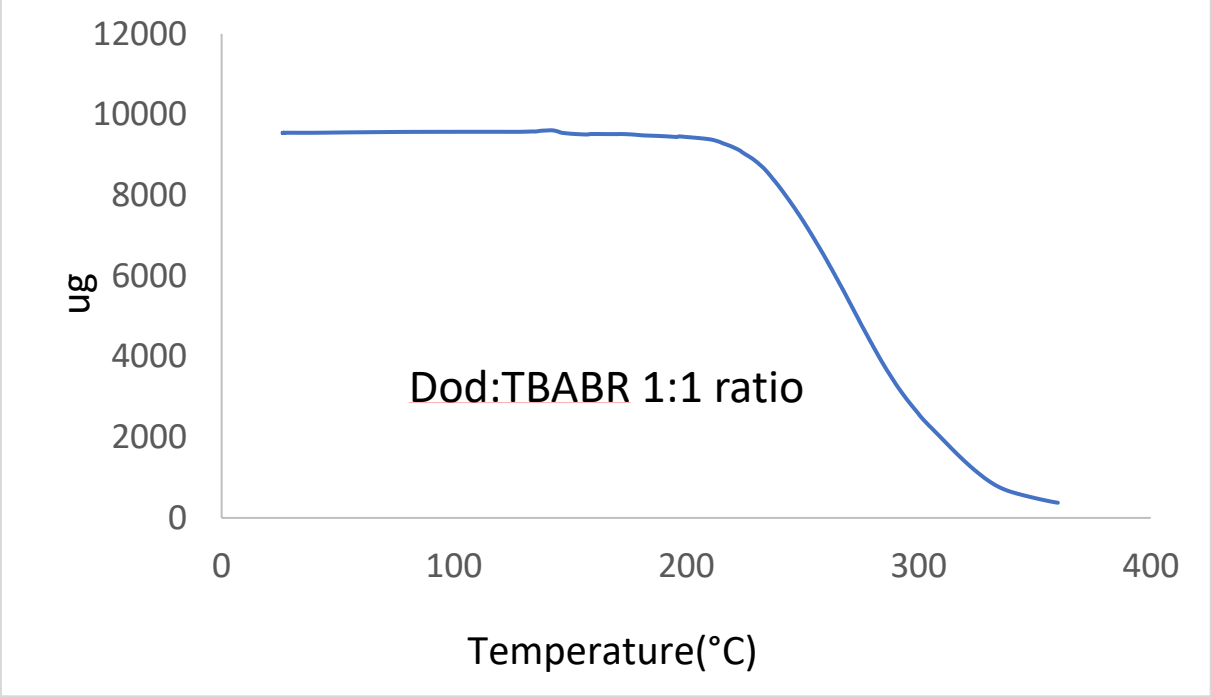

Figure 4.5. a) Thermal analysis of dodecyl gallate and TBABR and, b) dodecyl gallate and PEG400. Both formulations were stable up to 300 °C.

Heat tolerance capacity was analyzed using a Seiko 220 TG/DTA (Tokyo, Japan). High thermal stability indicates strong nonbonding interaction the components of deep eutectic solvent. According to the thermograms, major transition occurred for TBABR-based THEDES after 250 °C and for PEG400 based THEDES after 200 °C (Figure 4.5). Tight aluminum cap facilitated desired transition at high temperature. Thermal stability is one of remarkable physiological properties of DES [9]. Determination of highest temperature limits the maximum exposure of the solvent, set limit to make it suitable for use in industrial scale and ensure structural integrity. Thermal stability provides information to use low volatile compound so that it can prevent early degradation with increasing temperature [9,10]. In some previous studies excellent thermal stability were reported [10,11]. It also has been demonstrated that hydrogen bonds play important role in ensuring thermal stability of the solvent [12,13].

4.3.2. IR spectroscopic analysis of two dodecyl gallate based THEDES

IR spectroscopic analysis was performed to observe any nonbonding interaction between the DES components. In this study we performed infrared spectroscopic analysis of both THEDES prepared from dodecyl gallate along with pure dodecyl gallate. Spectral scanning was performed from 400 to 4000 cm^{-1}. The results are given below:

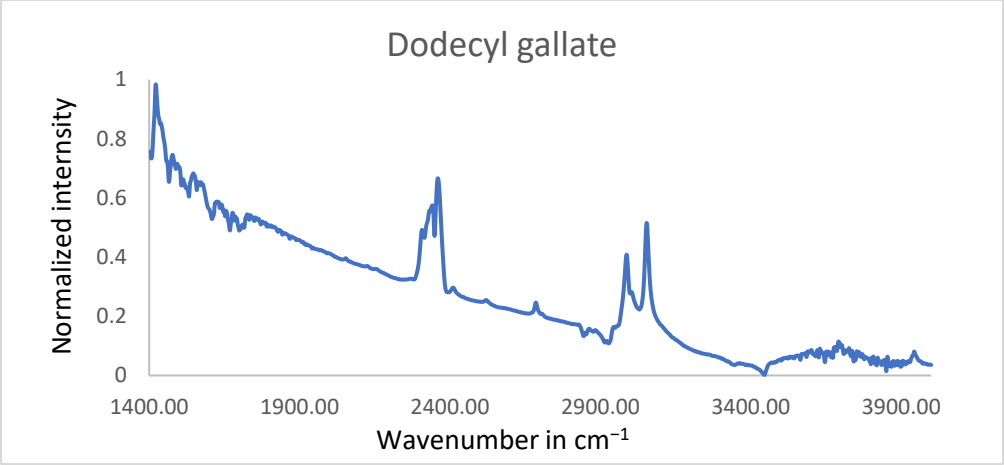

Pure dodecyl gallate

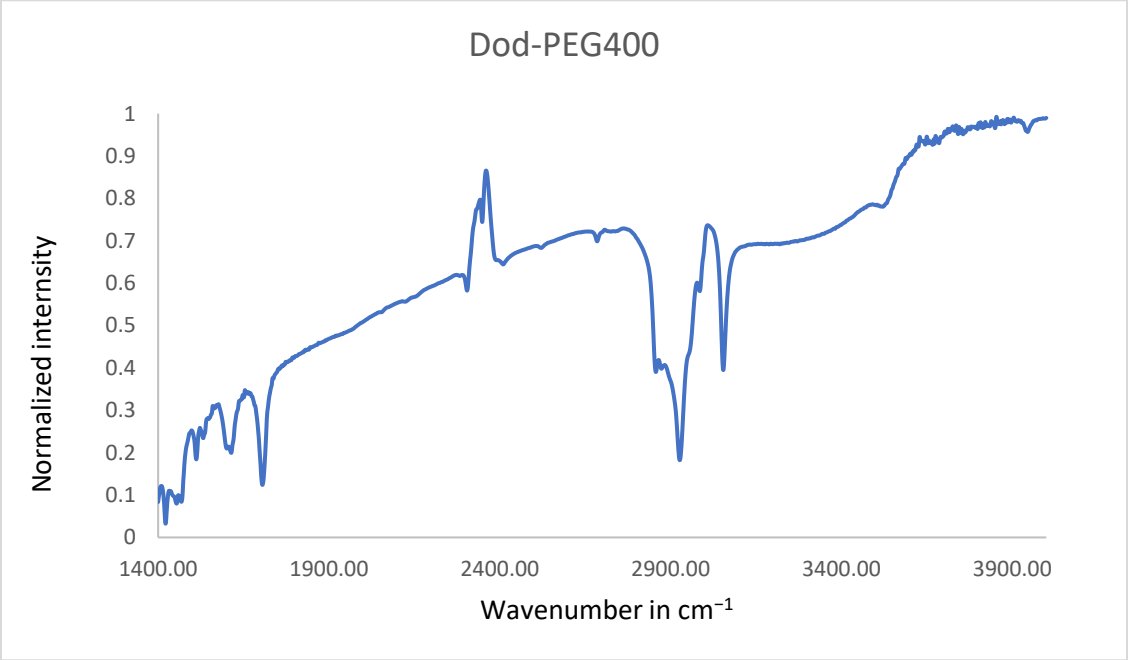

Dodecyl gallate-PEG400 (1:1)

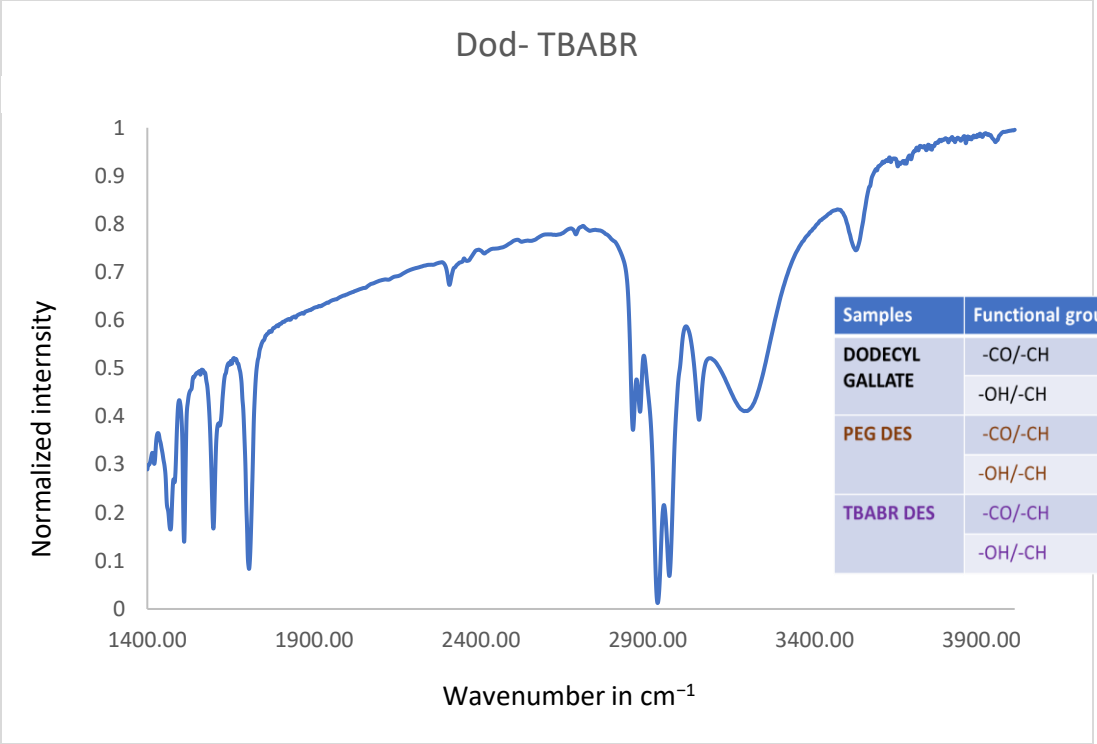

Samples	Functional group ratio	Value
DODECYL GALLATE	-CO/-CH	0.55
	-OH/-CH	1.05
PEG DES	-CO/-CH	0.87
	-OH/-CH	0.50
TBABR DES	-CO/-CH	0.88
	-OH/-CH	0.55

Dodecyl gallate-TBABR (1:1)

Figure 4.6. IR spectroscopic analysis of dodecyl gallate, PEG400, dodecyl gallate-TBABR and, dodecyl gallate- PEG400. Peak intensity ratio between core functional in each molecule was also calculated.

IR peak intensity is expressed as wavenumber vs normalized intensity. The pure molecule has some key functional groups namely -OH, -CH and -CO. When it forms nonbonding interactions with PEG400 and TBABR, peak intensity and position changed in the spectra (Figure 4.6). For -OH group stretching peak intensity became shaper and narrow compared to the pure dodecyl gallate and PEG 400. For carbonyl group we noticed sharp and intense peaks in both THEDES compared to pure dodecyl gallate and PEG400 (Figure 4.6). Peak intensity ratio was also calculated to add more insights in hydrogen bonding interaction. The eutectic interaction is predominantly between the -OH on the gallate to the PEG, or

TBABR. Intensity change was high (1.05, 0.5, and 0.55 for -OH/-CH in dodecyl gallate, PEG based DES and TBABR based DES respectively). It has been proved that classical and non-classical hydrogen bonding play vital role in forming DES and major contributor of peak shift, narrowing, broadening or intensification [12][14].

4.3.3. Solvatochromism analysis of THEDES

Solvatochromism analysis was for both THEDES prepared from dodecyl gallate. The assay determined polarity of the solvents in different temperature starting from 25 to 45 °C. All solvatochromic properties of the DESs were calculated using the following equations.

ET(NR)kcal.mol-1 = 28591.44/λmax(nm) …… (i)

π^* = 0.314 (27.52 – υN,N−diethyl−4−nitroaniline) …… (ii)

α = 0.0649 ET (NR) – 2.03 – 0.72 π^* …… (iii)

β = 1.035 υN,N−diethyl−4−nitroaniline+2.64− υ4−nitroaniline/2.80 ……..…2.2.6 (iv)

$ET^N = ET(solvent) - ET(TMS)/ET(water) - ET(TMS)$ …… (v)

Where, υ = wavenumber, α = hydrogen bond donor acidity, β = hydrogen bond acceptor basicity, π^* = polarizability, and ET^N (unitless) and ET(NR) refer to transition energy [15].

Results of different polarity parameters are given below for PEG 400 based THEDES.

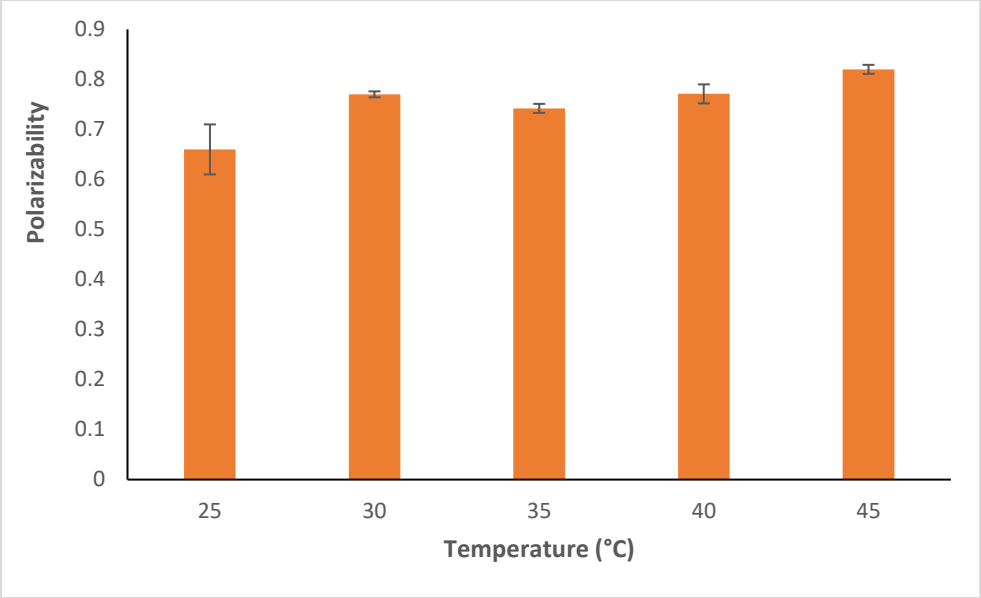

Dod: PEG400 polarity

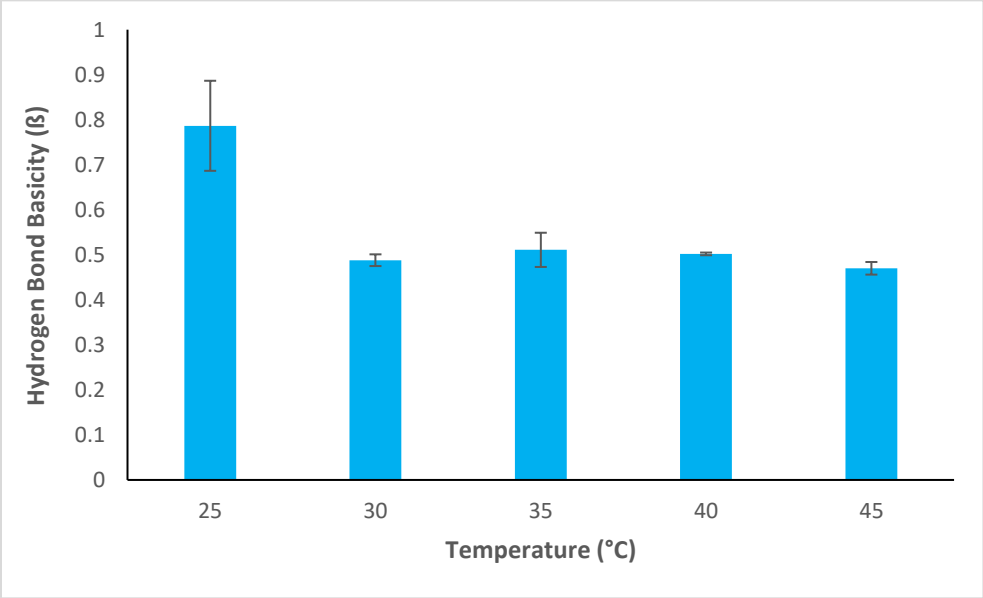

Hydrogen bond basicity of Dod:PEG400

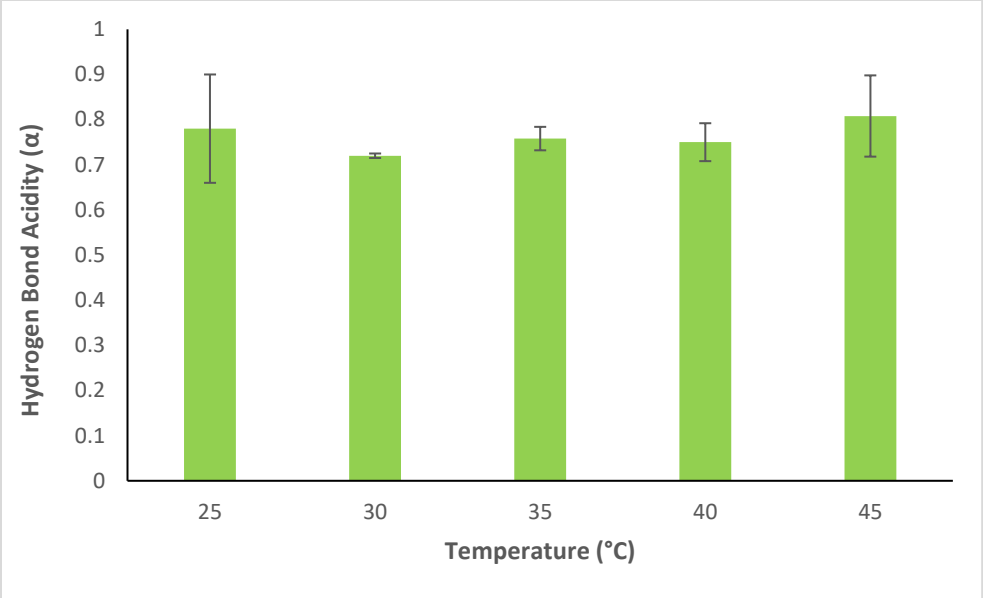

Hydrogen bond acidity of Dod:PEG400

Figure 4.7. Solvatochromism parameters of dodecyl gallate and PEG400 based DES. Results are presented as mean±SD. Two independent trials were performed to analyze the parameters.

Results of different polarity parameters are given below for TBABR based THEDES

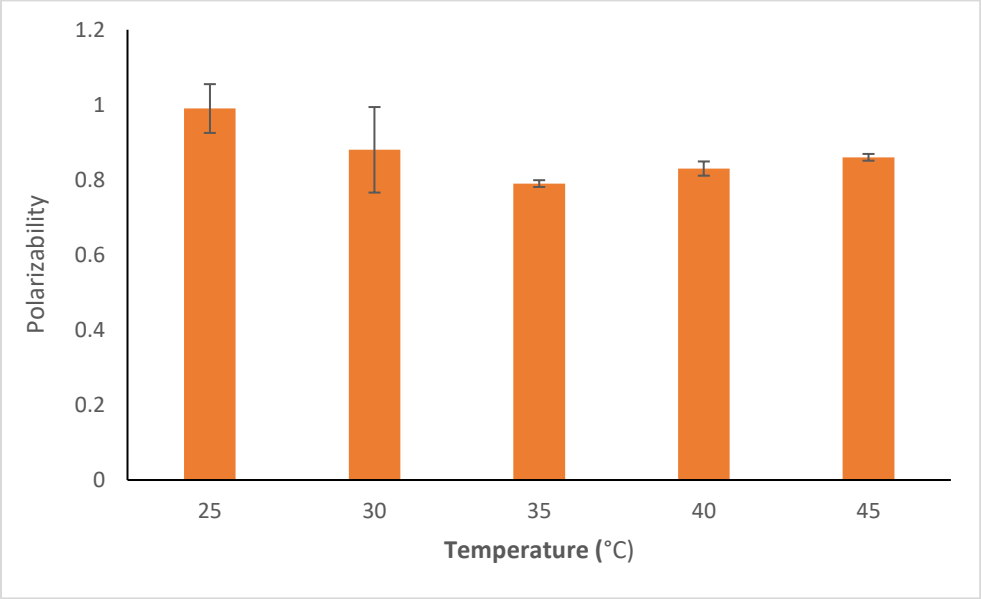

Dod:TBABR polarity

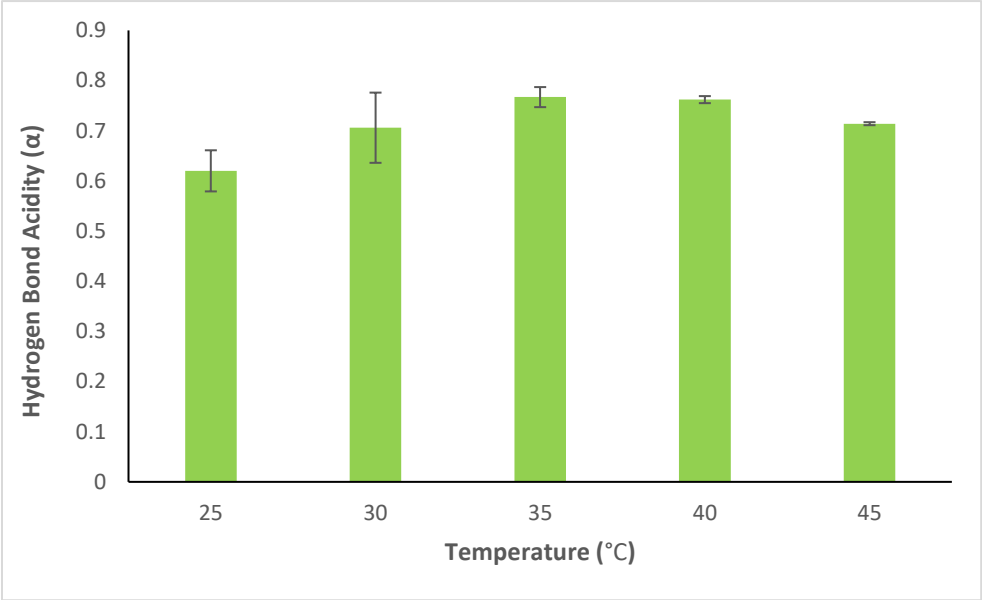

Hydrogen bond acidity of Dod:TBABR

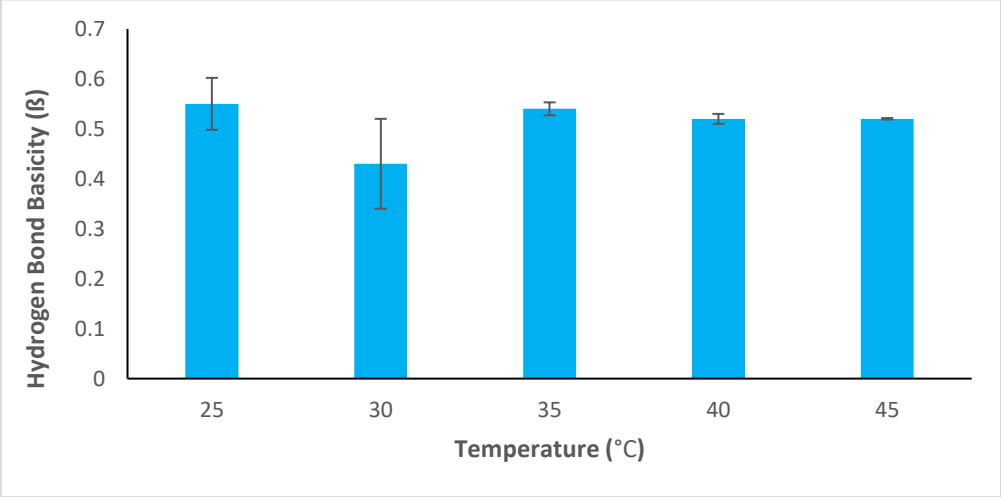

Hydrogen bond basicity of Dod:TBABR

Figure 4.8. Solvatochromism parameters of dodecyl gallate and TBABR based DES. Results are presented as mean only. Two independent trials were performed to analyze the parameters.

A)

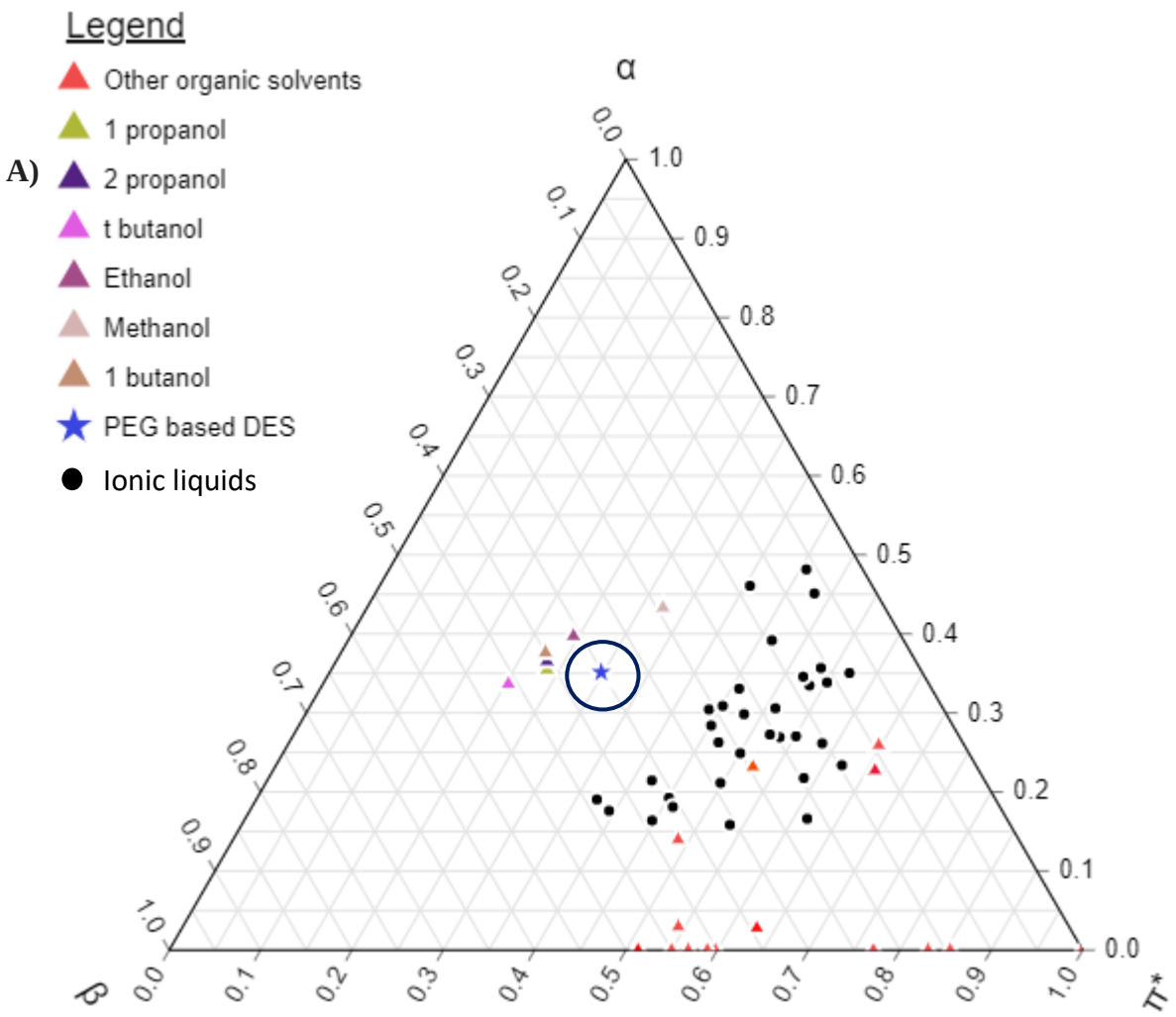
Legend
Other organic solvents
1 propanol
2 propanol
t butanol
Ethanol
Methanol
1 butanol
PEG based DES
Ionic liquids
α
β
π*

B)

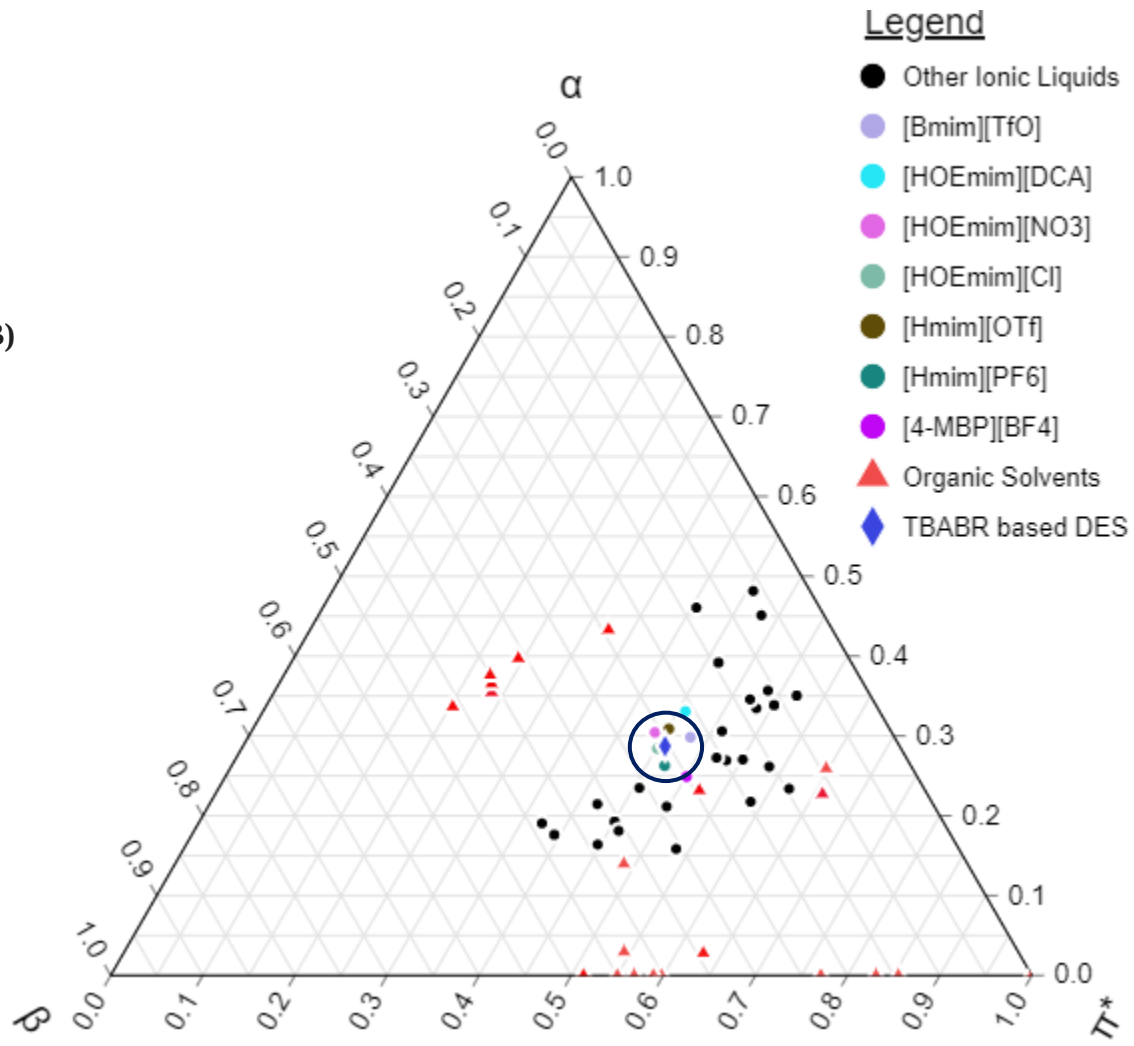

Figure 4.9A and 4.9B. Ternary plot of dodecyl gallate based DESs, ionic liquids, and organic solvents generated based on Kamlet-Taft parameters (α, β, and π*). Solvatochromism parameters were collected from previously published literature and plotted in ternary plot server [16][17]. Organic solvents and ionic liquids closely related to DESs are highlighted in different colors to provide understanding about probable polar nature of formulated DESs. Position of DESs in the plot are presented in circles.

We observed the effect of temperature on different polarity parameters for both solvents (Figure 4.7 and 4.8). In previous studies it has been found that polarity, hydrogen bond acidity, and hydrogen bond basicity govern the interaction between hydrogen bond donor (HBD) and hydrogen bond acceptor (HBA) [15,18,19]. At ambient temperature, polarizability of TBABR based DES is higher than PEG based DES. It indicates that electron cloud in both formulations are well distributed and localized [15,19]. Kamlet-Taft parameters of DESs were compared with parameters of selected ionic liquids and organic solvents. Solvent selectivity triangle plot was prepared from Kamlet-Taft parameters to describe polarity of test samples. TBABR based DES is mostly closed to polarity of ionic liquids. On the other hand. PEG based DES falls on the side of organic solvents. To produce solvent selectivity triangle, polarity parameters at ambient temperature were chosen. PEG based DES is closely related to organic solvents namely methanol, ethanol, propanol and butanol. We can assume that the therapeutic solvent shares similar polarity properties with traditional organic solvents routinely used in various drug discovery and development research. TBABR based DES share similar properties with ionic liquids namely [Bmim][TfO], [HOEmim][DCA], [HOEmim][NO3], [HOEmim][Cl], [Hmim][OTf], [Hmim][PF6] and, [4-MBP][BF4] (Figure 4.5B). Majority of ionic liquids that show similar properties contain 1-hexyl-3-methyl-imidazolium (Hmim) and 1-(2-hydroxylethyl)-3-methylimidazolium ([HOEMIm]) cations (Figure 4.9). Ionic liquids are excellent resources for using as catalytic agent in chemical synthesis, extraction, and separation of analytical samples.

4.3.4. Solubility profile of THEDES

Though DES is a viscous and thick liquid, it significantly improves solubility of poorly water-soluble anticancer agents. In this experiment we performed solubility of both therapeutic solvents in water and compared it to pure dodecyl gallate. We used a UV microplate reader to measure solubility. Standard curves were generated by running a known range of concentrations. Based on UV absorption spectra solubility profile was determined. The standard curve to determine the unknown concentration of soluble dodecyl gallate in THEDES format was $y=0.0088x-0.0005$, $R^2 = 0.9983$.

Results of solubility of dodecyl gallate in DES format are shown below:

Table 4.1. Solubility of Dod in water in pure and THEDES forms.

Samples	**Solubility in mg/mL**
Dod powder	0.0010 ± 0.00002
Dod:PEG400 (1:1)	0.0025± 0.00004
Dod:TBABR (1:1)	0.0019± 0.00005

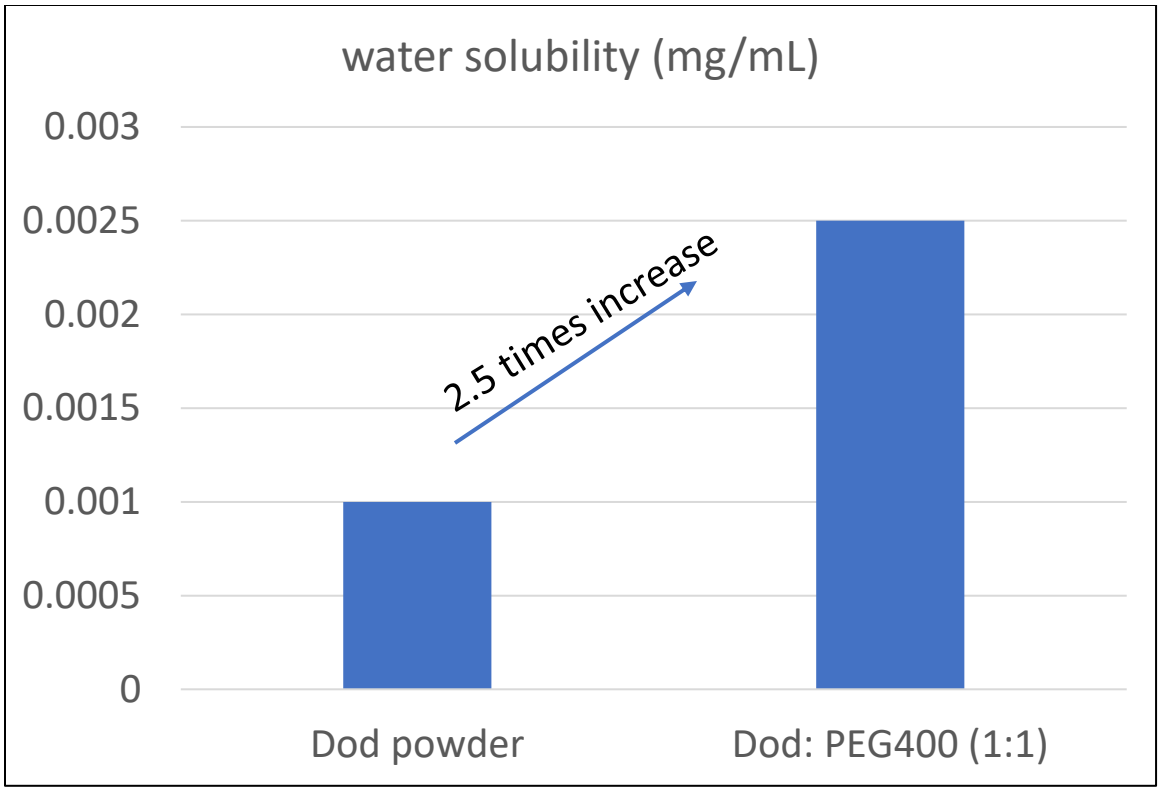

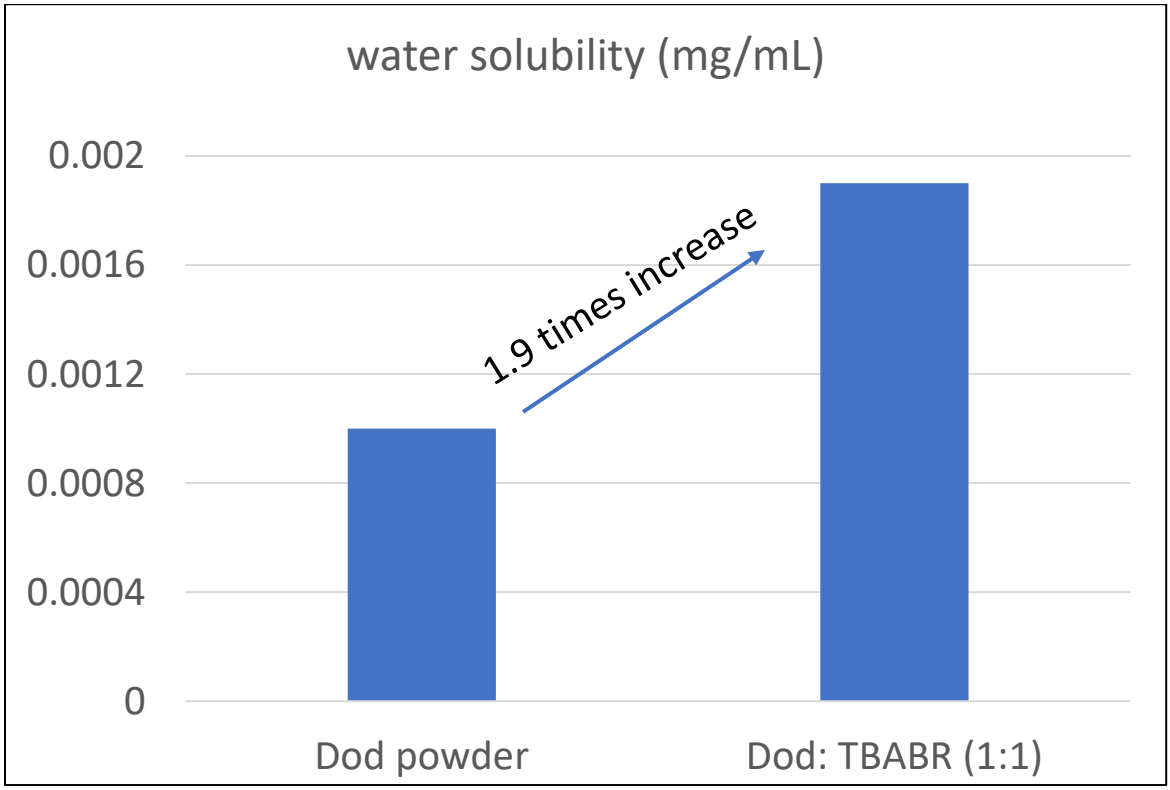

Figure 4.10. Solubility of Dod increased in THEDES format compared to powder form.

Solubility is a major issue in drug formulation in pharmaceutical industry. According to a recent study at least 40 % pharmaceutical API suffers from poor water solubility [20]. Solubility ensures desired drug concentrations to be achieved for exerting proper pharmacological effect. Poor water solubility significantly impacts pharmacokinetics parameters of API [20,21]. As a result, it reduces bioavailability, drug permeability and ultimately affect pharmacological action [20,21]. Due to poor solubility, formulation scientists struggle to design appropriate drug delivery system. As a new class of solvent, DES has emerged an excellent alternative formulation to improve drug solubility and drug delivery [22–25]. In our current experiment, PEG400-based solvent improved dodecyl gallate solubility 2.5 times more than pure compound. On the other hand, TBABR-based solvent enhanced solubility by 1.5 times (Table 4.1, Figure 4.10). Between both solvents, PEG400 showed improved performance.

4.3.5. Molecular modeling analysis of THEDES

To calculate molecular orbitals and associated energy parameters, at first molecule mechanistic optimization was performed for all molecules. Then the structures were proceeded for further image analysis.

Table 4.2. Molecular properties of all DES components.

DES components	**Total strain energy**	**Bond stretch**	**Angle bend**	**Stretch bend**	**OP bend**	**Torsion**	**Van der Waals**	**Electrostatic**
Dodecyl gallate	34.9230 kcal/mol	15.0378	4.3001	-1.3805	0.0050	-8.4566	26.8239	-1.4067
TBABR	26.0115 Kcal/mol	2.527	8.508	1.011	0.000	2.323	11.64	0.000
Ethylene glycol (unit of PEG400)	13.0748 kcal/mol	0.0822	0.3777	-0.13	0.00	-0.4235	12.34	0.8298

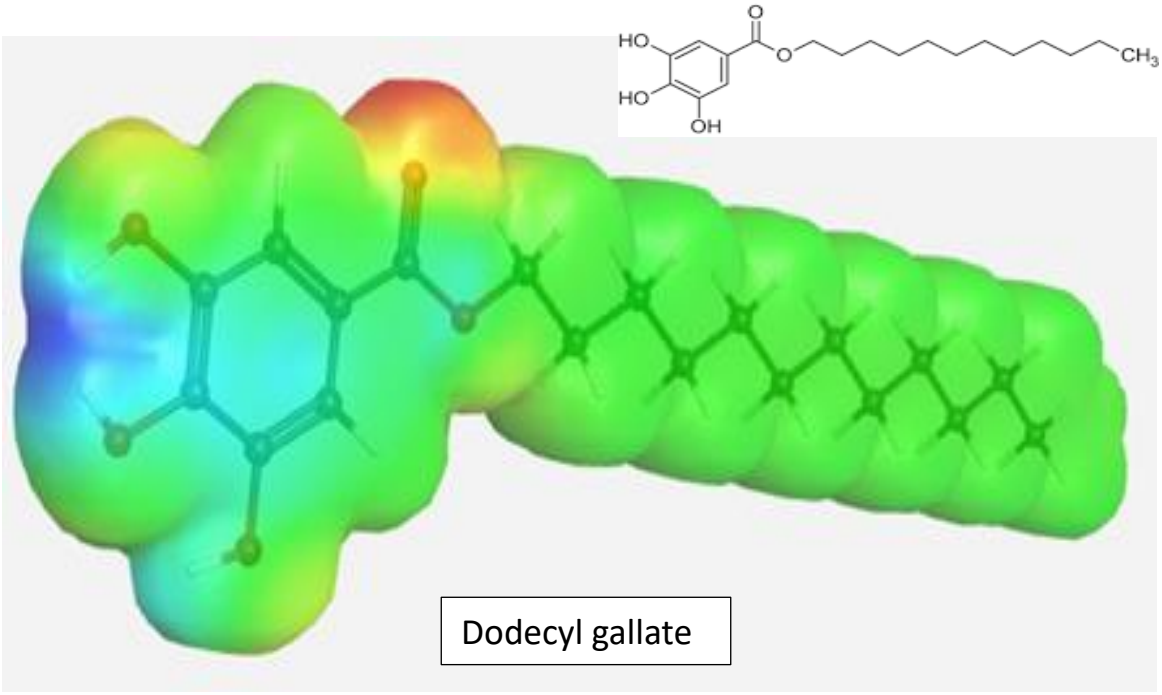

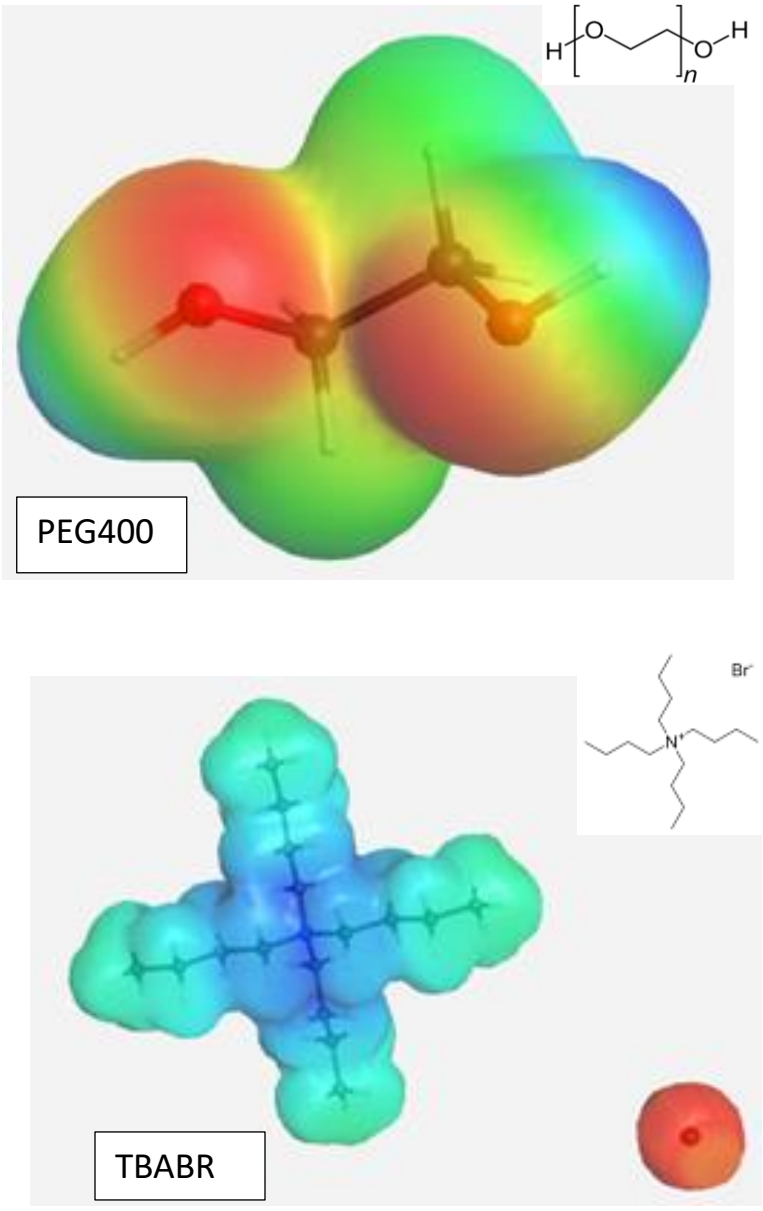

Figure 4.11. Electron density graph for dodecyl gallate, PEG 400 (ethylene glycol) and TBABR.

Quantum parameters were calculated for DES components. It indicates physicochemical properties of DES components [8,26]. Quantum parameters justify nonbonding interaction (hydrogen bond) takes place between DES components. Table 4.2. shows thermodynamic

properties of all DES components. From electrostatic potential surface analysis of dodecyl gallate, we see that red color is around oxygen of carbonyl group and blue color is around hydrogen of hydroxyl groups. For PEG400, we see that red and blue colors are around oxygen and hydrogen respectively. For TBABR, red color is on bromide ion and blue color is on Quaternary ammonium cation. The color indicates possible electrophile or nucleophile attacks (Figure 4.11). Electron rich and electron poor regions participate in hydrogen bonding interaction and solidify DES formation. [8].

In addition to electrostatic potential, electrostatic energy, strain energy, and solvatochromic parameters like hydrogen bond acidity, hydrogen bond basicity and polarizability provides insight about hydrogen bonding interaction between DES components [6,8,26,27].

4.4. Conclusion

In a nutshell, dodecyl gallate based DES tremendously improves water solubility of the molecule compared to pure form. Spectroscopic assessment describes rationale for hydrogen bonding interaction between DES components. DES shares similar polarity with some common ionic liquids and organic solvents. Thermal analysis shows that, both DES formulations are thermally stable at high temperature. Electrostatic potential provides deep insight on possible interaction area for hydrogen bonding attraction between DES components. The physicochemical studies will establish possible drug delivery applications of dodecyl gallate based DES in animal based models.

4.5. References

[1] C.-H. Cheng, Y.-P. Cheng, I.-L. Chang, H.-Y. Chen, C.-C. Wu, C.-P. Hsieh, Dodecyl gallate induces apoptosis by upregulating the caspase-dependent apoptotic pathway and inhibiting the expression of anti-apoptotic Bcl-2 family proteins in human osteosarcoma cells., Mol. Med. Rep. 13 (2016) 1495–1500. https://doi.org/10.3892/mmr.2015.4717.

[2] J.-C. Kim, B. Jeon, Novel adjuvant strategy to potentiate bacitracin against MDR MRSA., J. Antimicrob. Chemother. 71 (2016) 1260–1263. https://doi.org/10.1093/jac/dkv463.

[3] E.E. Alfonso, R. Troche, Z. Deng, T. Annamalai, P. Chapagain, Y.-C. Tse-Dinh, F. Leng, Potent Inhibition of Bacterial DNA Gyrase by Digallic Acid and Other Gallate Derivatives., ChemMedChem. (2022) e202200301. https://doi.org/10.1002/cmdc.202200301.

[4] M.R.A. Perazzoli, C.K. Perondi, C.M. Baratto, E. Winter, T.B. Creczynski-Pasa, C. Locatelli, Gallic Acid and Dodecyl Gallate Prevents Carbon Tetrachloride-Induced Acute and Chronic Hepatotoxicity by Enhancing Hepatic Antioxidant Status and Increasing p53 Expression., Biol. Pharm. Bull. 40 (2017) 425–434. https://doi.org/10.1248/bpb.b16-00782.

[5] M. Zhang, J.-Y. Wang, J. Su, J.-J. Wang, S.-T. Yan, Y.-C. Luan, C.-K. Cheng, Wear Assessment of Tibial Inserts Made of Highly Cross-Linked Polyethylene Supplemented with Dodecyl Gallate in the Total Knee Arthroplasty., Polymers (Basel). 13 (2021). https://doi.org/10.3390/polym13111847.

[6] M. Miar, A. Shiroudi, K. Pourshamsian, A.R. Oliaey, F. Hatamjafari, Theoretical investigations on the HOMO–LUMO gap and global reactivity descriptor studies, natural bond orbital, and nucleus-independent chemical shifts analyses of 3-phenylbenzo[d]thiazole-2(3H)-imine and its para-substituted derivatives: Solvent and subs, J. Chem. Res. 45 (2020) 147–158. https://doi.org/10.1177/1747519820932091.

[7] M.A. Mumit, T.K. Pal, M.A. Alam, M.A.-A.-A.-A. Islam, S. Paul, M.C. Sheikh, DFT studies on vibrational and electronic spectra, HOMO-LUMO, MEP, HOMA, NBO and molecular docking analysis of benzyl-3-N-(2,4,5-trimethoxyphenylmethylene)hydrazinecarbodithioate., J. Mol. Struct. 1220 (2020) 128715. https://doi.org/10.1016/j.molstruc.2020.128715.

[8] W.F. Polik, J.R. Schmidt, WebMO: Web-based computational chemistry calculations in education and research, WIREs Comput. Mol. Sci. 12 (2022) e1554. https://doi.org/https://doi.org/10.1002/wcms.1554.

[9] M. Marchel, H. Cieśliński, G. Boczkaj, Thermal Instability of Choline Chloride-Based Deep Eutectic Solvents and Its Influence on Their Toxicity─Important Limitations of DESs as Sustainable Materials, Ind. Eng. Chem. Res. 61 (2022) 11288–11300. https://doi.org/10.1021/acs.iecr.2c01898.

[10] J.A. Kist, M.T. Henzl, J.L. Bañuelos, G.A. Baker, Calorimetric Evaluation of the Operational Thermal Stability of Ribonuclease A in Hydrated Deep Eutectic Solvents, ACS Sustain. Chem. Eng. 7 (2019) 12682–12687. https://doi.org/10.1021/acssuschemeng.9b02585.

[11] K.-P. Lin, G.-J. Feng, F.-L. Pu, X.-D. Hou, S.-L. Cao, Enhancing the Thermostability of Papain by Immobilizing on Deep Eutectic Solvents-Treated Chitosan With Optimal Microporous Structure and Catalytic Microenvironment , Front. Bioeng. Biotechnol. . 8 (2020). https://www.frontiersin.org/articles/10.3389/fbioe.2020.576266.

[12] H. Wang, S. Liu, Y. Zhao, J. Wang, Z. Yu, Insights into the Hydrogen Bond Interactions in Deep Eutectic Solvents Composed of Choline Chloride and Polyols, ACS Sustain. Chem. Eng. 7 (2019) 7760–7767. https://doi.org/10.1021/acssuschemeng.8b06676.

[13] D.O. Abranches, L.P. Silva, M.A.R. Martins, S.P. Pinho, J.A.P. Coutinho, Understanding the Formation of Deep Eutectic Solvents: Betaine as a Universal Hydrogen Bond Acceptor, ChemSusChem. 13 (2020) 4916–4921. https://doi.org/https://doi.org/10.1002/cssc.202001331.

[14] R. Stefanovic, M. Ludwig, G.B. Webber, R. Atkin, A.J. Page, Nanostructure{,} hydrogen bonding and rheology in choline chloride deep eutectic solvents as a function of the hydrogen bond donor, Phys. Chem. Chem. Phys. 19 (2017) 3297–3306. https://doi.org/10.1039/C6CP07932F.

[15] A.K. Dwamena, D.E. Raynie, Solvatochromic Parameters of Deep Eutectic Solvents: Effect of Different Carboxylic Acids as Hydrogen Bond Donor, J. Chem. Eng. Data. 65 (2020) 640–646. https://doi.org/10.1021/acs.jced.9b00872.

[16] M.S. Rahman, D.E. Raynie, Thermal behavior, solvatochromic parameters, and metal halide solvation of the novel water-based deep eutectic solvents, J. Mol. Liq. 324 (2021) 114779. https://doi.org/https://doi.org/10.1016/j.molliq.2020.114779.

[17] Ternary Plot, (n.d.). https://www.ternaryplot.com/.

[18] A.R.R. Teles, E. V Capela, R.S. Carmo, J.A.P. Coutinho, A.J.D. Silvestre, M.G. Freire, Solvatochromic parameters of deep eutectic solvents formed by ammonium-based salts and carboxylic acids., Fluid Phase Equilib. 448 (2017) 15–21. https://doi.org/10.1016/j.fluid.2017.04.020.

[19] C. Florindo, A.J.S. McIntosh, T. Welton, L.C. Branco, I.M. Marrucho, A closer look into deep eutectic solvents: exploring intermolecular interactions using solvatochromic probes, Phys. Chem. Chem. Phys. 20 (2018) 206–213. https://doi.org/10.1039/C7CP06471C.

[20] K.T. Savjani, A.K. Gajjar, J.K. Savjani, Drug solubility: importance and enhancement techniques., ISRN Pharm. 2012 (2012) 195727. https://doi.org/10.5402/2012/195727.

[21] S. Sareen, G. Mathew, L. Joseph, Improvement in solubility of poor water-soluble drugs by solid dispersion., Int. J. Pharm. Investig. 2 (2012) 12–17. https://doi.org/10.4103/2230-973X.96921.

[22] A. Gutiérrez, M. Atilhan, S. Aparicio, A theoretical study on lidocaine solubility in deep eutectic solvents, Phys. Chem. Chem. Phys. 20 (2018) 27464–27473. https://doi.org/10.1039/C8CP05641B.

[23] Z. Li, P.I. Lee, Investigation on drug solubility enhancement using deep eutectic solvents and their derivatives., Int. J. Pharm. 505 (2016) 283–288. https://doi.org/10.1016/j.ijpharm.2016.04.018.

[24] S. Trombino, C. Siciliano, D. Procopio, F. Curcio, A.S. Laganà, M.L. Di Gioia, R. Cassano, Deep Eutectic Solvents for Improving the Solubilization and Delivery of Dapsone., Pharmaceutics. 14 (2022). https://doi.org/10.3390/pharmaceutics14020333.

[25] M. Mokhtarpour, H. Shekaari, M.T. Zafarani-Moattar, S. Golgoun, Solubility and solvation behavior of some drugs in choline based deep eutectic solvents at different temperatures, J. Mol. Liq. 297 (2020) 111799. https://doi.org/https://doi.org/10.1016/j.molliq.2019.111799.

[26] S. Sevvanthi, S. Muthu, M. Raja, S. Aayisha, S. Janani, PES, molecular structure, spectroscopic (FT-IR, FT-Raman), electronic (UV-Vis, HOMO-LUMO), quantum chemical and biological (docking) studies on a potent membrane permeable inhibitor: dibenzoxepine derivative, Heliyon. 6 (2020) e04724. https://doi.org/https://doi.org/10.1016/j.heliyon.2020.e04724.

[27] L.-G. Zhuo, W. Liao, Z.-X. Yu, A Frontier Molecular Orbital Theory Approach to Understanding the Mayr Equation and to Quantifying Nucleophilicity and Electrophilicity by Using HOMO and LUMO Energies, Asian J. Org. Chem. 1 (2012) 336–345. https://doi.org/https://doi.org/10.1002/ajoc.201200103.

CHAPTER FIVE

SUMMARY AND FUTURE DIRECTION

Chemoresistance is the most challenging situation faced in cancer science today. Due to chemoresistance, chemotherapy loses efficacy and as a result cancer cells survive. According to the National Cancer Institute, since 2022 chemoresistance has been exclusively focused on as a dominant barrier in the path of success of chemotherapy. There are several causes behind evolving chemoresistance. The major cause is overexpression of ABC transporters such as P-glycoprotein, MRP1 and BCRP. MRP1 is one of the major ABC transporters that play a significant role in pumping most of the anticancer drugs out of the cells. Overexpression of this transporter mainly exert this unwanted pharmacologic effect. Currently there are some available established protocols to detect possible MRP1 substrates, for example, fluorescence-based assay, flow cytometry, radiolabeled MRP1 substrate accumulation, FRET-based ABC biosensors to detect substrates, and bidirectional transport assays coupled with LCMS. However, all these established protocols have several disadvantages. The protocols are technically complicated to perform, require hand on experience, expensive instrument set up, complex image analysis, some protocols need preparation of complex inside out membrane vesicle, and are based on accumulation of secondary fluorescence or radiolabeled substrates. The novel assay will significantly overcome disadvantages associated with currently established protocols. The novel method will directly detect the substrates anticancer drugs. It is easy and simple to perform and requires less time and technical expertise. We already detected possible MRP1 substrates namely alisertib, mesalamine and celecoxib. The idea of novel *in vitro* cell based efflux assay will be applicable to other prominent Pgp or BCRP ABC transporters. The novel assay will assist in identifying exact substrates of MRP1 or other transporters. It will significantly improve the outcome of current cancer chemotherapy in treating direct

cancers. With the help of the novel protocol and identification of transporter-specific substrates, scientists could design transporter specific inhibitors to prevent efflux of substrates. It might also be helpful to selectively inhibit and kill the ABC transporter overexpressed cancer cells.

The research might be extended to further development of transporter specific 3D-tumoroid model assay in different cancer conditions to detect substrate and specific inhibitor more accurately because a 3D model represents human cells in better than 2D cell-based assay model. The extended knowledge will help us to further develop *in vivo* animal model-based transporter specific preclinical assay models. Overall, novel cell-based efflux assay will significantly contribute to drug discovery and development of new drug candidates and enhance potency of approved chemotherapeutic agents in the market. Recently, emerging immunotherapy approach is considered another effective approach to treat recurrent cancerous conditions. The assay will assist in designing selective antibody to target the transporter-overexpressed cells and overcome drug resistance. Moreover, we will get insight about novel transporter specific inhibitors and specific cytotoxic agents to kill the overexpressed cancer cells selectively.

Therapeutic deep eutectic solvents (THEDES) are specialized class of deep eutectic solvent that comprises one active pharmaceutical API and one biomolecule. It is known as a binary deep eutectic solvent. THEDES is a new concept in the field of pharmaceutics research. Nowadays, approximately 40% of pharmaceutical API face poor water solubility issue. Poor solubility significantly affects drug delivery, bioavailability, permeability, and pharmacological response of the API molecule. If the desired concentration is not achieved, API shows drastic reduction in pharmacological activity. Low solubility limits

possibility of proper drug formulation and unwanted side effects. As a safe solvent for human health, it preserves the integrity of pharmaceutical API and makes it compatible for administration into human patients. Traditional organic solvents are hazardous and not applicable for pharmaceutical application. THEDES is an excellent alternative. It improves solubility, dissolution profile, bioavailability, *in vivo* drug absorption, and pharmacological activity. In this project, solubility of poorly water-soluble anticancer agents, namely ethyl gallate and dodecyl gallate, were significantly improved compared to the pure compounds. Structural and biological activities were also performed to evaluate the therapeutic potential of the anticancer agents when incorporated as DES. This strategy might be applicable to other drug candidates or FDA-approved drugs that face pharmaceutical formulation related issues. THEDES based on ethyl gallate and dodecyl gallate can be incorporated in nanoparticle-based drug delivery strategies to improve performance.

As THEDES is a new concept, little research has been performed to assess the efficacy of new formulations. Further *in vitro* cell-based assay and *in vivo* animal model-based assay should be developed to check the drug delivery efficiency of the new formulation. Drug development costs have been spiking due to increased numbers of preclinical and clinical testing before FDA approval. Optimizing drug delivery has multiple promises to combat ongoing drug development costs. DES might be utilized as a novel approach to tackle these issues. In previous studies DES showed promise to optimize drug delivery strategies. Future pharmaceutical research should focus on the excellent physicochemical properties of DES and it might be a valuable resource for developing next generation drug delivery technologies.